

Gravity of quantum vacuum and the cosmological constant problem

by

Qingdi Wang

B.Sc., Wuhan University, 2008

M.Sc., The University of British Columbia, 2011

A THESIS SUBMITTED IN PARTIAL FULFILLMENT OF
THE REQUIREMENTS FOR THE DEGREE OF

DOCTOR OF PHILOSOPHY

in

The Faculty of Graduate and Postdoctoral Studies

(Physics)

THE UNIVERSITY OF BRITISH COLUMBIA

(Vancouver)

July 2018

© Qingdi Wang 2018

The following individuals certify that they have read, and recommend to the Faculty of Graduate and Postdoctoral Studies for acceptance, the dissertation entitled:

Gravity of Quantum Vacuum and the Cosmological Constant Problem

submitted by Qingdi Wang in partial fulfillment of the requirements for

the degree of Doctor of Philosophy

in Physics

Examining Committee:

William G. Unruh

Supervisor

Philip C.E. Stamp

Supervisory Committee Member

Mark Van Raamsdonk

Supervisory Committee Member

Joanna Karczmarek

University Examiner

Jingyi Chen

University Examiner

Additional Supervisory Committee Members:

Gordon Semenoff

Supervisory Committee Member

Ludovic Van Waerbeke

Supervisory Committee Member

Abstract

We investigate the gravitational property of the quantum vacuum by treating its large energy density predicted by quantum field theory seriously and assuming that it does gravitate to obey the equivalence principle of general relativity. We find that the quantum vacuum would gravitate differently from what people previously thought. The consequence of this difference is an accelerating universe with a small Hubble expansion rate $H \propto \Lambda e^{-\beta\sqrt{G}\Lambda} \rightarrow 0$ instead of the previous prediction $H = \sqrt{8\pi G\rho^{vac}/3} \propto \sqrt{G}\Lambda^2 \rightarrow \infty$ which was unbounded, as the high energy cutoff Λ is taken to infinity. In this sense, at least the “old” cosmological constant problem would be resolved. Moreover, it gives the observed slow rate of the accelerating expansion as Λ is taken to be some large value of the order of Planck energy or higher. This result suggests that there is no necessity to introduce the cosmological constant, which is required to be fine tuned to an accuracy of 10^{-120} , or other forms of dark energy, which are required to have peculiar negative pressure, to explain the observed accelerating expansion of the Universe.

Lay Summary

Based on two fundamental principles of modern physics — the uncertainty principle of quantum mechanics and the equivalence principle of general relativity, this study suggests that the space we live in is not as static as it appears. It is constantly moving. At each point, it oscillates between expansion and contraction. As it swings back and forth, the two almost cancel each other but a very small net effect drives the universe to expand slowly at an accelerating rate. This process happens at very tiny scales, billions and billions times smaller even than an electron. This research proposes an original idea to resolve one of the most important problems in fundamental physics—the cosmological constant problem and provides an explanation for the origin of “dark energy” which drives the accelerating expansion of the universe.

Preface

This work is a further development with major corrections to the numerical results from the following publication: [1] Qingdi Wang, Zhen Zhu, and William G. Unruh, “How the huge energy of quantum vacuum gravitates to drive the slow accelerating expansion of the Universe”, Phys. Rev. D 95, 103504 (2017).

- Chapter 2 to 9 are basically from the published paper [1] with a little bit more details and revisions. In particular, chapter 5.6 and 5.7 contains major corrections to the numerical work, chapter 7 contains more discussions about different metrics, chapter 9 contains more discussions about the singularity issue. We also include a different model (unsuccessful but still interesting) in chapter 10.
- Sam Cree repeated the numerical simulation in our published work [1] and found that his numerical result does not match with ours. He helped identifying the problem, improving the numeric technique and correcting the old result.
- The original work presented in this thesis was carried out by Qingdi Wang who also developed the conception and method of this research with various degrees of conception, methods, consultation and editing support from William G. Unruh. The numerical part of this research (Section 5.7 (also part of Section 10.3) and Appendix B) was mainly conducted by Zhen Zhu who also contributed some method development of this research and helped editing part of the manuscript of [1].

Table of Contents

Abstract	iii
Lay Summary	iv
Preface	v
Table of Contents	vi
List of Figures	ix
Acknowledgements	xii
Dedication	xiii
1 Introduction	1
2 The formulation of the cosmological constant problem	4
3 The fluctuating quantum vacuum energy density	7
4 Differences made by the inhomogeneous vacuum—a simple model	10
4.1 Beyond the FLRW metric	10
4.2 The fluctuating spacetime	11
4.3 Methods and assumptions in solving the system	16
5 The solution for $a(t, \mathbf{x})$	18
5.1 Parametric resonance	18
5.2 The solution for $P(t, \mathbf{x})$	21
5.3 The global Hubble expansion rate H	22
5.4 A more intuitive explanation	25
5.5 Meaning of our results	27
5.6 The slow varying condition	28

Table of Contents

5.7	Numerical verification	30
6	The back reaction	37
6.1	A simplified toy model	39
6.2	General case	47
7	The more general metrics	54
7.1	The full metric and Einstein equations	54
7.2	The Mixmaster-type metric	55
7.3	An alternative derivation from geodesic deviation equation	57
7.4	The physical picture	60
7.5	The Raychaudhuri equation	60
8	Similarity of effects of vacuum energy in non-gravitational system and gravitational system	63
8.1	Value of vacuum energy is relevant in Casimir effect	64
8.2	Effect of vacuum energy on the motion of mirrors	66
8.3	Analogies between the motion of mirror and the motion of $a(t, \mathbf{x})$	67
9	The singularities at $a(t, \mathbf{x}) = 0$	69
9.1	Is singularity an end or a new beginning?	69
9.2	Resolving singularity by multiplying a	70
9.3	Singularities do not cause problems	71
10	A different model with a large bare cosmological constant (unsuccessful)	75
10.1	The formulation of the cosmological constant problem is destroyed by density fluctuations of quantum vacuum	75
10.2	New relation between λ_{eff} and λ_b	77
10.3	Numerical simulation	81
10.4	Meaning of the results	86
10.5	Problem of this model	87
11	Conclusions	91
	Bibliography	92

Table of Contents

Appendices

A Real Massless Scalar Field	98
B Wigner-Weyl Description of Quantum Mechanics and Nu- meric simulations	104
C Fourier transforms of the coefficients in (6.42)	109

List of Figures

3.1	Plot of the expectation value of the square of the energy density difference as a function of spacial separation $\Lambda\Delta x$	9
4.1	Constant energy density requires negative pressure	15
5.1	Plot of the normalized covariance χ as a function of temporal separation $\Lambda\Delta t$	19
5.2	Plot of the power spectrum density of the varying part of $\Omega^2(t, \mathbf{0})$ (except for the constant Ω_0^2 part).	26
5.3	Numeric result for $\log a_o(t) $ when one scalar field is present. The slope represents the Hubble expansion rate H . It shows that as Λ increases, H also increases. The prediction (5.25) is not applicable in this case since the slow varying condition is violated when Ω^2 fluctuates to values smaller than $\sim \Lambda^3$	31
5.4	Numeric result for $\log a_o(t) $ when one scalar field with a negative bare cosmological constant $-\lambda_b \sim \Lambda^{3.5}$ are present. The slope represents the Hubble expansion rate H . It shows that as Λ increases, H decreases. The linear fit $\log(H/\Lambda)$ vs Λ gives the parameter $\alpha \sim e^{-4.1} \approx 0.017$, $\beta \sim 0.072$	32
5.5	Top: numeric result for five scalar fields without a bare cosmological constant and its linear fit $\log(H/\Lambda)$ vs Λ ; Bottom: five scalar fields with a negative bare cosmological constant $-\lambda_b \sim \Lambda^{3.5}$ and its linear fit $\log(H/\Lambda)$ vs Λ . The slope represents the Hubble expansion rate H . In both cases as Λ increases, H decreases. The linear fit gives the parameters $\alpha \sim e^{-3.8} \approx 0.022$, $\beta \sim 0.14$ for five scalar fields without the bare cosmological constant and the parameters $\alpha \sim e^{-4.2} \approx 0.015$, $\beta \sim 0.28$ for five scalar fields with the bare cosmological constant.	33

List of Figures

5.6	Top: numeric result for ten scalar fields without a bare cosmological constant and its linear fit $\log(H/\Lambda)$ vs Λ ; Bottom: ten scalar fields with a negative bare cosmological constant $-\lambda_b \sim \Lambda^{3.5}$ and its linear fit $\log(H/\Lambda)$ vs Λ . The slope represents the Hubble expansion rate H . In both cases as Λ increases, H decreases. The linear fit gives the parameters $\alpha \sim e^{-3.7} \approx 0.025$, $\beta \sim 0.6$ for ten scalar fields without the bare cosmological constant and the parameters $\alpha \sim e^{-3.5} \approx 0.03$, $\beta \sim 0.83$ for ten scalar fields with the bare cosmological constant.	34
5.7	Top: numeric result for twenty scalar fields without a bare cosmological constant and its linear fit $\log(H/\Lambda)$ vs Λ ; Bottom: twenty scalar fields with a negative bare cosmological constant $-\lambda_b \sim \Lambda^{3.5}$ and its linear fit $\log(H/\Lambda)$ vs Λ . The slope represents the Hubble expansion rate H . In both cases as Λ increases, H decreases. The linear fit gives the parameters $\alpha \sim e^{-2.6} \approx 0.074$, $\beta \sim 1.9$ for twenty scalar fields without the bare cosmological constant and the parameters $\alpha \sim e^{-2.1} \approx 0.12$, $\beta \sim 2.4$ for twenty scalar fields with the bare cosmological constant.	35
9.1	Plot of the correction function $f(\Theta) = \sum_{m=1}^{+\infty} x_m \sin 2m\Theta$ around the spacetime singularity at $\Theta = \Omega t + \mathbf{K} \cdot \mathbf{k} = \pi/2$, where the sum in the plot is from $m = 1$ to $m = 20000$	73
9.2	Plot of the derivative of the correction function $\frac{df(\Theta)}{d\Theta} = \sum_{m=1}^{+\infty} 2mx_m \cos 2m\Theta$ around the spacetime singularity at $\Theta = \Omega t + \mathbf{K} \cdot \mathbf{k} = \pi/2$, where the sum in the plot is from $m = 1$ to $m = 20000$	73
10.1	An illustration of the probability density distribution $P(\Omega^2)$. The shape of the graph is obtained from the histogram of a sample of $\Omega^2(t)$ we used in the numerical simulation 10.3. This is for one boson and one fermion field. The tails fall as $e^{-\kappa \Omega^2+\lambda_b/3 }$ (as shown in FIG. 10.2) for large argument where κ is some constant.	78
10.2	Plot of $\log(\Omega^2)$ which shows the tail of $P(\Omega^2)$ falls as $e^{-\kappa \Omega^2+\lambda_b/3 }$ for large argument where κ is some constant.	79

List of Figures

10.3	Numerical result for the dependence of $\log a $ on the bare cosmological constant λ_b as $ \lambda_b $ is small. The cutoff $\Lambda = 1$. 100 samples are averaged for each line. Planck units are used for convenience. The matter fields are one Boson field and one Fermion field. The magnitude of $\langle \rho + \sum_{i=1}^3 P_i \rangle$ for both fields are set equal but with opposite sign, i.e. we set $\langle \rho + \sum_{i=1}^3 P_i \rangle = 0$ in the simulation. It shows that the Hubble expansion rate decreases as $-\lambda_b$ increases.	82
10.4	Plot of $\log H$ over $ \lambda_b $ when $ \lambda_b $ is small. The fitting result shows that $\tilde{\beta} \sim 6$. Planck units are used for convenience. . . .	83
10.5	Numerical result for the dependence of $\log a $ on the bare cosmological constant λ_b as $ \lambda_b $ is large. The cutoff $\Lambda = 1$. 400 samples are averaged for each line. Planck units are used for convenience. The matter fields are one Boson field and one Fermion field. The magnitude of $\langle \rho + \sum_{i=1}^3 P_i \rangle$ for both fields are set equal but with opposite sign, i.e. we set $\langle \rho + \sum_{i=1}^3 P_i \rangle = 0$ in the simulation. It shows that the Hubble expansion rate decreases as $-\lambda_b$ increases. For larger $-\lambda_b$ the slope of $\log a $ grows too slow that the numerical rounding errors seem to dominant.	84
10.6	Plot of $\log H$ over $\sqrt{ \lambda_b }$ when $ \lambda_b $ is large. The fitting result shows that $\alpha \sim e^{18}, \beta \sim 14$. Planck units are used for convenience. The cutoff $\Lambda = 1$	85
A.1	Plot of correlation coefficient $\rho_{x,x'}$ as a function of time separation $\Lambda \Delta t$ in the case $\Delta x = 0$	100
A.2	Plot of correlation coefficient $\rho_{x,x'}$ as a function of spatial separation $\Lambda \Delta x$ in the case $\Delta t = 0$	100

Acknowledgements

I would like to express the deepest appreciation to my supervisor, Professor William George Unruh, whose expertise and generous guidance made it possible for me to work on a topic that was of great interest but also highly risky. It was lucky to had the opportunity to work with him. Without his guidance this dissertation would not have been possible.

I would also like to thank the many people with whom I discussed the related work and have benefited greatly from such discussion: Andrei Barvinsky, Gordon W. Semenoff, Mark Van Raamsdonk, Philip C. E. Stamp, Daniel Carney, Yin-Zhe Ma, Daoyan Wang, Michael Desrochers, Giorgio Torrieri, Niayesh Afshordi, Roland de Putter, Jérôme Gleyzes and Olivier Doré for helpful discussions and criticisms. I especially thank Michael Desrochers for helping revising the manuscript.

I would also specially thank Sam Cree who helped to identify and correct the mistakes we made in the numerical calculations in [1].

Most importantly, none of this would have been possible without the love and patience of my family. Especially I want to mention my grandfather Jiehua Wang, my parents Huan Wang and Shuangxiu Wang. My family has been a constant source of love, concern, support and strength all over these years. I would like to express my heart-felt gratitude to my family.

Dedication

To my grandfather Jiehua Wang

Chapter 1

Introduction

The two pillars that much of modern physics is based on are Quantum Mechanics (QM) and General Relativity (GR). QM is the most successful scientific theory in history, which has never been found to fail in repetitive experiments. GR is also a successful theory which has so far managed to survive every test [2]. In particular, the last major prediction of GR—the gravitational waves, has finally been directly detected on Sept 2015 [3]. However, these two theories seem to be incompatible at a fundamental level (see e.g. [4]). The unification of both theories is a big challenge to modern theoretical physicists.

While the test of the combination of QM and GR is still difficult in lab, our Universe already provides one of the biggest confrontations between both theories: the Cosmological Constant Problem [5]. Quantum field theory (QFT) predicts a huge vacuum energy density from various sources. Meanwhile, the equivalence principle of GR requires that every form of energy gravitates in the same way. When combining these concepts together, it is widely supposed that the vacuum energy gravitates as a cosmological constant. However, the observed effective cosmological constant λ_{eff} is so small compared with the QFT's prediction that an unknown bare cosmological constant λ_b (2.7) has to cancel this huge contribution from the vacuum to better than at least 50 to 120 decimal places! It is an extremely difficult fine-tuning problem that gets even worse when the higher loop corrections are included [6].

In 1998, the discovery of the accelerating expansion of the Universe [7, 8] has further strengthened the importance of this problem. Before this, one only needs to worry about the “old” cosmological constant problem of explaining why the effective cosmological constant is not large. Now, one also has to face the challenge of the “new” cosmological constant problem of explaining why it has such a specific small value from the observation, which is the same order of magnitude as the present mass density of the Universe (coincidence problem).

This problem is widely regarded as one of the major obstacles to further progress in fundamental physics (for example, see Witten 2001 [9]). Its

importance has been emphasized by various authors from different aspects. For example, it has been described as a “veritable crisis” (Weinberg 1989, [5] p.1), an “unexplained puzzle” (Kolb and Turner 1993, [10] p.198), “the most striking problem in contemporary physics” (Dolgov 1997 [11] p.1) and even “the mother of all physics problems”, “the worst prediction ever” (Susskind 2015 [12] chapter two). While it might be possible that people working on a particular problem tend to emphasize or even exaggerate its importance, those authors all agree that this is a problem that needs to be solved, although there is little agreement on what is the right direction to find the solution [13].

In this thesis, we make a proposal for addressing the cosmological constant problem. We treat the divergent vacuum energy density predicted by QFT seriously and assume that it does gravitate to obey the equivalence principle of GR. We notice that the magnitude of the vacuum fluctuation itself also fluctuates, which leads to a constantly fluctuating and extremely inhomogeneous vacuum energy density. As a result, the quantum vacuum gravitates differently from a cosmological constant. Instead, at each spatial point, the spacetime sourced by the vacuum oscillates alternatively between expansion and contraction, and the phases of the oscillations at neighboring points are different. In this manner of vacuum gravitation, although the gravitational effect produced by the vacuum energy is still huge at sufficiently small scales (Planck scale), its effect at macroscopic scales is largely canceled. Moreover, due to the weak parametric resonance of those oscillations, the expansion outweighs contraction a little bit during each oscillation. This effect accumulates at sufficiently large scales (cosmological scale), resulting in an observable effect—the slow accelerating expansion of the Universe. Our proposal harkens back to Wheeler’s spacetime foam [14, 15] and suggests that it is this foamy structure which leads to the cosmological constant we see today.

This thesis is organized as follows: in chapter 2, we first review several key steps in formulating the cosmological constant problem; in chapter 3, we point out that the vacuum energy density is not a constant but is constantly fluctuating and extremely inhomogeneous; in chapter 4, we investigate the differences made by the extreme inhomogeneity of the quantum vacuum by introducing a simple model; in chapter 5, we give the solutions to this model by solving the Einstein field equations and show how metric fluctuations leads to the slow accelerating expansion of the Universe; in chapter 6, we investigate the back reaction effect of the resulting spacetime on the matter fields propagating on it; in chapter 7, we generalize our results to more general metrics; in chapter 8 we discuss the role played by vacuum energy in

Chapter 1. Introduction

non-gravitational physics and gravitational physics; in chapter 9 we discuss the singularity issue; in chapter 10 we introduce another unsuccessful but interesting model.

The units and metric signature are set to be $c = \hbar = 1$ and $(-, +, +, +)$ throughout except otherwise specified.

Chapter 2

The formulation of the cosmological constant problem

The cosmological constant problem arises when trying to combine GR and QFT to investigate the gravitational property of the vacuum:

$$G_{\mu\nu} + \lambda_b g_{\mu\nu} = 8\pi G T_{\mu\nu}^{\text{vac}}, \quad (2.1)$$

where $G_{\mu\nu} \equiv R_{\mu\nu} - \frac{1}{2}Rg_{\mu\nu}$ is the Einstein tensor and the parameter λ_b is the bare cosmological constant.

One crucial step in formulating the cosmological constant problem is assuming that the vacuum energy density is equivalent to a cosmological constant. First, it is argued that the vacuum is Lorentz invariant and thus every observer would see the same vacuum. In Minkowski spacetime, $\eta_{\mu\nu}$ is the only Lorentz invariant $(0, 2)$ tensor up to a constant. Thus the vacuum stress-energy tensor must be proportional to $\eta_{\mu\nu}$ (see, e.g. [16], [13])

$$T_{\mu\nu}^{\text{vac}}(t, \mathbf{x}) = -\rho^{\text{vac}}\eta_{\mu\nu}. \quad (2.2)$$

The above vacuum equation of state (2.2) is then straightforwardly generalized from inertial coordinates to arbitrary coordinates by replacing $\eta_{\mu\nu}$ with $g_{\mu\nu}$ ¹,

$$T_{\mu\nu}^{\text{vac}}(t, \mathbf{x}) = -\rho^{\text{vac}}g_{\mu\nu}(t, \mathbf{x}). \quad (2.3)$$

Then from the principle of general covariance, it is asserted that $T_{\mu\nu}^{\text{vac}}$ has also to be a constant times $g_{\mu\nu}$ when $g_{\mu\nu}$ describes a real gravitational field:

$$T_{\mu\nu}^{\text{vac}}(t, \mathbf{x}) = -\rho^{\text{vac}}g_{\mu\nu}(t, \mathbf{x}). \quad (2.4)$$

¹Note that the $g_{\mu\nu}$ here is still describing flat spacetime. Do not be confused with the $g_{\mu\nu}$ in (2.4), which is describing curved spacetime (with non-zero Riemann curvature tensor components).

If $T_{\mu\nu}^{\text{vac}}$ does take the above form (2.4), the vacuum energy density ρ^{vac} has to be a constant, which is the requirement of the conservation of the stress-energy tensor

$$\nabla^\mu T_{\mu\nu}^{\text{vac}} = 0. \quad (2.5)$$

The effect of a stress-energy tensor of the form (2.4) is equivalent to that of a cosmological constant, as can be seen by moving the term $8\pi G T_{\mu\nu}^{\text{vac}}$ in (2.1) to the left-hand side

$$G_{\mu\nu} + \lambda_{\text{eff}} g_{\mu\nu} = 0, \quad (2.6)$$

where,

$$\lambda_{\text{eff}} = \lambda_b + 8\pi G \rho^{\text{vac}}; \quad (2.7)$$

Or equivalently by moving the term $\lambda_b g_{\mu\nu}$ in (2.1) to the right-hand side

$$G_{\mu\nu} = -8\pi G \rho_{\text{eff}}^{\text{vac}} g_{\mu\nu}, \quad (2.8)$$

where,

$$\rho_{\text{eff}}^{\text{vac}} = \rho^{\text{vac}} + \frac{\lambda_b}{8\pi G}. \quad (2.9)$$

So anything that contributes to the energy density of the vacuum acts like a cosmological constant and thus contributes to the effective cosmological constant. Or equivalently we can say that the bare cosmological constant acts like a source of vacuum energy and thus contributes to the total effective vacuum energy density. This equivalence is the origin of the identification of the cosmological constant with the vacuum energy density.

Following the above formulations, the effective cosmological constant λ_{eff} or the total effective vacuum energy density $\rho_{\text{eff}}^{\text{vac}}$ are the quantities that can be constrained and measured through experiments. While solar system and galactic observations have placed a small upper bound on λ_{eff} , large scale cosmological observations provide the most accurate measurement. It is interpreted as a form of “dark energy”, which drives the observed accelerating expansion of the Universe [7, 8].

Based on the assumption of homogeneity and isotropy of the Universe, the metric has the cosmology’s standard FLRW form, which is, for the spatially flat case,

$$ds^2 = -dt^2 + a^2(t) (dx^2 + dy^2 + dz^2). \quad (2.10)$$

Then by applying the equations (2.6) or (2.8) for the above special metric (2.10), one obtains the contributions to the Hubble expansion rate $H = \dot{a}/a$

and the acceleration of the scale factor \ddot{a} from λ_{eff} and/or $\rho_{\text{eff}}^{\text{vac}}$ are

$$3H^2 = \lambda_{\text{eff}} = 8\pi G\rho_{\text{eff}}^{\text{vac}}, \quad (2.11)$$

$$\ddot{a} = \frac{\lambda_{\text{eff}}}{3}a = \frac{8\pi G\rho_{\text{eff}}^{\text{vac}}}{3}a. \quad (2.12)$$

The solution to the dynamic equation (2.12) is

$$a(t) = a(0)e^{Ht}, \quad (2.13)$$

where H is determined by the initial value constraint equation (2.11).

According to the Lambda-CDM model of the big bang cosmology, the effective cosmological constant is responsible for the accelerating expansion of the Universe as shown in (2.12) and contributes about 69% to the current Hubble expansion rate [17]:

$$\lambda_{\text{eff}} = 3\Omega_\lambda H_0^2 \approx 4.32 \times 10^{-84}(\text{GeV})^2, \quad (2.14)$$

or

$$\rho_{\text{eff}}^{\text{vac}} = \Omega_\lambda \rho_{\text{crit}} \approx 2.57 \times 10^{-47}(\text{GeV})^4, \quad (2.15)$$

where $\Omega_\lambda = 0.69$ is the dark energy density parameter, H_0 is the current observed Hubble constant and $\rho_{\text{crit}} = \frac{3H_0^2}{8\pi G}$ is the critical density.

Unfortunately the predicted energy density of the vacuum from QFT is much larger than this. It receives contributions from various sources, including the zero point energies ($\sim 10^{72}(\text{GeV})^4$) of all fundamental quantum fields due to vacuum fluctuations, the phase transitions due to the spontaneous symmetry breaking of electroweak theory ($\sim 10^9(\text{GeV})^4$) and any other known and unknown phase transitions in the early Universe (e.g. from chiral symmetry breaking in QCD ($\sim 10^{-2}(\text{GeV})^4$), grand unification ($\sim 10^{64}(\text{GeV})^4$) etc)[13, 18]. Each contribution is larger than the observed value (2.15) by 50 to 120 orders of magnitude. There is no mechanism in the standard model which suggests any relations between the individual contributions, so it is customary to assume that the total vacuum energy density is at least as large as any of the individual contributions [13]. One thus has to fine tune the unknown bare cosmological constant λ_b to a precision of at least 50 decimal places to cancel the excess vacuum energy density.

Chapter 3

The fluctuating quantum vacuum energy density

The vacuum energy density is treated as a constant in the usual formulation of the cosmological constant problem. While this is true for the expectation value, it is not true for the actual energy density.

That's because the vacuum is not an eigenstate of the local energy density operator T_{00} , although it is an eigenstate of the global Hamiltonian operator $H = \int d^3x T_{00}$. This implies that the total vacuum energy all over the space is constant but its density fluctuates at individual points.

To see this more clearly, consider a quantized real massless scalar field ϕ in Minkowski spacetime as an example:

$$\phi(t, \mathbf{x}) = \int \frac{d^3k}{(2\pi)^{3/2}} \frac{1}{\sqrt{2\omega}} \left(a_{\mathbf{k}} e^{-i(\omega t - \mathbf{k} \cdot \mathbf{x})} + a_{\mathbf{k}}^\dagger e^{+i(\omega t - \mathbf{k} \cdot \mathbf{x})} \right), \quad (3.1)$$

where the temporal frequency ω and the spatial frequency \mathbf{k} in (3.1) are related to each other by $\omega = |\mathbf{k}|$.

The vacuum state $|0\rangle$, which is defined as

$$a_{\mathbf{k}}|0\rangle = 0, \quad \text{for all } \mathbf{k}, \quad (3.2)$$

is an eigenstate of the Hamiltonian operator

$$H = \int d^3x T_{00} = \frac{1}{2} \int d^3k \omega \left(a_{\mathbf{k}} a_{\mathbf{k}}^\dagger + a_{\mathbf{k}}^\dagger a_{\mathbf{k}} \right), \quad (3.3)$$

where T_{00} is defined as

$$T_{00} = \frac{1}{2} \left(\dot{\phi}^2 + (\nabla\phi)^2 \right). \quad (3.4)$$

But, $|0\rangle$ is not an eigenstate of the energy density operator

$$T_{00}(t, \mathbf{x}) = \frac{1}{2} \int \frac{d^3k d^3k'}{(2\pi)^3} \frac{1}{2} \left(\sqrt{|\mathbf{k}||\mathbf{k}'|} + \frac{\mathbf{k} \cdot \mathbf{k}'}{\sqrt{|\mathbf{k}||\mathbf{k}'|}} \right) \cdot \left(a_{\mathbf{k}} a_{\mathbf{k}'}^\dagger e^{-i[(|\mathbf{k}|-|\mathbf{k}'|)t - (\mathbf{k}-\mathbf{k}') \cdot \mathbf{x}]} + a_{\mathbf{k}}^\dagger a_{\mathbf{k}'} e^{+i[(|\mathbf{k}|-|\mathbf{k}'|)t - (\mathbf{k}-\mathbf{k}') \cdot \mathbf{x}]} - a_{\mathbf{k}} a_{\mathbf{k}'} e^{-i[(|\mathbf{k}+|\mathbf{k}'|)t - (\mathbf{k}+\mathbf{k}') \cdot \mathbf{x}]} - a_{\mathbf{k}}^\dagger a_{\mathbf{k}'}^\dagger e^{+i[(|\mathbf{k}+|\mathbf{k}'|)t - (\mathbf{k}+\mathbf{k}') \cdot \mathbf{x}]} \right), \quad (3.5)$$

because of the terms of the form $a_{\mathbf{k}} a_{\mathbf{k}'}$ and $a_{\mathbf{k}}^\dagger a_{\mathbf{k}'}^\dagger$.

Direct calculation shows the magnitude of the fluctuation of the vacuum energy density diverges as the same order as the energy density itself,

$$\langle (T_{00} - \langle T_{00} \rangle)^2 \rangle = \frac{2}{3} \langle T_{00} \rangle^2, \quad (3.6)$$

where

$$\langle T_{00} \rangle = \frac{\Lambda^4}{16\pi^2}, \quad (3.7)$$

where Λ is the effective QFT's high energy cutoff. (For more details on this calculation, see equation (A.6) in Appendix A.) Thus the energy density fluctuates as violently as its own magnitude. With such huge fluctuations, the vacuum energy density ρ^{vac} is not a constant in space or time.

Furthermore, the energy density of the vacuum is not only not a constant in time at a fixed spatial point, it also varies from place to place. In other words, the energy density of vacuum is varying wildly at every spatial point and the variation is not in phase for different spatial points. This results in an extremely inhomogeneous vacuum. The extreme inhomogeneity can be illustrated by directly calculating the expectation value of the square of difference between energy density at different spatial points,

$$\Delta\rho^2(\Delta x) = \frac{\langle \{ (T_{00}(t, \mathbf{x}) - T_{00}(t, \mathbf{x}'))^2 \} \rangle}{\frac{4}{3} \langle T_{00}(t, \mathbf{x}) \rangle^2}, \quad (3.8)$$

where $\Delta x = |\mathbf{x} - \mathbf{x}'|$ and we have normalized $\Delta\rho^2$ by dividing its asymptotic value $\frac{4}{3} \langle T_{00} \rangle^2$ (the curly bracket $\{ \}$ is the symmetrization operator which is defined by (A.2)). The behavior of $\Delta\rho^2$ for the scalar field (3.1) in Minkowski vacuum is plotted in FIG. 3.1, which shows that the magnitude of the energy density difference between two spacial points quickly goes up to the order of

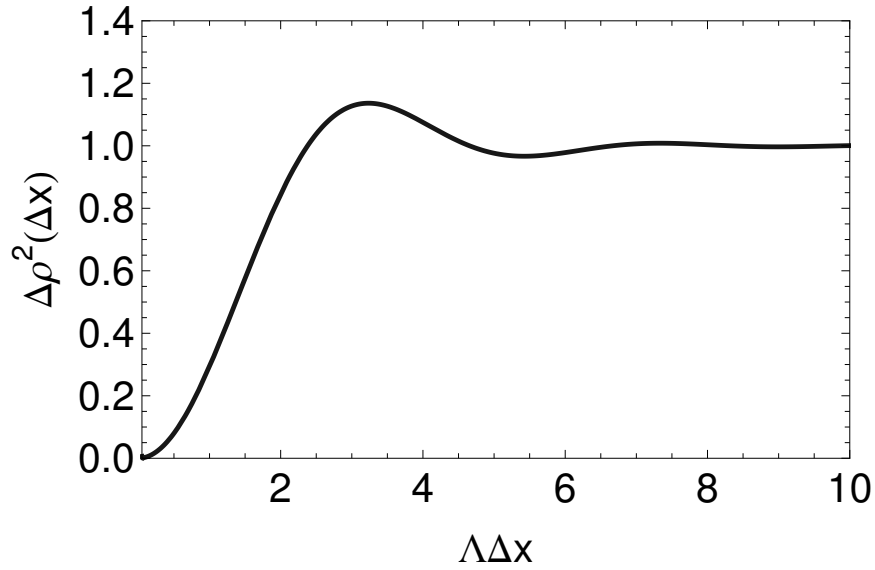


Figure 3.1: Plot of the expectation value of the square of the energy density difference as a function of spatial separation $\Lambda\Delta x$.

$\langle T_{00} \rangle$ itself as their distance increases by only the order of $1/\Lambda$. (For more details on the calculations and how the energy density fluctuates all over the spacetime, see Appendix A.)

As the vacuum is clearly not homogeneous, equation (2.11) is not valid as it depends on a homogeneous and isotropic matter field and metric. Therefore a new method of relating vacuum energy density to the observed Hubble expansion rate is required.

Chapter 4

Differences made by the inhomogeneous vacuum—a simple model

The extreme inhomogeneity of the vacuum means its gravitational effect cannot be treated perturbatively, so another method is required. As solutions to the fully general Einstein equations are difficult to obtain, we will first look at a highly simplified model.

4.1 Beyond the FLRW metric

To describe the gravitational property of the inhomogeneous quantum vacuum, we must allow inhomogeneity in the metric. This is accomplished by allowing the scale factor $a(t)$ in the FLRW metric (2.10) to have spatial dependence,

$$ds^2 = -dt^2 + a^2(t, \mathbf{x})(dx^2 + dy^2 + dz^2). \quad (4.1)$$

The full Einstein field equations for the coordinate (4.1) are

$$G_{00} = 3 \left(\frac{\dot{a}}{a} \right)^2 + \frac{1}{a^2} \left(\frac{\nabla a}{a} \right)^2 - \frac{2}{a^2} \left(\frac{\nabla^2 a}{a} \right) = 8\pi GT_{00}, \quad (4.2)$$

$$\begin{aligned} G_{ii} &= -2a\ddot{a} - \dot{a}^2 - \left(\frac{\nabla a}{a} \right)^2 + \frac{\nabla^2 a}{a} + 2 \left(\frac{\partial_i a}{a} \right)^2 - \frac{\partial_i^2 a}{a} \\ &= 8\pi GT_{ii}, \end{aligned} \quad (4.3)$$

$$G_{0i} = 2 \frac{\dot{a}}{a} \frac{\partial_i a}{a} - 2 \frac{\partial_i \dot{a}}{a} = 8\pi GT_{0i}, \quad (4.4)$$

$$G_{ij} = 2 \frac{\partial_i a}{a} \frac{\partial_j a}{a} - \frac{\partial_i \partial_j a}{a} = 8\pi GT_{ij}, \quad i, j = 1, 2, 3, \quad i \neq j, \quad (4.5)$$

where $\nabla = (\partial_1, \partial_2, \partial_3)$ is the ordinary gradient operator with respect to the spatial coordinates x, y, z .

By choosing the above simplest inhomogeneous metric (4.1), we are assuming a mini-superspace type model, and will choose which of these equations do apply later. This treatment might result in inconsistencies as general vacuum fluctuations of the matter fields possess rich structures that they may not produce spacetime described by the metric (4.1). To fully describe the resulting inhomogeneous spacetime, one needs a more general metric. However, as a first approximation, using (4.1) is relatively easy to calculate and leads to interesting results. We are also going to do the calculations for more general metrics in chapter 7.

4.2 The fluctuating spacetime

The role played by the value of vacuum energy density in the above equations (4.2), (4.3), (4.4) and (4.5) is different from (2.11). The value of vacuum energy density is no longer directly related to the Hubble rate H through the equation (2.11). This is evident from the 00 component of the Einstein equation (4.2). The equation (2.11) is only the special case of (4.2) when the spatial derivatives ∇a and $\nabla^2 a$ are zero, which requires that the matter distribution is strictly homogeneous and isotropic. However, as shown in the last section, the quantum vacuum is extremely inhomogeneous and necessarily anisotropic, which requires ∇a and $\nabla^2 a$ be huge. This can be seen through the ij component of the Einstein equation (4.5). In fact, due to symmetry properties of the quantum vacuum, we have the expectation value of shear stress T_{ij} on the right side of (4.5)

$$\langle T_{ij} \rangle = 0, \quad i, j = 1, 2, 3, \quad i \neq j. \quad (4.6)$$

Meanwhile, T_{ij} must fluctuate since the quantum vacuum is not its eigenstate either, and the magnitude of the fluctuation is on the same order of the vacuum energy density

$$\langle T_{ij}^2 \rangle \sim \langle T_{00} \rangle^2. \quad (4.7)$$

This means that the T_{ij} is constantly fluctuating around zero with a huge magnitude of the order of vacuum energy density. As a result, in (4.5), the spatial derivatives of $a(t, \mathbf{x})$ must also constantly fluctuate with huge magnitudes.

More importantly, since the scale factor $a(t, \mathbf{x})$ is spatially dependent, the physical distance L between two spatial points with comoving coordinates \mathbf{x}_1 and \mathbf{x}_2 is no longer related to their comoving distance $\Delta x = |\mathbf{x}_1 - \mathbf{x}_2|$

4.2. The fluctuating spacetime

by the simple equation $L(t) = a(t)\Delta x$ and the observed global Hubble rate H is no longer equal to the local Hubble rate \dot{a}/a . Instead, the physical distance and the global Hubble rate are defined as

$$L(t) = \int_{\mathbf{x}_1}^{\mathbf{x}_2} \sqrt{a^2(t, \mathbf{x})} dl \quad (4.8)$$

and

$$H(t) = \frac{\dot{L}}{L} = \frac{\int_{\mathbf{x}_1}^{\mathbf{x}_2} \frac{\dot{a}}{a}(t, \mathbf{x}) \sqrt{a^2(t, \mathbf{x})} dl}{\int_{\mathbf{x}_1}^{\mathbf{x}_2} \sqrt{a^2(t, \mathbf{x})} dl}, \quad (4.9)$$

where the line element $dl = \sqrt{dx^2 + dy^2 + dz^2}$.

Equation (4.9) shows the key difference between the gravitational behavior of quantum vacuum predicted by the homogeneous FLRW metric (2.10) and by the inhomogeneous metric (4.1).

For the homogeneous metric (2.10), the scale factor a is spatially independent and (4.9) just reduces to

$$H(t) = \frac{\dot{a}}{a}(t). \quad (4.10)$$

In this case, there are only two distinct choices for Hubble rates on a spatial slice $t = Const$ under the initial value constraint equation (2.11)

$$\frac{\dot{a}}{a} = \pm \sqrt{\frac{8\pi G \rho^{\text{vac}}}{3}}, \quad (4.11)$$

which implies that all points in space have to be simultaneously expanding or contracting at the same constant rate (Here we do not include the cosmological constant λ).

But for the inhomogeneous metric (4.1), the scale factor a is spatially dependent and there is much more freedom in choosing different local Hubble rates at different spatial points of the slice $t = Const$ under the corresponding initial value constraint equation (4.2).

In fact, the local Hubble rates must be constantly changing over spatial directions within very small length scales. This can be seen from the initial value constraint equations (4.4), which can be rewritten as

$$\nabla \left(\frac{\dot{a}}{a} \right) = -4\pi G \mathbf{J}, \quad (4.12)$$

4.2. The fluctuating spacetime

where $\mathbf{J} = (T_{01}, T_{02}, T_{03})$ is vacuum energy flux².

The solution to (4.12) or (4.4) is

$$\frac{\dot{a}}{a}(t, \mathbf{x}) = \frac{\dot{a}}{a}(t, \mathbf{x}_0) - 4\pi G \int_{\mathbf{x}_0}^{\mathbf{x}} \mathbf{J}(t, \mathbf{x}') \cdot d\mathbf{l}', \quad (4.13)$$

where $d\mathbf{l}' = (dx', dy', dz')$ and \mathbf{x}_0 is an arbitrary spatial point. The above solution (4.13) shows that the difference in the local Hubble rates \dot{a}/a between \mathbf{x}_0 and \mathbf{x}_1 is determined by the spatial accumulations (integral) of the vacuum energy flux \mathbf{J} . Similar to the shear stress, \mathbf{J} has zero expectation value

$$\langle \mathbf{J} \rangle = \mathbf{0} \quad (4.14)$$

but huge fluctuations

$$J = \sqrt{\langle \mathbf{J}^2 \rangle} \sim \langle T_{00} \rangle \sim \Lambda^4 \rightarrow +\infty, \quad (4.15)$$

which implies that the local Hubble rates differ from point to point due to the fluctuations. The average of the absolute value of \dot{a}/a can be estimated with the constraint equation (4.2)

$$\sqrt{\left\langle \left(\frac{\dot{a}}{a} \right)^2 \right\rangle} \sim \sqrt{G \langle T_{00} \rangle} \sim \sqrt{G} \Lambda^2. \quad (4.16)$$

By using (4.13), we find that the difference in local Hubble rates becomes comparable with itself for points separated by only a distance of the order $\Delta x \sim \frac{1}{\sqrt{G} \Lambda^2}$ as $\Lambda \rightarrow +\infty$:

$$\Delta \left(\frac{\dot{a}}{a} \right) \sim 4\pi G J \Delta x \sim \sqrt{G} \Lambda^2 \sim \sqrt{\left\langle \left(\frac{\dot{a}}{a} \right)^2 \right\rangle}. \quad (4.17)$$

Up to this point, we have used the equations (4.2), (4.4) and (4.5). These equations are all initial value constraint equations which do not contain the scale factor's second order time derivative \ddot{a} . To get the information about

²One might notice that (4.12) requires $\nabla \times \mathbf{J} = 0$, which means that to produce the metric of the form (4.1), the energy flux of the matter field needs to be curl free. As mentioned in the last paragraph of section 4.1, this is not true for general matter fields, but here as a first approximation we will use (4.12) to estimate the magnitude of change in \dot{a}/a .

4.2. The fluctuating spacetime

the time evolution of $a(t, \mathbf{x})$, we also need to use (4.3). A linear combination of equations (4.2) and (4.3) gives,

$$G_{00} + \frac{1}{a^2} (G_{11} + G_{22} + G_{33}) = -\frac{6\ddot{a}}{a}, \quad (4.18)$$

where all the spatial derivatives of a cancel and only the second order time derivative left. Therefore we reach the following dynamic evolution equation for $a(t, \mathbf{x})$:

$$\ddot{a} + \Omega^2(t, \mathbf{x})a = 0, \quad (4.19)$$

where

$$\Omega^2 = \frac{4\pi G}{3} \left(\rho + \sum_{i=1}^3 P_i \right), \quad \rho = T_{00}, P_i = \frac{1}{a^2} T_{ii}. \quad (4.20)$$

(4.19) is just a generalization of the second Friedman equation. Its solution depends on the property of Ω^2 , especially its sign.

If still treating the energy density $\rho \equiv \text{constant}$, then to satisfy the conservation equation (2.5), one must have $P = P_1 = P_2 = P_3 = -\rho$ that ³

$$\Omega^2 = \frac{4\pi G}{3}(\rho + 3P) = -\frac{8\pi G\rho}{3} < 0, \quad \text{if } \rho > 0. \quad (4.21)$$

In this case, gravity becomes “repulsive” and the solution to (4.19) is just the exponential expansion (2.13).

However, when ρ is not a constant, fundamental difference happens—the sign of Ω^2 may change. For example, consider a real massless scalar field ϕ , its stress energy tensor for a general spacetime metric $g_{\mu\nu}$ is

$$T_{\mu\nu} = \nabla_\mu \phi \nabla_\nu \phi - \frac{1}{2} g_{\mu\nu} \nabla^\lambda \phi \nabla_\lambda \phi. \quad (4.22)$$

Direct calculation using the inhomogeneous metric (4.1) gives that

$$\rho + \sum_{i=1}^3 P_i = 2\dot{\phi}^2, \quad (4.23)$$

where all the spatial derivatives and explicit dependence on the metric a are canceled. Thus we obtain

$$\Omega^2 = \frac{8\pi G\dot{\phi}^2}{3} > 0. \quad (4.24)$$

³This is easy to understand by considering the matter illustrated in Fig.4.2. The matter must have negative pressure to be able to do negative work to the environment to maintain constant energy density.

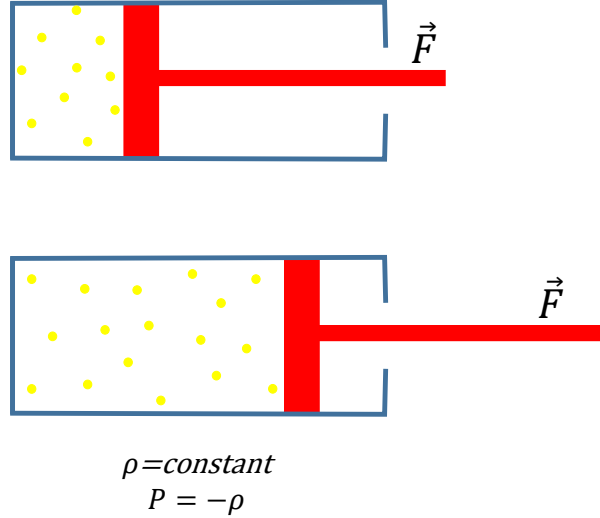


Figure 4.1: Constant energy density requires negative pressure

In this case, gravity is still attractive⁴ as usual and (4.19) describes a harmonic oscillator with time dependent frequency. The most basic behavior of a harmonic oscillator is that it oscillates back and forth around its equilibrium point, which implies that the local Hubble rates \dot{a}/a are periodically changing signs over time. By using equation (4.17) you can find that \dot{a}/a must also have this periodic sign change in a given spatial direction.

Physically, these fluctuating features of \dot{a}/a imply that, at any instant of time, if the space is expanding in a small region, it has to be contracting in neighboring regions; and at any spatial point, if the space is expanding now, it has to be contracting later.

These features result in huge cancellations when calculating the averaged H through (4.9). The observable overall net Hubble rate can be small although the absolute value of the local Hubble rate $|\dot{a}/a|$ at each individual point has to be huge to satisfy the constraint equation (4.2). In other words, while the instantaneous rates of expansion or contraction at a fixed spatial point can be large, their effects can be canceled in a way that the physical

⁴This is true if the matter fields satisfy normal energy conditions. We will assume that $\Omega^2 > 0$ even after considering all the contributions from known and unknown fundamental fields, i.e. gravity is always attractive as usual, no mysteries “dark energy” with peculiar negative pressure.

distance (4.8) would not grow 10^{120} times larger than what is observed.

This picture of fluctuating spacetime is not completely new. It is similar to the concept of spacetime foam devised by John Wheeler [14, 15] that in a quantum theory of gravity spacetime would have a foamy, jittery nature and would consist of many small, ever-changing, regions in which spacetime are not definite, but fluctuates. His reason for this “foamy” picture is the same as ours—at sufficiently small scales the energy of vacuum fluctuations would be large enough to cause significant departures from the smooth spacetime we see at macroscopic scales.

The solution for $a(t, \mathbf{x})$ will be given by equations (5.4), (5.8) and (5.9) in the next chapter 5 to describe this foamy structure more precisely.

4.3 Methods and assumptions in solving the system

In principle, we need a full quantum theory of gravity to solve the evolution details of this quantum gravitational system. Unfortunately, no satisfactory theory of quantum gravity exists yet.

In this paper, we are not trying to quantize gravity. Instead, we are still keeping the spacetime metric $a(t, \mathbf{x})$ as classical, but quantizing the fields propagating on it. The key difference from the usual semiclassical gravity is that we go one more step—instead of assuming the semiclassical Einstein equation, where the curvature of the spacetime is sourced by the expectation value of the quantum field stress energy tensor, we also take the huge fluctuations of the stress energy tensor into account. In our method, the sources of gravity are stochastic classical fields whose stochastic properties are determined by their quantum fluctuations, i.e. our method is using stochastic gravity framework [19].⁵

The evolution details of the scale factor $a(t, \mathbf{x})$ described by equation(4.19) depends on the property of the time dependent frequency $\Omega(t, \mathbf{x})$ given by (4.20). For both simplicity and clarity, in the following chapters we investigate the properties of Ω by considering the contribution from a real massless scalar field ϕ , whose stress energy tensor is given by (4.22). (4.24) shows that Ω^2 is not explicitly dependent on the metric $a(t, \mathbf{x})$. However, the resulting spacetime sourced by this massless scalar field ϕ does have back reaction effect on ϕ itself. This is because ϕ obeys the equation of motion in curved

⁵The difference from the usual stochastic gravity framework is that we do not try to regularize the divergent stress energy tensor.

4.3. Methods and assumptions in solving the system

spacetime

$$\nabla^\mu \nabla_\mu \phi = \frac{1}{\sqrt{-g}} \partial_\mu (\sqrt{-g} g^{\mu\nu} \partial_\nu \phi) = 0, \quad (4.25)$$

which reduces to

$$\partial_t (a^3 \partial_t \phi) - \nabla \cdot (a \nabla \phi) = 0 \quad (4.26)$$

for the special metric (4.1).

Incorporating the back reaction effect by solving both the Einstein equations (4.2), (4.3), (4.4), (4.5) for the metric a and the equation of motion (4.26) for the field ϕ at the same time is difficult. Fortunately, solving the system in this way is unnecessary. Physically, the quantum vacuum locally behaves as a huge energy reservoir, so that the back reaction effect on it should be small and can be neglected. In our method, we will first assume that the quantized field ϕ is still taking the flat spacetime form of (3.1) for field modes below the effective QFT's high frequency cutoff Λ . We use (3.1) to calculate the stochastic property of the time dependent frequency Ω and then solve (4.19) to get the resulting curved spacetime described by the metric $a(t, \mathbf{x})$. This will be done in the next chapter 5.

We then investigate the back reaction effect in chapter 6 by quantizing the field ϕ in the resulting curved spacetime. It turns out that, while the resulting spacetime is fluctuating, the fluctuation happens at scales which are much smaller than the length scale $1/\Lambda$. Therefore the corrections to the field modes with frequencies below the cutoff Λ is quite small and thus the flat spacetime quantization (3.1) is valid to high precision. (See equations (6.38) (or (6.69)), (6.39) and (6.41) for quantitatively how high this precision is.) In this way we justify neglecting the aforementioned back reaction.

Empirically, this must be true since ordinary QFT has achieved great successes by assuming flat Minkowski background and using the expansion (3.1). So if our method is correct, (3.1) has to be still valid even the background spacetime is no longer flat but wildly fluctuating at small scales. In other words, the resulting spacetime should still look like Minkowskian for low frequency field modes. Long wavelength fields ride over the Wheeler's foam as if it is not there. This is similar to the behavior of very long wavelength water waves which do not notice the rapidly fluctuating atomic soup over which they ride.

Chapter 5

The solution for $a(t, \mathbf{x})$

In this chapter we give the solution for the local scale factor $a(t, \mathbf{x})$.

5.1 Parametric resonance

One important feature of a harmonic oscillator with time dependent frequency is that it may exhibit parametric resonance behavior.

If the $\Omega(t, \mathbf{x})$ is strictly periodic in time with a period T , the property of the solutions of (4.19) has been thoroughly studied by Floquet theory [20]. Under certain conditions (for example, the condition (5.28)), the parametric resonance phenomenon occurs and the general solution of (4.19) is (see e.g. Eq(27.6) in Chapter V of [21])

$$a(t, \mathbf{x}) = c_1 e^{H_{\mathbf{x}} t} P_1(t, \mathbf{x}) + c_2 e^{-H_{\mathbf{x}} t} P_2(t, \mathbf{x}), \quad (5.1)$$

where $H_{\mathbf{x}} > 0$, c_1 and c_2 are constants. The P_1 and P_2 are purely periodic functions of time with period T . They are in general functions oscillating around zero. The amplitude of the first term in (5.1) increases exponentially with time while the second term decreases exponentially. Therefore the first term will become dominant and the solution will approach a pure exponential evolution

$$a(t, \mathbf{x}) \simeq e^{H_{\mathbf{x}} t} P(t, \mathbf{x}), \quad (5.2)$$

where we have absorbed the constant c_1 into $P(t, \mathbf{x})$ by letting $P(t, \mathbf{x}) = c_1 P_1(t, \mathbf{x})$.

Physically, the exponential evolution of the amplitude of $a(t, \mathbf{x})$ is easy to understand. If Ω is strictly periodic, the system will finally reach a steady pattern of evolution (when the second term in (5.1) has been highly suppressed). In this pattern, after each period of evolution of the system, a increases by a fixed ratio, i.e. $a(t + T, \mathbf{x}) = \mu_{\mathbf{x}} a(t, \mathbf{x})$, which results in the exponential increase since after n cycles, $a(t + nT, \mathbf{x}) = \mu_{\mathbf{x}}^n a(t, \mathbf{x})$. Here the $\mu_{\mathbf{x}}$ is related to the $H_{\mathbf{x}}$ by $H_{\mathbf{x}} = \frac{\ln \mu_{\mathbf{x}}}{T}$.

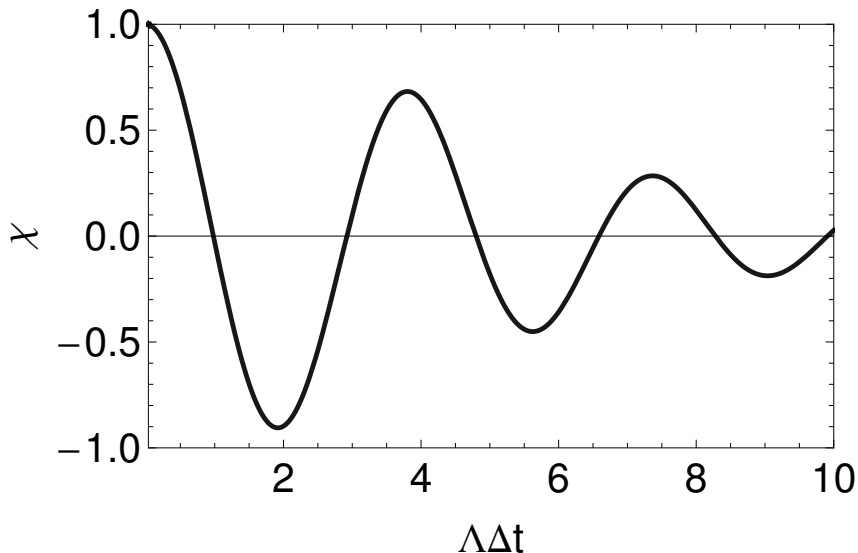


Figure 5.1: Plot of the normalized covariance χ as a function of temporal separation $\Lambda\Delta t$.

Due to the stochastic nature of quantum fluctuations, the $\Omega(t, \mathbf{x})$ in (4.19) is not strictly periodic. However, its behavior is still similar to a periodic function. In fact, Ω exhibits quasiperiodic behavior in the sense that it is always varying around its mean value back and forth on an approximately fixed time scale. To see this, we calculate the following normalized covariance:

$$\begin{aligned} \chi(\Delta t) &= \text{Cov}(\Omega^2(t_1, \mathbf{x}), \Omega^2(t_2, \mathbf{x})) \\ &= \frac{\langle \{(\Omega^2(t_1) - \langle \Omega^2(t_1) \rangle) (\Omega^2(t_2) - \langle \Omega^2(t_2) \rangle)\} \rangle}{\langle (\Omega^2 - \langle \Omega^2 \rangle)^2 \rangle}, \end{aligned} \quad (5.3)$$

where $\Delta t = t_1 - t_2$ and we have dropped the label \mathbf{x} in the second line of the above definition (5.3) since the final result is independent with \mathbf{x} .

Explicit expression for χ as a function of Δt is given by (A.12), which is plotted in FIG. 5.1. It describes how Ω^2 at different times change around their mean values together. We say that two Ω^2 separated by time difference Δt are positively (negatively) correlated if $\chi(\Delta t) > 0 (< 0)$, since it means that they are most likely to be at the same (opposite) side of their mean value $\langle \Omega^2 \rangle$.

5.1. Parametric resonance

FIG. 5.1 and (A.12) show that Ω^2 at different times are strongly correlated at close range. Especially, the negative correlation is strongest when $\Delta t \sim 2/\Lambda$, which implies that if at $t = 0$ the Ω^2 is above its mean value $\langle \Omega^2 \rangle$, then at $t \sim 2/\Lambda$, it is most likely below $\langle \Omega^2 \rangle$. So basically, Ω^2 varies around its mean value quasiperiodically on the time scale $T \sim 1/\Lambda$.

This quasiperiodic behavior of Ω should also lead to parametric resonance behavior seen in (5.2), instead with a difference in that $H_{\mathbf{x}}$ would become time dependent, i.e. the solution would take the following form

$$a(t, \mathbf{x}) \simeq e^{\int_0^t H_{\mathbf{x}}(t') dt'} P(t, \mathbf{x}), \quad (5.4)$$

where $P(t, \mathbf{x})$ here is no longer a strictly periodic function as in (5.2) but a quasiperiodic function with the same quasiperiod of the order $1/\Lambda$ as the time dependent frequency $\Omega(t, \mathbf{x})$. (The solution (5.8) for $P(t, \mathbf{x})$ in the next section 5.2 reveals this property.)

The physical mechanism is similar. The system will also reach a final steady evolution pattern. In this pattern, after each quasiperiod of evolution of the system, a will increase by an approximately fixed ratio. Suppose that during the i th cycle of quasiperiod T_i , a increases by a factor $\mu_{i\mathbf{x}}$, i.e. $a(t + T_i, \mathbf{x}) = \mu_{i\mathbf{x}} a(t, \mathbf{x})$. Then after the n cycles, we have $a(t + \sum_{i=1}^n T_i, \mathbf{x}) = \left(\prod_{i=1}^n \mu_{i\mathbf{x}} \right) a(t, \mathbf{x})$. Because the quasiperiods T_i and the factors $\mu_{i\mathbf{x}}$ are generally different from each other, the exponent in (5.4) would need to take the form of integration.

The detailed oscillating behavior of $P(t, \mathbf{x})$ is not observable at macroscopic scales. However, the factor of the exponential increase $e^{\int_0^t H_{\mathbf{x}}(t') dt'}$ can be observed. In fact, inserting (5.4) into (4.8), the observable physical distance would become

$$L(t) = L(0) e^{Ht}, \quad (5.5)$$

where

$$L(0) = \int_{\mathbf{x}_1}^{\mathbf{x}_2} \sqrt{P^2(t, \mathbf{x})} dl \quad (5.6)$$

and the global Hubble expansion rate H is

$$H = \frac{1}{t} \int_0^t H_{\mathbf{x}}(t') dt'. \quad (5.7)$$

In the next two sections, we are going to give the solution for $P(t, \mathbf{x})$ and the global Hubble expansion rate H .

5.2 The solution for $P(t, \mathbf{x})$

The magnitude of the time dependent frequency Ω is of the order $\sim \sqrt{G \langle T_{00} \rangle} \sim \sqrt{G} \Lambda^2$, while Ω itself varies roughly with a characteristic frequency Λ (this has been shown by FIG. 5.1). Then according to (4.19), the scale factor a would oscillate with a period that roughly goes as $T = 2\pi/\Omega \sim 1/\sqrt{G} \Lambda^2 \ll 1/\Lambda$, as $\Lambda \rightarrow \infty$, where $1/\Lambda$ is the time scale on which the Ω itself would change significantly.

So comparing to the oscillating period T of the scale factor a , the variation of Ω itself is very slow, although the time $1/\Lambda$ is already very short for large Λ . Therefore, during one period of the oscillation of a , Ω is almost constant since it has not have a chance to change significantly during such a short time scale. In this sense the time dependent frequency Ω is slowly varying and the evolution of the scale factor a is an adiabatic process.

The leading order solution of the equation (4.19) for a harmonic oscillator with the slowly varying frequency Ω can be obtained by a first order WKB approximation. This adiabatic approximation neglects the small exponential factor in (5.4). It gives the solution $P(t, \mathbf{x})$ which is describing the oscillating behavior of $a(t, \mathbf{x})$. The result is,

$$P(t, \mathbf{x}) = \frac{A_0}{\sqrt{\Omega(t, \mathbf{x})}} \cos \left(\int_0^t \Omega(t', \mathbf{x}) dt' + \theta_{\mathbf{x}} \right). \quad (5.8)$$

The $P(t, \mathbf{x})$ above is a quasiperiodic function with the same quasiperiod of the order $1/\Lambda$ as the time dependent frequency $\Omega(t, \mathbf{x})$ just as expected. The two constants of integration A_0 and $\theta_{\mathbf{x}}$ in (5.8) can be determined by the initial values $a(0, \mathbf{x})$ and $\dot{a}(0, \mathbf{x})$.

The quantum vacuum is fluctuating everywhere, but its statistical property must be still the same everywhere. Correspondingly, the statistical property of $P(t, \mathbf{x})$ must also be the same everywhere, which requires that the constant A_0 to be independent with respect to the spatial coordinate \mathbf{x} . In addition, the constant A_0 can be chosen as any nonzero value since the scale factor a multiplying by any nonzero constant describes physically equivalent spacetimes.

The initial phase $\theta_{\mathbf{x}}$ at different places must be dependent on \mathbf{x} . In applying the initial value constraint equation (4.13), neglecting the small exponential factor in (5.4) and neglecting the relatively small time derivative terms of the slowly varying frequency Ω , we obtain the result,

$$\tan \theta_{\mathbf{x}} = \frac{\Omega(0, \mathbf{x}_0)}{\Omega(0, \mathbf{x})} \tan \theta_{\mathbf{x}_0} + \frac{4\pi G}{\Omega(0, \mathbf{x})} \int_{\mathbf{x}_0}^{\mathbf{x}} \mathbf{J}(0, \mathbf{x}') \cdot d\mathbf{l}', \quad (5.9)$$

where $\theta_{\mathbf{x}_0}$ is the initial phase of the scale factor a at an arbitrary spatial point \mathbf{x}_0 .

In solutions (5.8) and (5.9) we see the fluctuating nature of spacetime at very small scales as described in the previous chapter 4.2. In particular, (5.9) shows that the phases of $a(t, \mathbf{x})$ vary on a given initial Cauchy slice; some locations contract while others expand. In this new physical picture the catastrophic vacuum energy density is confined to very small scales.

5.3 The global Hubble expansion rate H

As the system is adiabatic, the parametric resonance effect is weak. The adiabatic solution (5.8) in the last section does not include the parametric resonance and thus misses the small exponential factor expected in (5.4). In this section we go beyond the adiabatic approximation and investigate the exact strength of the weak parametric resonance.

When considering the weak parametric resonance effect, the constant A_0 in (5.8) would become time and space dependent and take the following form

$$A(t, \mathbf{x}) = A_0 e^{\int_0^t H_{\mathbf{x}}(t') dt'} \quad (5.10)$$

in order to satisfy (5.4).

To determine how the $H_{\mathbf{x}}(t)$ depends on the spacetime dependent frequency $\Omega(t, \mathbf{x})$, we consider the adiabatic invariant of a harmonic oscillator with time dependent frequency, which is defined as

$$I(t, \mathbf{x}) = \frac{E}{\Omega}, \quad (5.11)$$

where

$$E = \frac{1}{2}(\dot{a}^2 + \Omega^2 a^2). \quad (5.12)$$

Replace the constant A_0 in (5.8) by $A(t, \mathbf{x})$ and then plug it into the above expression (5.11) we get that

$$I(t, \mathbf{x}) = \frac{1}{2} A^2(t, \mathbf{x}), \quad (5.13)$$

where we have neglected the time derivatives of A and Ω in the above equation (5.13), which are higher order infinitesimals. I is invariant in the first order adiabatic approximation. When going to higher orders, I will slowly change with time. Through the relation (5.13) between I and A we can obtain how the $A(t, \mathbf{x})$ changes by investigating how accurately the adiabatic invariant is preserved and how it changes with time.

5.3. The global Hubble expansion rate H

It has been proved by Robnik and Romanovski [22, 23] that, in full generality (no restrictions on the function $\Omega(t, \mathbf{x})$), the final value of the adiabatic invariant for the average energy $\bar{I} = \bar{E}/\Omega$ is always greater or equal to the initial value $I_0 = E_0/\Omega_0$ (see the references [22, 23] for precise definition about the average energy). In other words, the average value of the adiabatic invariant $\bar{I} = \bar{E}/\Omega$ for the mean value of the energy never decreases, which is a kind of irreversibility statement. It is conserved only for infinitely slow process, i.e. an ideal adiabatic process.

Therefore, in the case of our quasiperiodic frequency $\Omega(t, \mathbf{x})$ in (4.19), \bar{I} will also always increase. Moreover, it will increase by a fixed factor after each quasiperiod of evolution, which results in an exponentially increasing \bar{I} . This is in fact evident because of the weak parametric resonance effect. In the following we investigate this exponential behavior in detail.

First we construct the evolution equation for the adiabatic invariant I . Do the canonical transformation

$$a = \sqrt{2I/\Omega} \sin \varphi, \quad (5.14)$$

$$\dot{a} = \sqrt{2I\Omega} \cos \varphi. \quad (5.15)$$

Then the evolution equations for a and its conjugate momentum \dot{a} transfer to the evolution equation for the new action variable I and the angle variable φ ,

$$\frac{dI}{dt} = -I \frac{\dot{\Omega}}{\Omega} \cos 2\varphi, \quad (5.16)$$

$$\frac{d\varphi}{dt} = \Omega + \frac{\dot{\Omega}}{2\Omega} \sin 2\varphi. \quad (5.17)$$

Integrating (5.16) yields

$$I(t) = I(0) \exp \left(2 \int_0^t H_{\mathbf{x}}(t') dt' \right), \quad (5.18)$$

where

$$H_{\mathbf{x}}(t') = -\frac{\dot{\Omega}}{2\Omega} \cos 2\varphi. \quad (5.19)$$

The $H_{\mathbf{x}}(t')$ in the above equation (5.19) is just the same with the $H_{\mathbf{x}}(t')$ defined in (5.4) and (5.10), which can be seen by applying equation (5.13). Thus equation (5.19) constructed the dependence of $H_{\mathbf{x}}(t')$ on the time dependent frequency $\Omega(t', \mathbf{x})$.

5.3. The global Hubble expansion rate H

The observable global Hubble expansion rate H is the average of $H_{\mathbf{x}}(t')$ over time, which was defined by equation (5.7). Plugging (5.19) into (5.7) gives,

$$H = \text{Re} \left(-\frac{1}{t} \int_0^t \frac{\dot{\Omega}}{2\Omega} e^{2i\varphi} dt' \right). \quad (5.20)$$

When the slow varying condition (5.35) holds, from equation (5.17) we know that $d\varphi/dt$ is positive, i.e. φ is a monotonic function in time. Thus we can change the integral in (5.20) from the integration over t' to integration over φ' :

$$H = \text{Re} \left(-\frac{1}{t} \int_{\varphi_0}^{\varphi} \frac{\dot{\Omega}}{2\Omega} e^{2i\varphi} \frac{dt'}{d\varphi'} d\varphi' \right), \quad (5.21)$$

where $\varphi_0 = \varphi(0)$ and $\varphi = \varphi(t)$.

To evaluate H , we formally treat φ as a complex variable and close the contour integral in the upper half plane. The integrand in (5.21) has no singularities for real φ if the slow varying condition (5.35) holds. Equation (5.17) implies that $\varphi \sim \Omega t \sim \sqrt{G}\Lambda^2 t$, so the length of the interval $\varphi - \varphi_0 \sim \sqrt{G}\Lambda^2 t$ goes to infinity as $\Lambda \rightarrow +\infty$. Hence the principle contribution to the integral in (5.21) comes from the residue values at singularities $\varphi_{(k)}$ inside the contour:

$$H = \frac{1}{t} \text{Re} \left(2\pi i \sum_k \text{Res} \left(-\frac{\dot{\Omega}}{2\Omega} e^{2i\varphi} \frac{dt}{d\varphi}, \varphi_{(k)} \right) \right). \quad (5.22)$$

Each term in (5.22) gives a contribution containing a factor $\exp(-2 \text{Im} \varphi_{(k)})$. So the dominant contribution in (5.22) comes from the singularities near the real axis, i.e. those with the smallest positive imaginary part. To keep the calculation simple, we retain only those terms. Since $\Omega(t)$ varies quasiperiodically with a characteristic time $\tau \sim 1/\Lambda$, the number of singularities near the real axis would roughly be on the order $t/\tau \sim \Lambda t$. Therefore the H in (5.22) is roughly

$$H \sim \Lambda \exp(-2 \text{Im} \varphi_{(k)}). \quad (5.23)$$

Let $t_{(k)}$ be the (complex) ‘‘instant’’ corresponding to the singularity $\varphi_{(k)}$: $\varphi_{(k)} = \varphi(t_{(k)}) \sim \Omega t_{(k)}$. In general, $|t_{(k)}|$ has the same order of magnitude as the characteristic time $\tau \sim 1/\Lambda$ of variation of the Ω . Remember that $\Omega \sim \sqrt{G}\Lambda^2$, thus the order of magnitude of the exponent in (5.23) is

$$\text{Im} \varphi_{(k)} \sim \Omega \tau \sim \sqrt{G}\Lambda. \quad (5.24)$$

5.4. A more intuitive explanation

Therefore, inserting (5.24) into (5.23) gives

$$H = \alpha \Lambda e^{-\beta \sqrt{G} \Lambda}, \quad (5.25)$$

where α and β are two dimensionless constants which depend on the variation details of the time dependent frequency $\Omega(t, \mathbf{x})$. Therefore H becomes exponentially small in the limit of taking Λ to infinity. This is a manifestation of the well-established result that the error in adiabatic invariant is exponentially small for analytic Ω [22, 24]. In fact, the technique we used in deriving (5.25) is very similar to the one used in deriving the error in adiabatic invariant in the pages “160 – 161” of [24].

5.4 A more intuitive explanation

So far we have obtained our key result (5.25) for the global Hubble expansion rate H . To understand the mechanism of weak parametric resonance better, we give a more intuitive explanation in this section.

Consider the following simplest parametric oscillator:

$$\ddot{x} + \omega^2(t)x = 0, \quad (5.26)$$

where

$$\omega^2(t) = \omega_0^2 (1 + h \cos \gamma t). \quad (5.27)$$

The behavior of the above harmonic oscillator with time dependent frequency has been thoroughly studied (see e.g. eq(27.7) in Chapter V of [21]). The parametric resonance occurs when the frequency γ with which $\omega(t)$ varies is close to any value $2\omega_0/n$, i.e.

$$\gamma \sim \frac{2\omega_0}{n}, \quad (5.28)$$

where n is an integer. The strength of the parametric resonance is strongest if γ is nearly twice ω_0 , i.e. if $n = 1$. As n increases to infinity, the strength of the parametric resonance decreases to zero. This is easy to understand since as n increases, the varying frequency γ of $\omega(t)$ becomes slower compared to the oscillator’s natural frequency ω_0 and as $n \rightarrow \infty$, (5.26) reduces to an ordinary harmonic oscillator with constant frequency which has no parametric resonance behavior.

Now let us go back to Eq.(4.19) for $a(t, \mathbf{x})$. The time dependent frequency $\Omega(t, \mathbf{x})$ in (4.19) is more complicated than the $\omega(t)$ given in our

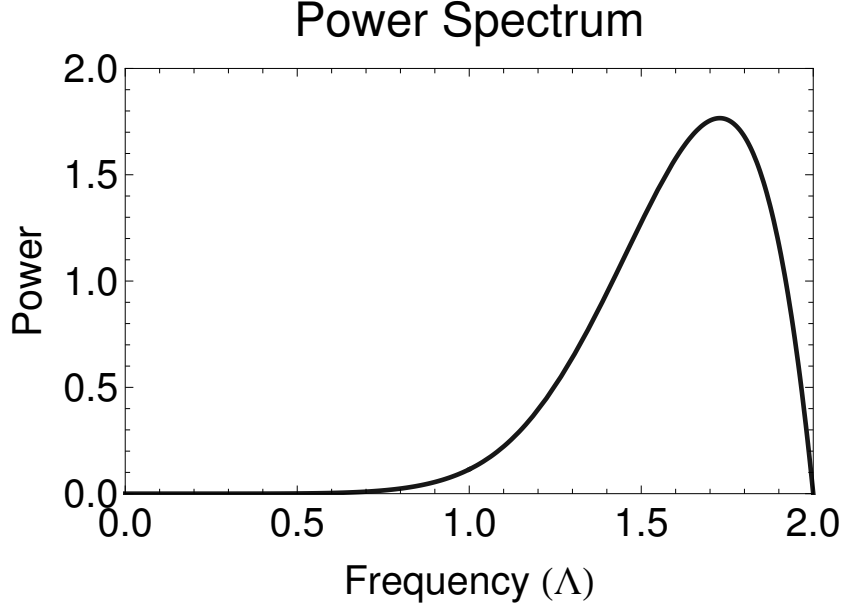


Figure 5.2: Plot of the power spectrum density of the varying part of $\Omega^2(t, \mathbf{0})$ (except for the constant Ω_0^2 part).

example (5.27). However, it can be written in a similar form:

$$\Omega^2(t, \mathbf{0}) = \Omega_0^2 \left(1 + \int_0^{2\Lambda} d\gamma (f(\gamma) \cos \gamma t + g(\gamma) \sin \gamma t) \right), \quad (5.29)$$

where

$$\Omega_0^2 = \langle \Omega^2 \rangle = \frac{G\Lambda^4}{6\pi}, \quad (5.30)$$

and $f(\gamma)$, $g(\gamma)$ are operator coefficients, whose exact form are given by (A.15) and (A.16) in Appendix A. The behavior of $\Omega^2(t, \mathbf{x})$ for an arbitrary \mathbf{x} is the same with $\Omega^2(t, \mathbf{0})$ except phase differences. The power spectrum density of the varying part of $\Omega^2(t, \mathbf{0})$ (except for the constant Ω_0^2 part) given by (A.18) is plotted in FIG. 5.2.

Unlike the case (5.27) where the $\omega(t)$ varies with a single frequency γ , the $\Omega(t, \mathbf{0})$ in (5.29) varies with frequencies continuously distributed in the range $(0, 2\Lambda)$ with a peak around 1.7Λ (see FIG. 5.2). From (5.30) we have that, as taking the cutoff frequency Λ to infinity, $\Omega_0 \sim \sqrt{G}\Lambda^2 \gg 2\Lambda$. Because of the continuity of the spectrum of Ω , we can always find integers n such that

if

$$n \geq \sqrt{\frac{G}{6\pi}}\Lambda, \quad \Lambda \rightarrow +\infty, \quad (5.31)$$

then

$$\frac{2\Omega_0}{n} \in (0, 2\Lambda). \quad (5.32)$$

So $\Omega(t, \mathbf{x})$ always contains frequencies $2\Omega_0/n$ that may excite resonances. From (5.31) we see that $n \rightarrow \infty$ as taking the cutoff Λ to infinity. While as n increases, the relative magnitude of the resonance frequency $2\Omega_0/n$ decreases comparing to the $a(t, \mathbf{x})$'s natural frequency Ω_0 . Then for reasons similar to the simplest parametric oscillator (5.26), the strength of the parametric resonance of (4.19) would also decrease to zero. This weak parametric resonance effect leads to the global Hubble expansion rate

$$H \rightarrow 0, \quad \text{as } \Lambda \rightarrow +\infty. \quad (5.33)$$

5.5 Meaning of our results

It is interesting to notice that both (2.13) and (5.5) give the exponential evolution and predict an accelerated expanding Universe. However, the underlying mechanisms are completely different, which leads to opposite results on the predicted magnitude of the observable Hubble expansion rate H .

The solution (2.13) is based on the assumption that quantum vacuum energy density is constant all over the spacetime, which is a necessary requirement if one suppose that vacuum acts as a cosmological constant. This assumption leads to a huge Hubble expansion rate

$$H = \sqrt{\frac{8\pi G\rho^{vac}}{3}} \propto \sqrt{G}\Lambda^2 \rightarrow +\infty \quad (5.34)$$

as taking the high energy cutoff Λ to infinity.

Our proposal (5.5) is based on the fact that quantum vacuum energy density is constantly fluctuating and extremely inhomogeneous all over the whole spacetime. This fact leads to a small Hubble expansion rate given by (5.25) which goes to zero as taking the high energy cutoff Λ to infinity.

If we can literally take the cutoff Λ in (5.25) to infinity, then $H = 0$. In this sense, at least the ‘‘old’’ cosmological constant problem would be resolved.

In principle, this effective theory is valid only up to a large but finite cutoff Λ , which leads to a tiny but nonzero H . Since $H \rightarrow 0$ as $\Lambda \rightarrow +\infty$,

there always exists a very large cutoff value of Λ such that $H = \sqrt{\Omega_\lambda} H_0 \approx 1.2 \times 10^{-42} \text{ GeV}$ to match the observation, where H_0 is current observed Hubble constant.

So our result suggests that there is no necessity to introduce the cosmological constant, which is required to be fine tuned to an accuracy of 10^{-120} , or other forms of dark energy, which are required to have peculiar negative pressure, to explain the observed accelerating expansion of the Universe.

The exact value of Λ cannot be determined since we do not know the values of the two dimensionless parameters α and β in (5.25). In principle, we need the knowledge of all fundamental fields in the Universe to determine α and β , this deserves further investigations in the future and might provide some hint on elementary particle physics.

We will use a couple of scalar fields to estimate the order of magnitude of the parameters α and β in the numerical simulation presented in section 5.7.

5.6 The slow varying condition

The key requirement for our derivation of (5.25) to work is that Ω^2 is slowly varying that the whole process is adiabatic. The mathematical description of the slow varying condition is (see equation (49.1) in Chapter VII of [24])

$$\Delta\Omega \sim T d\Omega/dt \ll \Omega, \quad (5.35)$$

where $T \sim 2\pi/\Omega$ is the period of the oscillation of a . Then the above condition can be rewritten as

$$\frac{\dot{\Omega}}{\Omega^2} \ll 1. \quad (5.36)$$

If there is only one scalar field we have $\Omega^2 = \frac{8\pi G}{3} \dot{\phi}^2$ and $\left(\frac{d\Omega}{dt}\right)^2 = \frac{8\pi G}{3} \ddot{\phi}^2$. Using (3.1), we have the expectation values

$$\begin{aligned} \langle \Omega^2 \rangle &= \frac{8\pi G}{3} \frac{1}{(2\pi)^3} \int d^3k \frac{1}{2} \omega \\ &= \frac{8\pi G}{3} \frac{1}{4\pi^2} \int_0^\Lambda k^3 dk = \frac{1}{6\pi} G \Lambda^4, \end{aligned} \quad (5.37)$$

$$\begin{aligned} \left\langle \left(\frac{d\Omega}{dt} \right)^2 \right\rangle &= \frac{8\pi G}{3} \frac{1}{(2\pi)^3} \int d^3k \frac{1}{2} \omega^3 \\ &= \frac{8\pi G}{3} \frac{1}{4\pi^2} \int_0^\Lambda k^5 dk = \frac{1}{9\pi} G \Lambda^6. \end{aligned} \quad (5.38)$$

5.6. The slow varying condition

(5.37) just gives $\langle \Omega^2 \rangle \sim G\Lambda^4$ as expected, (5.38) gives $\langle d\Omega/dt \rangle \sim \sqrt{G}\Lambda^3$, therefore, we would have

$$\frac{\langle \dot{\Omega} \rangle}{\langle \Omega^2 \rangle} \sim \frac{\sqrt{G}\Lambda^3}{G\Lambda^4} = \frac{1}{\sqrt{G}\Lambda} \ll 1, \quad \text{as } \Lambda \rightarrow +\infty, \quad (5.39)$$

i.e. the slow varying condition (5.35) is satisfied on average for one scalar field.

However, the quantum fluctuation of Ω^2 is as big as its expectation value, so there is still possibility that $\Omega^2 = 8\pi G\dot{\phi}^2/3$ fluctuates to values smaller than $\sqrt{G}\Lambda^3$ or even close to 0 where the slow varying condition (5.35) is not satisfied. These extreme points have large contribution to the growth of the amplitude of a and destroy the key result $H = \alpha\Lambda e^{-\beta\sqrt{G}\Lambda}$ as $\Lambda \rightarrow +\infty$ (Eq.(5.25)).

To resolve this problem, one has to make sure Ω always satisfy (5.35) (or at least the probability of violating (5.35) is low enough). This can be done in two ways: i) increase the number of fields or ii) add a small negative bare cosmological constant in the Einstein equations. We will discuss this two solutions in the following.

I). Adding more fields

The real Universe contains many different quantum fields. From central limit theorem, when more fields are added, the probability distribution for Ω^2 would approach Gaussian. Moreover, the magnitude of the fluctuation of Ω^2 would become relatively smaller compared to its expectation value. In fact, if we have n fields, the expectation value of Ω^2 goes as $nG\Lambda^4$ while the magnitude of the fluctuation (standard deviation of Ω^2) goes as $\sqrt{n}G\Lambda^4$. Therefore the probability for Ω^2 to fluctuate to values smaller than $\sqrt{G}\Lambda^3$ goes to zero as the number of fields n go to infinity, i.e. the probability for Ω^2 violating (5.35) becomes vanishingly small.

In addition, when more fields are added, the expectation value of Ω^2 grows but the time scale of the variation of Ω^2 stay the same, this makes the variation of Ω^2 becomes even slower for the same cutoff Λ . So the cutoff needed to match the observed rate of accelerating expansion is reduced.

II). Adding a small cosmological constant

When a bare cosmological constant λ_b is included, Ω^2 becomes

$$\Omega^2 = \frac{4\pi G}{3} \left(\rho + \sum_{i=1}^3 P_i \right) - \frac{\lambda_b}{3}, \quad \rho = T_{00}, P_i = \frac{1}{a^2} T_{ii}. \quad (5.40)$$

If $-\lambda_b$ is greater than $\sqrt{G}\Lambda^3$, then the slow varying condition (5.36) will

always be satisfied. This can reduce the number of fields needed to achieve our key result (5.25).

5.7 Numerical verification

In this section, Planck units will be used, so all instances of Newton's constant are set to unity, $G = 1$.

The main idea is to rewrite the time dependent frequency $\Omega(t)$ in phase space. (To see more details about this numeric method, please check Appendix B. Here we only list the most crucial results.) For a real massless scalar field, we have

$$\begin{aligned} \Omega^2(\{x_{\mathbf{k}}\}, \{p_{\mathbf{k}}\}, t) &= \frac{8\pi}{3} \int \frac{d^3k d^3k'}{(2\pi)^3} x_{\mathbf{k}} x_{\mathbf{k}'} \omega \omega' \sin \omega t \sin \omega' t \\ &+ p_{\mathbf{k}} p_{\mathbf{k}'} \cos \omega t \cos \omega' t - 2x_{\mathbf{k}} p_{\mathbf{k}'} \omega \sin \omega t \cos \omega' t. \end{aligned} \quad (5.41)$$

This is the Weyl transformation of the operator $\hat{\Omega}^2(t)$. Here $\{x_{\mathbf{k}}, p_{\mathbf{k}}\}$ are phase space points of a particular field mode with momentum \mathbf{k} . Approximately, for a particular choice of $\{x_{\mathbf{k}}\}, \{p_{\mathbf{k}}\}$, we can get an classic equation for a :

$$\ddot{a}(\{x_{\mathbf{k}}\}, \{p_{\mathbf{k}}\}, t) + \Omega^2(\{x_{\mathbf{k}}\}, \{p_{\mathbf{k}}\}, t) a(\{x_{\mathbf{k}}\}, \{p_{\mathbf{k}}\}, t) = 0 \quad (5.42)$$

The observed value $a_o(t)$ is the average of $a(\{x_{\mathbf{k}}\}, \{p_{\mathbf{k}}\}, t)$ over the Wigner pseudo distribution function $W(\{x_{\mathbf{k}}\}, \{p_{\mathbf{k}}\}, t)$, which is based on the wave function of the quantum field:

$$a_o(t) = \int \left(\prod_{\mathbf{k}} dx_{\mathbf{k}} dp_{\mathbf{k}} \right) a(\{x_{\mathbf{k}}\}, \{p_{\mathbf{k}}\}, t) W(\{x_{\mathbf{k}}\}, \{p_{\mathbf{k}}\}, t). \quad (5.43)$$

If the quantum field is in its ground state, we have

$$W(\{x_{\mathbf{k}}\}, \{p_{\mathbf{k}}\}, t) = \prod_{\mathbf{k}} \frac{1}{\pi} e^{-\frac{p_{\mathbf{k}}^2}{\omega} - x_{\mathbf{k}}^2 \omega} \quad (5.44)$$

which means $\{x_{\mathbf{k}}\}, \{p_{\mathbf{k}}\}$ are all Gaussian variables. Based on this observation, our method to simulate this equation is as following: i) at first we generate a set of random Gaussian numbers for $\{x_{\mathbf{k}}\}, \{p_{\mathbf{k}}\}$; ii) we solve the equation (5.42) for this particular set of numbers; iii) then we repeat the process for another set of random numbers until a certain amount of repetitions; iv) The result $a_o(t)$ is the average over all samples we have generated.

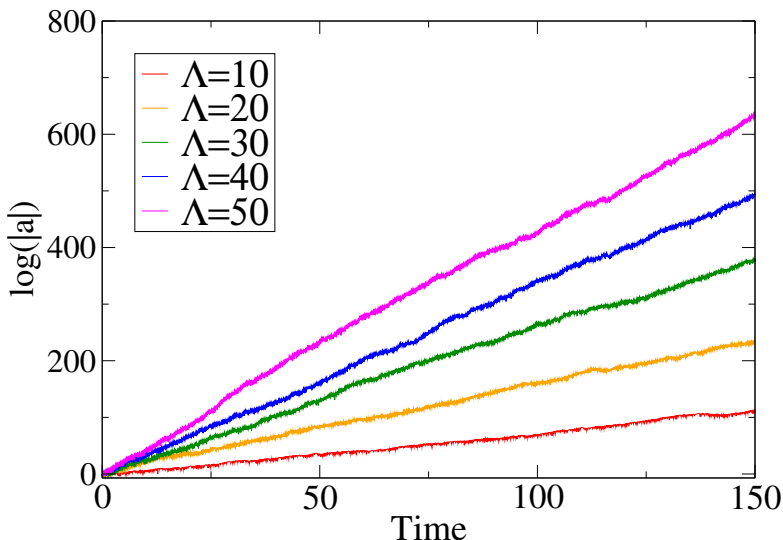


Figure 5.3: Numeric result for $\log |a_o(t)|$ when one scalar field is present. The slope represents the Hubble expansion rate H . It shows that as Λ increases, H also increases. The prediction (5.25) is not applicable in this case since the slow varying condition is violated when Ω^2 fluctuates to values smaller than $\sim \Lambda^3$.

Fig. 5.3 is the result for only one scalar field contributing to Ω^2 . The slope represents the Hubble expansion rate H . It shows that as Λ increases, H also increases. The prediction (5.25) is not applicable in this case since the probability for the slow varying condition (when Ω^2 fluctuates to values smaller than $\sim \Lambda^3$) can not be neglected as explained in the last section.

Fig. 5.4 is the result for one scalar field with a negative bare cosmological constant $-\lambda_b \sim \Lambda^{3.5}$ contributing to Ω^2 . It shows that as Λ increases, H decreases. The linear fit $\log(H/\Lambda)$ vs Λ gives the parameter $\alpha \sim e^{-4.1} \approx 0.017$, $\beta \sim 0.072$. In this case, the prediction (5.25) is observed since λ_b makes Ω^2 always greater than Λ^3 and has it be adiabatic.

Fig. 5.5 is the result for five scalar fields with and without a bare cosmological constant $-\lambda_b \sim \Lambda^{3.5}$ contributing to Ω^2 . In both cases as Λ increases, H decreases and the prediction (5.25) is observed. The linear fit gives the parameters $\alpha \sim e^{-3.8} \approx 0.022$, $\beta \sim 0.14$ for the case without the bare cosmological constant and the parameters $\alpha \sim e^{-4.2} \approx 0.015$, $\beta \sim 0.28$ for the case with the bare cosmological constant.

Fig. 5.6 is the result for ten scalar fields with and without a bare cosmological constant $-\lambda_b \sim \Lambda^{3.5}$ contributing to Ω^2 . In both cases as Λ increases,

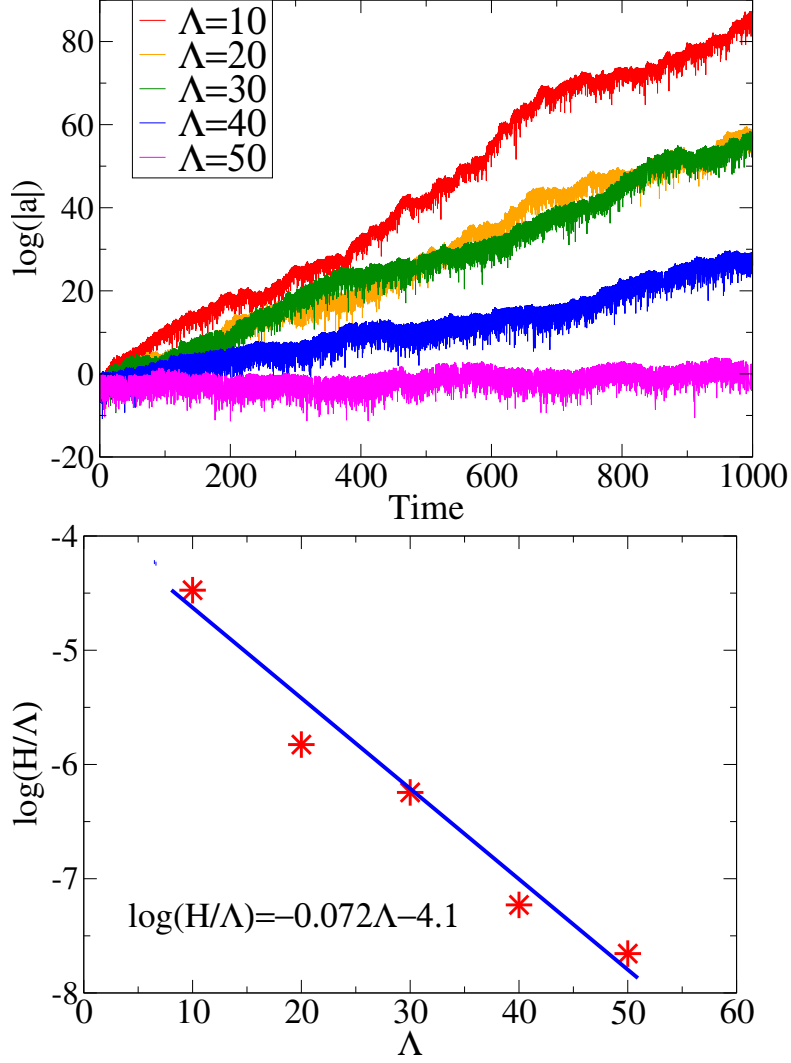


Figure 5.4: Numeric result for $\log |a_o(t)|$ when one scalar field with a negative bare cosmological constant $-\lambda_b \sim \Lambda^{3.5}$ are present. The slope represents the Hubble expansion rate H . It shows that as Λ increases, H decreases. The linear fit $\log(H/\Lambda)$ vs Λ gives the parameter $\alpha \sim e^{-4.1} \approx 0.017$, $\beta \sim 0.072$.

5.7. Numerical verification

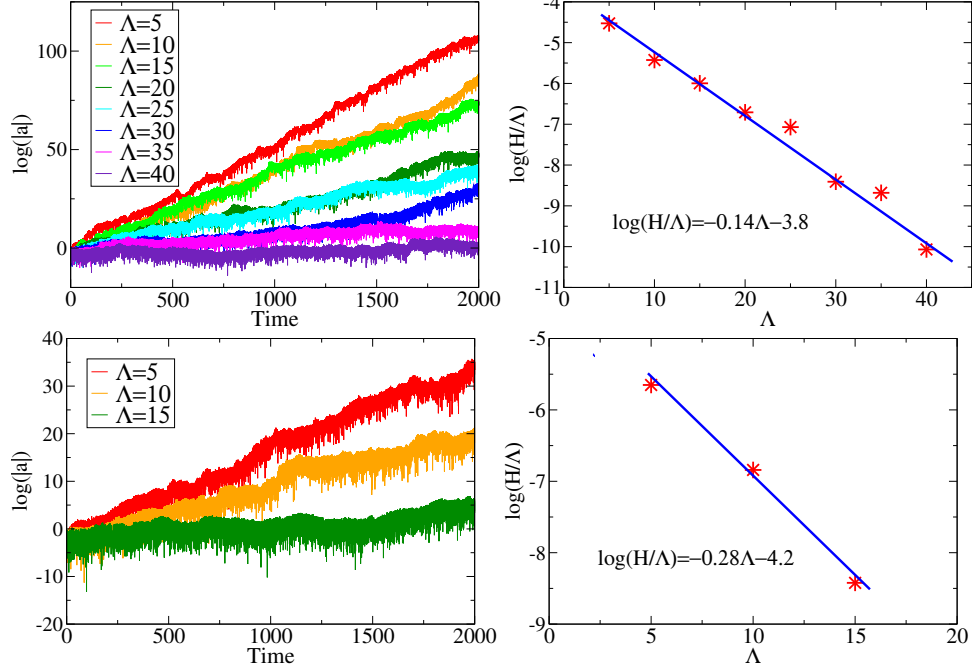


Figure 5.5: Top: numeric result for five scalar fields without a bare cosmological constant and its linear fit $\log(H/\Lambda)$ vs Λ ; Bottom: five scalar fields with a negative bare cosmological constant $-\lambda_b \sim \Lambda^{3.5}$ and its linear fit $\log(H/\Lambda)$ vs Λ . The slope represents the Hubble expansion rate H . In both cases as Λ increases, H decreases. The linear fit gives the parameters $\alpha \sim e^{-3.8} \approx 0.022$, $\beta \sim 0.14$ for five scalar fields without the bare cosmological constant and the parameters $\alpha \sim e^{-4.2} \approx 0.015$, $\beta \sim 0.28$ for five scalar fields with the bare cosmological constant.

5.7. Numerical verification

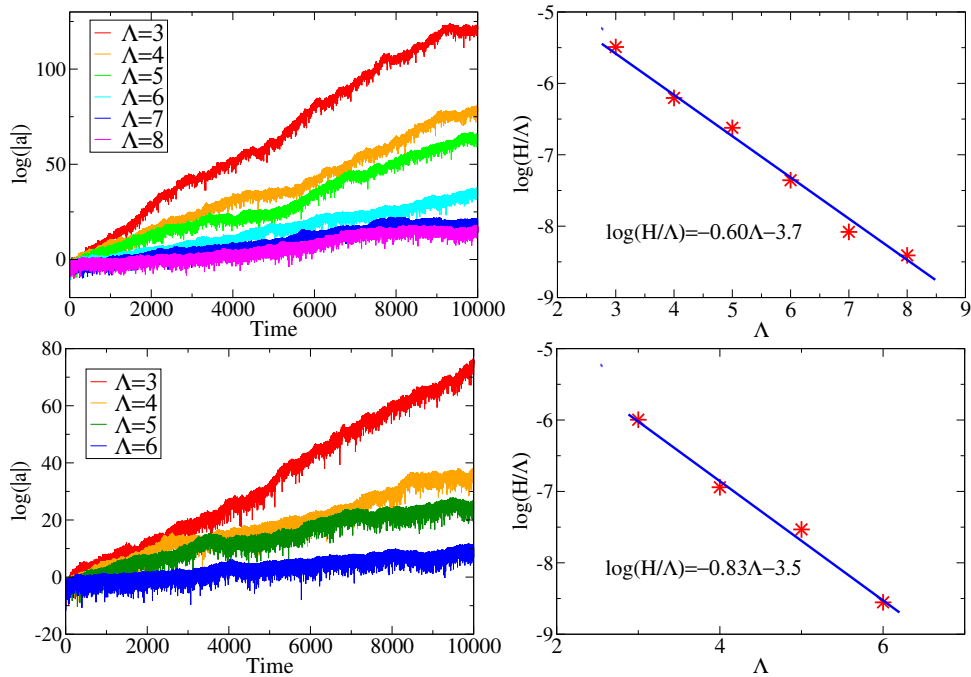


Figure 5.6: Top: numeric result for ten scalar fields without a bare cosmological constant and its linear fit $\log(H/\Lambda)$ vs Λ ; Bottom: ten scalar fields with a negative bare cosmological constant $-\lambda_b \sim \Lambda^{3.5}$ and its linear fit $\log(H/\Lambda)$ vs Λ . The slope represents the Hubble expansion rate H . In both cases as Λ increases, H decreases. The linear fit gives the parameters $\alpha \sim e^{-3.7} \approx 0.025$, $\beta \sim 0.6$ for ten scalar fields without the bare cosmological constant and the parameters $\alpha \sim e^{-3.5} \approx 0.03$, $\beta \sim 0.83$ for ten scalar fields with the bare cosmological constant.

H decreases and the prediction (5.25) is observed. The linear fit gives the parameters $\alpha \sim e^{-3.7} \approx 0.025$, $\beta \sim 0.6$ for the case without the bare cosmological constant and the parameters $\alpha \sim e^{-3.5} \approx 0.03$, $\beta \sim 0.83$ for the case with the bare cosmological constant.

Fig. 5.7 is the result for twenty scalar fields with and without a bare cosmological constant $-\lambda_b \sim \Lambda^{3.5}$ contributing to Ω^2 . In both cases as Λ increases, H decreases and the prediction (5.25) is observed. The linear fit gives the parameters $\alpha \sim e^{-2.6} \approx 0.074$, $\beta \sim 1.9$ for the case without the bare cosmological constant and the parameters $\alpha \sim e^{-2.1} \approx 0.12$, $\beta \sim 2.4$ for the case with the bare cosmological constant.

We can see from Fig. 5.5, 5.6 and 5.7 that as more fields are added, the

5.7. Numerical verification

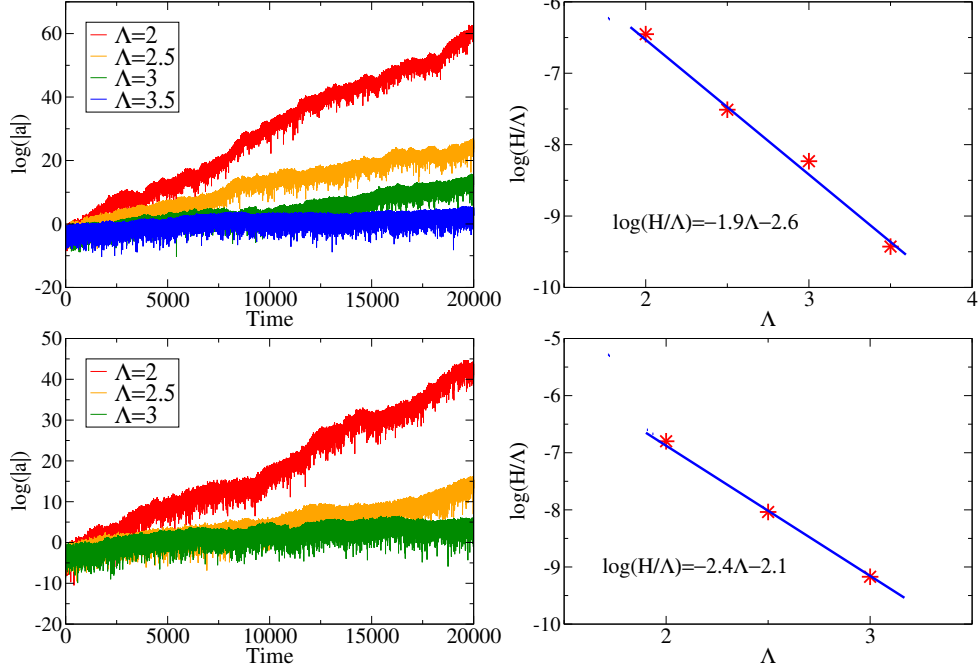


Figure 5.7: Top: numeric result for twenty scalar fields without a bare cosmological constant and its linear fit $\log(H/\Lambda)$ vs Λ ; Bottom: twenty scalar fields with a negative bare cosmological constant $-\lambda_b \sim \Lambda^{3.5}$ and its linear fit $\log(H/\Lambda)$ vs Λ . The slope represents the Hubble expansion rate H . In both cases as Λ increases, H decreases. The linear fit gives the parameters $\alpha \sim e^{-2.6} \approx 0.074$, $\beta \sim 1.9$ for twenty scalar fields without the bare cosmological constant and the parameters $\alpha \sim e^{-2.1} \approx 0.12$, $\beta \sim 2.4$ for twenty scalar fields with the bare cosmological constant.

5.7. Numerical verification

fitting parameter β increases, which implies that the parametric resonance effect becomes weaker and the cutoff needed to match the observation is reduced. The observed H is on the order of $10^{-61} \sim e^{-140}$, so for five fields the cutoff needed is about $\Lambda \sim 140/\beta \sim 140/0.14 \sim 1000$, for ten fields the cutoff needed is about $\Lambda \sim 140/\beta \sim 140/0.6 \sim 230$, for twenty fields the cutoff needed is about $\Lambda \sim 140/\beta \sim 140/1.9 \sim 74$.

If we also add a negative bare cosmological constant, the cutoff needed would be further reduced. For a bare cosmological constant on the order of $-\lambda_b \sim \Lambda^{3.5}$, the cutoffs needed are $\Lambda \sim 140/\beta \sim 140/0.28 \sim 500$ for five fields, $\Lambda \sim 140/\beta \sim 140/0.83 \sim 168$ for ten fields $\Lambda \sim 140/\beta \sim 140/2.4 \sim 58$ for twenty fields.

Chapter 6

The back reaction

In this chapter, we investigate the back reaction effect by quantizing the field ϕ in the resulting curved spacetime to justify our method of using the quantized field expansion (3.1) in Minkowski spacetime as an approximation.

The standard way to quantize the scalar field ϕ in a generic curved spacetime $g_{\mu\nu}$ is by first defining the following inner product on a spacelike hypersurface Σ with induced metric h_{ij} and unit normal vector n^μ (see e.g. [16, 25]):

$$(\phi_1, \phi_2) = -i \int_{\Sigma} (\phi_1 \partial_\mu \phi_2^* - \phi_2^* \partial_\mu \phi_1) n^\mu \sqrt{h} d^3x, \quad (6.1)$$

where $h = \det h_{ij}$ and ϕ_1, ϕ_2 are solutions to the equation (4.25). The above inner product is independent of the choice of Σ .

One then choose a complete set of mode solutions $u_{\mathbf{k}}$ of (4.25) which are orthonormal in the product (6.1):

$$(u_{\mathbf{k}}, u_{\mathbf{k}'}) = \delta(\mathbf{k} - \mathbf{k}'), \quad (6.2)$$

$$(u_{\mathbf{k}}^*, u_{\mathbf{k}'}^*) = -\delta(\mathbf{k} - \mathbf{k}'), \quad (6.3)$$

$$(u_{\mathbf{k}}, u_{\mathbf{k}'}^*) = 0. \quad (6.4)$$

Then the field ϕ may be expanded as

$$\phi = \sum_{\mathbf{k}} \left(a_{\mathbf{k}} u_{\mathbf{k}} + a_{\mathbf{k}}^\dagger u_{\mathbf{k}}^* \right). \quad (6.5)$$

For the flat Minkowski spacetime, i.e. $g_{\mu\nu} = \eta_{\mu\nu}$, (4.25) reduces to the usual wave equation

$$\ddot{\phi} - \nabla^2 \phi = 0. \quad (6.6)$$

In this case, the mode solutions are usually chosen as

$$u_{\mathbf{k}}(t, \mathbf{x}) = \frac{1}{(2\pi)^{3/2}} \frac{1}{\sqrt{2\omega}} e^{-i(\omega t - \mathbf{k} \cdot \mathbf{x})}, \quad (6.7)$$

where $\omega = |\mathbf{k}|$. Plugging (6.7) into (6.5) just gives the usual quantum field expansion (3.1).

For our specific metric (4.1), (4.25) reduces to (4.26). In this case, since the rate of accelerating expansion is extremely small, the back reaction effect due to the macroscopic expansion of the Universe is only important on large cosmological time scales. For this reason, we only worry about the back reaction due to the wildly fluctuating spacetime at small scales. i.e. we neglect the small exponential factor in (5.4) and use the form of the a based on the solution (5.8):

$$a(t, \mathbf{x}) = \frac{A_0}{\sqrt{\Omega(t, \mathbf{x})}} \cos(\Theta(t, \mathbf{x})), \quad (6.8)$$

where

$$\Theta(t, \mathbf{x}) = \int_0^t \Omega(t', \mathbf{x}) dt' + \theta_{\mathbf{x}}. \quad (6.9)$$

Then (4.26) becomes

$$\begin{aligned} & \frac{A_0^2}{\Omega} \cos^2 \Theta \ddot{\phi} - \nabla^2 \phi \\ & - \frac{3A_0^2}{2} \left(\frac{\dot{\Omega}}{\Omega^2} \cos^2 \Theta + \sin 2\Theta \right) \dot{\phi} + \left(\frac{\nabla \Omega}{2\Omega} + \tan \Theta \nabla \Theta \right) \cdot \nabla \phi = 0. \end{aligned} \quad (6.10)$$

In order to understand the effect from back reaction, we need to find out how the mode solutions of the above equation (6.10) in the resulting curved spacetime change from the mode solutions (6.7) of the equation (6.6) in the flat Minkowski spacetime.

Physically, the correction to (6.7) should be small for wave modes with frequencies lower than the cutoff frequency Λ . That is because the wave length of those field modes is larger than $2\pi/\Lambda$, while our spacetime fluctuates on the length scale $2\pi/\Omega \sim 1/(\sqrt{G}\Lambda^2) \ll 2\pi/\Lambda$. The relatively long wave length modes should not be sensitive to what is happening on small scales. This is analogous to the situation of sound waves traveling in the medium such as air or water or solids. The medium is constantly fluctuating at atomic scales, but this fluctuation does not affect the propagation of the sound wave whose wavelength is much larger than the atomic scale. Similarly, the propagation of the field modes in the “medium”—the spacetime, which is constantly fluctuating on scales much smaller than the wavelength of the field modes, should also not be affected.

Mathematical demonstration will be given in the following sections.

6.1 A simplified toy model

It is complicated to obtain the mode solutions of (6.10) for a generic stochastic function $\Theta(t, \mathbf{x})$ whose stochastic property is determined by the quantum nature of the field ϕ . To illustrate the underlying physical mechanism more clearly, we start with a simplified toy model by restricting the phase angle $\Theta(t, \mathbf{x})$ defined by (6.9) to take the following form:

$$\Theta(t, \mathbf{x}) = \Omega t + \mathbf{K} \cdot \mathbf{x}, \quad (6.11)$$

where both Ω and \mathbf{K} are constants and they have the same order of magnitude $\Omega \sim |\mathbf{K}| \sim \sqrt{G}\Lambda^2$.

Of course this toy model does not describe the real spacetime sourced by the quantum vacuum since the Ω is by no means a constant but always varying, although the varying is slow compared to its own magnitude. However, this toy model possesses the key property needed — the spacetime is constantly fluctuating. It will be convenient for visualizing the back reaction effect from a fluctuating spacetime.

After setting the $\Omega \equiv \text{Constant}$ and the phase angle $\Theta(t, \mathbf{x})$ to be the form of (6.11), the equation of motion (6.10) for ϕ becomes

$$\begin{aligned} (1 + \cos 2(\Omega t + \mathbf{K} \cdot \mathbf{x})) \ddot{\phi} - \nabla^2 \phi \\ - 3\Omega \sin 2(\Omega t + \mathbf{K} \cdot \mathbf{x}) \dot{\phi} + \tan(\Omega t + \mathbf{K} \cdot \mathbf{x}) \mathbf{K} \cdot \nabla \phi = 0, \end{aligned} \quad (6.12)$$

where we have set $A_0 = \sqrt{2\Omega}$ such that the average of the coefficient $\frac{A_0^2}{\Omega} \cos^2 \Theta$ before $\ddot{\phi}$ is 1 for convenience.

In the flat spacetime case (6.6), each mode solution $u_{\mathbf{k}}$ in (6.7) contains only one single frequency. However, for the above fluctuating spacetime case (6.12), high frequencies mix with low frequencies and each mode solution must contain multiple frequencies. In fact, since (6.12) describes a strictly periodic system with time period π/Ω and spatial period $\pi/|\mathbf{K}|$, each mode solution $u_{\mathbf{k}}$ must change from (6.7) to the following form:

$$u_{\mathbf{k}}(t, \mathbf{x}) = e^{-i(\omega t - \mathbf{k} \cdot \mathbf{x})} \left(c_0 + \sum_{\substack{m=-\infty \\ m \neq 0}}^{+\infty} c_m e^{i2m(\Omega t + \mathbf{K} \cdot \mathbf{x})} \right), \quad (6.13)$$

where c_m are constants.

6.1. A simplified toy model

Inserting (6.13) into (6.12) and using the orthogonality of $e^{2im(\Omega t + \mathbf{K} \cdot \mathbf{x})}$, we obtain the following infinite system of linear equations:

m th equation:

$$\begin{aligned}
 & \sum_{n=-\infty}^{m-2} (-1)^{m+n} \mathbf{K} \cdot (\mathbf{k} + 2n\mathbf{K}) c_n \\
 & + \left[\frac{1}{2} (\omega - 2(m-1)\Omega)^2 - \frac{3}{2} \Omega (\omega - 2(m-1)\Omega) \right. \\
 & \left. - \mathbf{K} \cdot (\mathbf{k} + 2(m-1)\mathbf{K}) \right] c_{m-1} \\
 & + \left[(\omega - 2m\Omega)^2 - (\mathbf{k} + 2m\mathbf{K})^2 \right] c_m \\
 & + \left[\frac{1}{2} (\omega - 2(m+1)\Omega)^2 + \frac{3}{2} \Omega (\omega - 2(m+1)\Omega) \right. \\
 & \left. + \mathbf{K} \cdot (\mathbf{k} + 2(m+1)\mathbf{K}) \right] c_{m+1} \\
 & + \sum_{n=m+2}^{+\infty} (-1)^{m+n+1} \mathbf{K} \cdot (\mathbf{k} + 2n\mathbf{K}) c_n \\
 & = 0, \qquad \qquad \qquad m = 0, \pm 1, \pm 2, \pm 3, \dots \quad (6.14)
 \end{aligned}$$

In the above calculations, we have used the Fourier series expansion

$$\tan x = -2 \sum_{n=1}^{+\infty} (-1)^n \sin 2nx \quad (6.15)$$

to expand the term $\tan(\Omega t + \mathbf{K} \cdot \mathbf{x})$ in (6.12).

For the equations of $m \leq -1$, we successively add the $(m+1)$ th equation to the m th equation by the order from $m = -\infty$ to $m = -1$; and for the equations of $m \geq 1$, we successively add the $(m-1)$ th equation to the m th equation by the order from $m = +\infty$ to $m = 1$. Most terms can be eliminated by these elementary row operations and the above infinite system

6.1. A simplified toy model

of linear equations (6.14) becomes

$$\begin{aligned}
& \text{if } m \leq -1, \\
& \frac{1}{2} (\omega - 2(m-1)\Omega) (\omega - (2m+1)\Omega) c_{m-1} \\
& + \left[\frac{3}{2} (\omega - 2m\Omega) (\omega - (2m+1)\Omega) - (\mathbf{k} + 2m\mathbf{K}) \cdot (\mathbf{k} + (2m+1)\mathbf{K}) \right] c_m \\
& + \left[\frac{3}{2} (\omega - 2(m+1)\Omega) (\omega - (2m+1)\Omega) \right. \\
& \left. - (\mathbf{k} + 2(m+1)\mathbf{K}) \cdot (\mathbf{k} + (2m+1)\mathbf{K}) \right] c_{m+1} \\
& + \frac{1}{2} (\omega - 2(m+2)\Omega) (\omega - (2m+1)\Omega) c_{m+2} = 0;
\end{aligned}$$

$$\begin{aligned}
& \text{if } m = 0, \\
& \sum_{n=-\infty}^{-2} (-1)^n \mathbf{K} \cdot (\mathbf{k} + 2n\mathbf{K}) c_n \\
& + \left[\frac{1}{2} (\omega + 2\Omega) (\omega - \Omega) - \mathbf{K} \cdot (\mathbf{k} - 2\mathbf{K}) \right] c_{-1} \\
& + (\omega^2 - \mathbf{k}^2) c_0 \\
& + \left[\frac{1}{2} (\omega - 2\Omega) (\omega + \Omega) + \mathbf{K} \cdot (\mathbf{k} + 2\mathbf{K}) \right] c_1 \\
& + \sum_{n=2}^{+\infty} (-1)^{n+1} \mathbf{K} \cdot (\mathbf{k} + 2n\mathbf{K}) c_n = 0;
\end{aligned}$$

$$\begin{aligned}
& \text{if } m \geq 1, \\
& \frac{1}{2} (\omega - 2(m-2)\Omega) (\omega - (2m-1)\Omega) c_{m-2} \\
& + \left[\frac{3}{2} (\omega - 2(m-1)\Omega) (\omega - (2m-1)\Omega) \right. \\
& \left. - (\mathbf{k} + 2(m-1)\mathbf{K}) \cdot (\mathbf{k} + (2m-1)\mathbf{K}) \right] c_{m-1} \\
& + \left[\frac{3}{2} (\omega - 2m\Omega) (\omega - (2m-1)\Omega) - (\mathbf{k} + 2m\mathbf{K}) \cdot (\mathbf{k} + (2m-1)\mathbf{K}) \right] c_m \\
& + \frac{1}{2} (\omega - 2(m+1)\Omega) (\omega - (2m-1)\Omega) c_{m+1} = 0. \tag{6.16}
\end{aligned}$$

6.1. A simplified toy model

To characterize the property of the solutions of this system more clearly, we define the following parameters for convenience:

$$\epsilon = \frac{\omega}{\Omega}, \quad v = \frac{|\mathbf{k}|}{\Omega}, \quad \delta = \frac{|\mathbf{K}|}{\Omega}, \quad \cos \gamma = \frac{\mathbf{K} \cdot \mathbf{k}}{|\mathbf{K}||\mathbf{k}|}. \quad (6.17)$$

As mentioned before that our effective theory has a cutoff Λ such that only modes with $\omega, |\mathbf{k}| \leq \Lambda$ are relevant, which are much smaller than $\Omega \sim |\mathbf{K}| \sim \sqrt{G}\Lambda^2$ as Λ grows large. Therefore, we are only interested in the solutions of (6.14) or (6.16) when $\omega, |\mathbf{k}| \ll \Omega$, i.e. when $\epsilon, v \rightarrow 0$.

Dividing both sides of (6.16) by Ω^2 and doing some necessary algebraic

6.1. A simplified toy model

manipulations, (6.16) can be rewritten as

$$\begin{aligned}
& \text{if } m \leq -1, \\
& \left[(m-1) - \frac{\epsilon}{2} \right] c_{m-1} \\
+ & \left[(3-2\delta^2)m - \frac{3\epsilon}{2} - 2m\delta^2 \sum_{n=1}^{+\infty} \left(\frac{\epsilon}{2m+1} \right)^n \right. \\
& \left. - \frac{v}{2m+1} ((4m+1)\delta \cos \gamma + v) \sum_{n=0}^{+\infty} \left(\frac{\epsilon}{2m+1} \right)^n \right] c_m \\
+ & \left[(3-2\delta^2)(m+1) - \frac{3\epsilon}{2} - 2(m+1)\delta^2 \sum_{n=1}^{+\infty} \left(\frac{\epsilon}{2m+1} \right)^n \right. \\
& \left. - \frac{v}{2m+1} ((4m+3)\delta \cos \gamma + v) \sum_{n=0}^{+\infty} \left(\frac{\epsilon}{2m+1} \right)^n \right] c_{m+1} \\
+ & \left[(m+2) - \frac{\epsilon}{2} \right] c_{m+2} = 0; \\
& \text{if } m = 0, \\
& \sum_{n=-\infty}^{-2} (-1)^n (2n\delta^2 + \delta v \cos \gamma) c_n + \left[-1 + 2\delta^2 + \frac{\epsilon}{2} - \delta v \cos \gamma + \frac{\epsilon^2}{2} \right] c_{-1} \\
+ & (\epsilon^2 - v^2) c_0 \tag{6.18} \\
+ & \left[-1 + 2\delta^2 - \frac{\epsilon}{2} + \delta v \cos \gamma + \frac{\epsilon^2}{2} \right] c_1 + \sum_{n=2}^{+\infty} (-1)^{n+1} (2n\delta^2 + \delta v \cos \gamma) c_n = 0; \\
& \text{if } m \geq 1, \\
& \left[(m-2) - \frac{\epsilon}{2} \right] c_{m-2} \\
+ & \left[(3-2\delta^2)(m-1) - \frac{3\epsilon}{2} - 2(m-1)\delta^2 \sum_{n=1}^{+\infty} \left(\frac{\epsilon}{2m-1} \right)^n \right. \\
& \left. - \frac{v}{2m-1} ((4m-3)\delta \cos \gamma + v) \sum_{n=0}^{+\infty} \left(\frac{\epsilon}{2m-1} \right)^n \right] c_{m-1} \\
+ & \left[(3-2\delta^2)m - \frac{3\epsilon}{2} - 2m\delta^2 \sum_{n=1}^{+\infty} \left(\frac{\epsilon}{2m-1} \right)^n \right. \\
& \left. - \frac{v}{2m-1} ((4m-1)\delta \cos \gamma + v) \sum_{n=0}^{+\infty} \left(\frac{\epsilon}{2m-1} \right)^n \right] c_m \\
+ & \left[(m+1) - \frac{\epsilon}{2} \right] c_{m+1} = 0.
\end{aligned}$$

6.1. A simplified toy model

As $\epsilon, v \rightarrow 0$, the leading order asymptotic solution for $\{c_n\}$ of the above system of linear equations (6.18) depends only on the leading order of the coefficients before $\{c_n\}$. By keeping only the leading term for each coefficient, (6.18) is asymptotic to the following infinite system of linear equations:

$$BC = 0, \quad (6.19)$$

where the infinite matrix B is

$$B = \begin{pmatrix} \ddots & \vdots & \ddots \\ \cdots & -3(3-2\delta^2) & -2(3-2\delta^2) & -1 & 0 & 0 & 0 & 0 & \cdots \\ \cdots & -3 & -2(3-2\delta^2) & -(3-2\delta^2) & -\frac{\epsilon}{2} & 0 & 0 & 0 & \cdots \\ \cdots & 0 & -2 & -(3-2\delta^2) & -\frac{3\epsilon}{2} - \delta v \cos \gamma & 1 & 0 & 0 & \cdots \\ \cdots & 6\delta^2 & -4\delta^2 & -1 + 2\delta^2 & \epsilon^2 - v^2 & -1 + 2\delta^2 & -4\delta^2 & 6\delta^2 & \cdots \\ \cdots & 0 & 0 & -1 & -\frac{3\epsilon}{2} - \delta v \cos \gamma & 3 - 2\delta^2 & 2 & 0 & \cdots \\ \cdots & 0 & 0 & 0 & -\frac{\epsilon}{2} & 3 - 2\delta^2 & 2(3-2\delta^2) & 3 & \cdots \\ \cdots & 0 & 0 & 0 & 0 & 1 & 2(3-2\delta^2) & 3(3-2\delta^2) & \cdots \\ \ddots & \vdots & \ddots \end{pmatrix}$$

and $C = (\cdots, c_{-3}, c_{-2}, c_{-1}, c_0, c_1, c_2, c_3, \cdots)^T$.

We will denote the matrix elements of B by b_{mn} with $-\infty < m, n < +\infty$. In order to have a nonzero solution, the determinant of B must be zero. This gives us the dispersion relation that ϵ and v must satisfy in the asymptotic regime $\epsilon, v \rightarrow 0$.

The determinant can be calculated by Laplace expansion:

$$\det(B) = b_{00}M_{00} + \sum_{\substack{n=-\infty \\ n \neq 0}}^{+\infty} (-1)^n b_{0n}M_{0n}, \quad (6.20)$$

where M_{0n} is the $0, n$ minor of B , i.e. the infinite determinant that results from deleting the 0th row and the n th column of B . Due to the symmetry property of B , we have that, for each $n \neq 0$,

$$b_{0n} = b_{0,-n}, \quad M_{0n} = -M_{0,-n}, \quad (6.21)$$

6.1. A simplified toy model

which implies that all the terms inside the summation symbol \sum of (6.20) exactly cancel. Therefore, only the first term in (6.20) survive and thus we have that

$$\det(B) = M_{00}(\delta^2) (\epsilon^2 - v^2) = 0, \quad (6.22)$$

which leads to

$$\epsilon^2 = v^2, \quad (6.23)$$

or equivalently

$$\omega^2 = \mathbf{k}^2. \quad (6.24)$$

This proves that the usual dispersion relation still holds for low frequency field modes.

After setting $\epsilon^2 = v^2$, we start solving the infinite system (6.19).

First, we rewrite (6.19) as the following form:

$$\sum_{\substack{n=-\infty \\ n \neq 0}}^{+\infty} b_{mn} c_n = -b_{m0} c_0, \quad m = 0, \pm 1, \pm 2, \pm 3, \dots \quad (6.25)$$

Notice that the matrix elements of B has the following symmetry properties:

$$b_{mn} = -b_{-m, -n}, \quad \text{if } m, n \neq 0 \quad (6.26)$$

$$b_{m0} = b_{-m, 0}, \quad b_{0n} = b_{0, -n}. \quad (6.27)$$

The above symmetry properties leads to the following relation

$$c_n = -c_{-n}, \quad n \neq 0, \quad (6.28)$$

which implies that we only need to solve c_n for $n > 0$ to solve the whole system.

For convenience, we define the following new variables x_n by

$$c_n = \epsilon c_0 x_n, \quad n \neq 0. \quad (6.29)$$

Then using the relation (6.28), the infinite system of linear equations (6.25) simplifies to the following infinite recurrence equations:

$$(4 - 2\delta^2) x_1 + 2x_2 = \frac{3}{2} + \delta \cos \gamma, \quad (6.30)$$

$$(3 - 2\delta^2) x_1 + (3 - 2\delta^2) 2x_2 + 3x_3 = \frac{1}{2}, \quad (6.31)$$

$$(m - 2)x_{m-2} + (3 - 2\delta^2)(m - 1)x_{m-1} + (3 - 2\delta^2)mx_m + (m + 1)x_{m+1} = 0, \quad \text{if } m \geq 3, \quad (6.32)$$

6.1. A simplified toy model

where the dependence on ϵ in the equation (6.19) or (6.25) has been eliminated by introducing the new variables $x_n, n \neq 0$ through (6.29) and the solution for x_n depends only on δ .

In order to find for the sequence $\{x_m\}$, we define the following new variables:

$$y_m = (m-1)x_{m-1} + mx_m, \quad m \geq 3. \quad (6.33)$$

Then the recurrence equations (6.32) become

$$y_{m-1} + 2(1-\delta^2)y_m + y_{m+1} = 0, \quad m \geq 3. \quad (6.34)$$

Sequences satisfying (6.34) must take the following form:

$$y_m = D \cos(m\vartheta + \psi), \quad m \geq 3, \quad (6.35)$$

where D and ψ are two constants and ϑ is determined by

$$\cos \vartheta = -1 + \delta^2, \quad \sin \vartheta = \delta\sqrt{2 - \delta^2}. \quad (6.36)$$

Combining (6.35) and (6.33), the general formula for x_m can be obtained by iteration

$$\begin{aligned} x_m &= \frac{1}{m} \left(D \sum_{n=3}^m (-1)^{m-n} \cos(n\vartheta + \psi) + (-1)^m 2x_2 \right) \\ &= \frac{(-1)^m}{m} \left(-D \sec\left(\frac{\vartheta}{2}\right) \sin\left(\frac{(m-2)\vartheta}{2} + \frac{m\pi}{2}\right) \right. \\ &\quad \left. \cdot \sin\left(\frac{(m+3)\vartheta}{2} + \psi + \frac{m\pi}{2}\right) + 2x_2 \right), \quad m \geq 3. \end{aligned} \quad (6.37)$$

Replacing the c_m in (6.13) by x_m through (6.29) we obtain that, as $\epsilon \rightarrow 0$, the mode solution $u_{\mathbf{k}}(t, \mathbf{x})$ is asymptotic to

$$u_{\mathbf{k}}(t, \mathbf{x}) = c_0 e^{-i(\omega t - \mathbf{k} \cdot \mathbf{x})} \left(1 + \epsilon \sum_{\substack{m=-\infty \\ m \neq 0}}^{+\infty} x_m e^{i2m(\Omega t + \mathbf{K} \cdot \mathbf{x})} \right), \quad (6.38)$$

where x_m is determined by (6.28), (6.29), (6.30), (6.31), (6.32) and (6.37).

Using the orthogonality of $e^{i2m(\Omega t + \mathbf{K} \cdot \mathbf{x})}$, the relative magnitude of the correction to $u_{\mathbf{k}}$ from the usual plane wave mode $e^{-i(\omega t - \mathbf{k} \cdot \mathbf{x})}$ in Minkowski

6.2. General case

spacetime can be characterized by applying Parseval's identity:

$$|\Delta u_{\mathbf{k}}(t, \mathbf{x})| = \epsilon \left(\sum_{\substack{m=-\infty \\ m \neq 0}}^{+\infty} x_m^2 \right)^{\frac{1}{2}}. \quad (6.39)$$

From the solution (6.37) we know that as $m \rightarrow \infty$,

$$x_m^2 \sim \frac{1}{m^2}. \quad (6.40)$$

Thus the summation inside the bracket of (6.39) converges and the correction

$$|\Delta u_{\mathbf{k}}(t, \mathbf{x})| \sim \epsilon \rightarrow 0, \quad \text{as } \epsilon \rightarrow 0. \quad (6.41)$$

Thus we have demonstrated that the low frequency wave modes ($\omega \leq \Lambda$) are almost not affected by the fluctuating spacetime with much higher frequency ($\Omega \sim \sqrt{G}\Lambda^2$).

6.2 General case

The methods used and results obtained in the last section for the particular simplified toy model (6.12) can be generalized to the generic case (6.10). To start, we rewrite (6.10) to the following form:

$$(1 + f_1) \ddot{\phi} - \nabla^2 \phi - \Omega_0 f_2 \dot{\phi} + K_0 \mathbf{f}_3 \cdot \nabla \phi = 0, \quad (6.42)$$

where

$$f_1 = \frac{A_0^2}{\Omega} \cos^2 \Theta - 1, \quad (6.43)$$

$$f_2 = \frac{3A_0^2}{2} \left(\frac{\dot{\Omega}}{\Omega^2} \cos^2 \Theta + \sin 2\Theta \right) / \Omega_0, \quad (6.44)$$

$$\mathbf{f}_3 = \left(\frac{\nabla \Omega}{2\Omega} + \tan \Theta \nabla \Theta \right) / K_0, \quad (6.45)$$

$$\Omega_0 = \langle \Omega \rangle, \quad K_0 = \langle |\nabla \Theta| \rangle. \quad (6.46)$$

For convenience, we choose the constant A_0 such that the average of f_1

$$\langle f_1(t, \mathbf{x}) \rangle = 0. \quad (6.47)$$

6.2. General case

Unlike the toy model (6.12) we used in the last section, (6.42) is not strictly periodic. However, (6.42) is quasiperiodic and its quasiperiod is the same as the period of (6.12). This property is reflected in the Fourier transforms $f_1(\omega, \mathbf{k})$, $f_2(\omega, \mathbf{k})$ and $\mathbf{f}_3(\omega, \mathbf{k})$ of the functions $f_1(t, \mathbf{x})$, $f_2(t, \mathbf{x})$ and $\mathbf{f}_3(t, \mathbf{x})$ respectively which are defined by

$$f_1(t, \mathbf{x}) = \int d\omega d^3k f_1(\omega, \mathbf{k}) e^{i(\omega t + \mathbf{k} \cdot \mathbf{x})}, \quad (6.48)$$

$$f_2(t, \mathbf{x}) = \int d\omega d^3k f_2(\omega, \mathbf{k}) e^{i(\omega t + \mathbf{k} \cdot \mathbf{x})}, \quad (6.49)$$

$$\mathbf{f}_3(t, \mathbf{x}) = \int d\omega d^3k \mathbf{f}_3(\omega, \mathbf{k}) e^{i(\omega t + \mathbf{k} \cdot \mathbf{x})}. \quad (6.50)$$

For the function $f_1(t, \mathbf{x})$ defined by (6.43), after setting the constant A_0 by (6.47) and considering the slow varying property of $\Omega(t, \mathbf{x})$ and $\Theta(t, \mathbf{x})$ in both temporal and spatial directions, its leading order goes as

$$f_1(t, \mathbf{x}) \sim \cos 2\Theta, \quad (6.51)$$

which implies that the Fourier transform $f_1(\omega, \mathbf{k})$ would have two peaks centered at

$$\omega = \pm 2\Omega_0, \quad |\mathbf{k}| = 2K_0. \quad (6.52)$$

For the function $f_2(t, \mathbf{x})$ defined by (6.44), the second term which includes the factor $\sin 2\Theta$ is dominant since the first term which includes the factor $\dot{\Omega}/\Omega^2$ goes as $\sim 1/\Lambda \rightarrow 0$ due to the slow varying condition described by (5.37) and (5.38). Thus, its leading order goes as

$$f_2(t, \mathbf{x}) \sim 3 \sin 2\Theta, \quad (6.53)$$

which implies that the Fourier transform $f_2(\omega, \mathbf{k})$ would also have two peaks centered at

$$\omega = \pm 2\Omega_0, \quad |\mathbf{k}| = 2K_0. \quad (6.54)$$

Similarly, for the function $\mathbf{f}_3(t, \mathbf{x})$ defined by (6.45), the second term which includes the factor $\tan \Theta$ is dominant since the absolute value of the first term which includes the factor $\nabla\Omega/(\Omega K_0)$ also goes as $\sim 1/\Lambda \rightarrow 0$ due to the slow varying property of Ω in spatial directions. Thus, its leading order goes as

$$\mathbf{f}_3(t, \mathbf{x}) \sim \tan \Theta \frac{\nabla\Theta}{K_0}. \quad (6.55)$$

6.2. General case

Then using the Fourier series expansion (6.15) for $\tan \Theta$, we know that the Fourier transform $\mathbf{f}_3(\omega, \mathbf{k})$ would have infinitely many peaks centered at

$$\omega = \pm 2n\Omega_0, \quad |\mathbf{k}| = 2nK_0, \quad n = 1, 2, 3, \dots \quad (6.56)$$

(For a rough calculation of the above Fourier transforms, see Appendix C)

In addition, we have the zero frequency component (see (C.6) in Appendix C)

$$f_i(\omega = 0, \mathbf{k} = 0) \sim 0, \quad i = 1, 2, 3. \quad (6.57)$$

In summary, the system described by (6.42) is very similar to the system described by the simplified toy model (6.12). The only difference is that the Fourier transforms of the coefficients f_1 , f_2 , and \mathbf{f}_3 in (6.42) spread around center points given by (6.52), (6.54) and (6.56) while the Fourier transforms of the corresponding coefficients in (6.12) are ideal delta functions exactly located at same points given by (6.52), (6.54) and (6.56).

Therefore, the mode solution of (6.42) would take the form similar to (6.13):

$$u_{\mathbf{k}}(t, \mathbf{x}) = e^{-i(\omega t - \mathbf{k} \cdot \mathbf{x})} \left(c_0 + \int_{\substack{\omega' \neq 0 \\ \mathbf{k}' \neq \mathbf{0}}} d\omega' d^3 k' u_{\mathbf{k}}(\omega', \mathbf{k}') e^{i(\omega' t + \mathbf{k}' \cdot \mathbf{x})} \right), \quad (6.58)$$

where $u_{\mathbf{k}}(\omega', \mathbf{k}')$ is non-negligible only when ω', \mathbf{k}' are taking values around the centers given by (6.52), (6.54) and (6.56).

Inserting (6.58) into (6.42) and replacing the coefficients $f_1(t, \mathbf{x})$, $f_2(t, \mathbf{x})$ and $\mathbf{f}_3(t, \mathbf{x})$ in (6.42) by the equations (6.48), (6.49) and (6.50) and then using the orthogonality of $e^{i(\omega' t + \mathbf{k}' \cdot \mathbf{x})}$, we obtain the following uncountably infinite system of linear equations which are similar to (6.14):

$$\begin{aligned} & (\omega', \mathbf{k}')\text{th equation :} \\ & \left[(\omega - \omega')^2 - (\mathbf{k} + \mathbf{k}')^2 \right] u_{\mathbf{k}}(\omega', \mathbf{k}') \\ & + \int d\omega'' d^3 k'' \left[(\omega - (\omega' - \omega''))^2 f_1(\omega'', \mathbf{k}'') \right. \\ & - i\Omega_0 (\omega - (\omega' - \omega'')) f_2(\omega'', \mathbf{k}'') \\ & \left. - iK_0 (\mathbf{k} + (\mathbf{k}' - \mathbf{k}'')) \cdot \mathbf{f}_3(\omega'', \mathbf{k}'') \right] u_{\mathbf{k}}(\omega' - \omega'', \mathbf{k}' - \mathbf{k}'') = 0, \end{aligned} \quad (6.59)$$

where we have defined the notation $u_{\mathbf{k}}(0, \mathbf{0}) = c_0 \delta(0, \mathbf{0})$ for convenience.

6.2. General case

To characterize the property of the solutions of this system more clearly, we define the following parameters similar to (6.17) for convenience:

$$\begin{aligned}\epsilon &= \frac{\omega}{\Omega_0}, \quad v = \frac{|\mathbf{k}|}{\Omega_0}, \quad \delta = \frac{K_0}{\Omega_0}, \quad \cos \gamma = \frac{\mathbf{k} \cdot \mathbf{k}'}{|\mathbf{k}||\mathbf{k}'|}, \\ \cos \mu &= \frac{\mathbf{k} \cdot \mathbf{f}_3}{|\mathbf{k}||\mathbf{f}_3|}, \quad \cos \mu' = \frac{\mathbf{k}' \cdot \mathbf{f}_3}{|\mathbf{k}'||\mathbf{f}_3|}, \quad \cos \mu'' = \frac{\mathbf{k}'' \cdot \mathbf{f}_3}{|\mathbf{k}''||\mathbf{f}_3|}.\end{aligned}$$

Dividing both sides of (6.59) by Ω_0^2 gives

$$\begin{aligned}(\omega', \mathbf{k}')\text{th equation :} \\ \left[\left(\epsilon - \frac{\omega'}{\Omega_0} \right)^2 - \left(v^2 + \frac{\mathbf{k}'^2}{\Omega_0^2} + 2v \frac{|\mathbf{k}'|}{\Omega_0} \cos \gamma \right) \right] u_{\mathbf{k}}(\omega', \mathbf{k}') \\ + \int d\omega'' d^3 k'' \left[\left(\epsilon - \left(\frac{\omega'}{\Omega_0} - \frac{\omega''}{\Omega_0} \right) \right)^2 f_1(\omega'', \mathbf{k}'') \right. \\ - i \left(\epsilon - \left(\frac{\omega'}{\Omega_0} - \frac{\omega''}{\Omega_0} \right) \right) f_2(\omega'', \mathbf{k}'') \\ \left. - i \delta \left(v \cos \mu + \left(\frac{|\mathbf{k}'|}{\Omega_0} \cos \mu' - \frac{|\mathbf{k}''|}{\Omega_0} \cos \mu'' \right) \right) |\mathbf{f}_3(\omega'', \mathbf{k}'')| \right] \\ \cdot u_{\mathbf{k}}(\omega' - \omega'', \mathbf{k}' - \mathbf{k}'') = 0.\end{aligned}\tag{6.60}$$

Similar to the toy model case, as $\epsilon, v \rightarrow 0$, the leading order solution of (6.60) for $u_{\mathbf{k}}(\omega', \mathbf{k}')$ satisfies the following uncountably infinite system of

6.2. General case

linear equations:

if $(\omega', \mathbf{k}') = (0, \mathbf{0})$:

$$\begin{aligned}
& (\epsilon^2 - v^2) \delta(0, \mathbf{0}) c_0 \\
+ & \int d\omega'' d^3 k'' \left[\left(\frac{\omega''}{\Omega_0} \right)^2 f_1(\omega'', \mathbf{k}'') - i \left(\frac{\omega''}{\Omega_0} \right) f_2(\omega'', \mathbf{k}'') \right. \\
+ & \left. i\delta \left(\frac{|\mathbf{k}''|}{\Omega_0} \cos \mu'' \right) |f_3(\omega'', \mathbf{k}'')| \right] u_{\mathbf{k}}(-\omega'', -\mathbf{k}'') = 0,
\end{aligned} \tag{6.61}$$

if $(\omega', \mathbf{k}') \neq (0, \mathbf{0})$:

$$\begin{aligned}
& (-i\epsilon f_2(\omega', \mathbf{k}') - i\delta v \cos \mu |f_3(\omega', \mathbf{k}')|) c_0 \\
+ & \left[\left(\frac{\omega'}{\Omega_0} \right)^2 - \left(\frac{|\mathbf{k}'|}{\Omega_0} \right)^2 \right] u_{\mathbf{k}}(\omega', \mathbf{k}') \\
+ & \int_{\substack{\omega'' \neq \omega' \\ \mathbf{k}'' \neq \mathbf{k}'}} d\omega'' d^3 k'' \left[\left(\frac{\omega'}{\Omega_0} - \frac{\omega''}{\Omega_0} \right)^2 f_1(\omega'', \mathbf{k}'') + i \left(\frac{\omega'}{\Omega_0} - \frac{\omega''}{\Omega_0} \right) f_2(\omega'', \mathbf{k}'') \right. \\
- & \left. i\delta \left(\frac{|\mathbf{k}'|}{\Omega_0} \cos \mu' - \frac{|\mathbf{k}''|}{\Omega_0} \cos \mu'' \right) |f_3(\omega'', \mathbf{k}'')| \right] u_{\mathbf{k}}(\omega' - \omega'', \mathbf{k}' - \mathbf{k}'') = 0,
\end{aligned}$$

where we have used the property (6.57) in obtaining (6.61) from (6.60).

The above uncountably infinite system of linear equations (6.61) can also be written formally in matrix form similar to (6.19). We use similar notations that denoting the matrix here by B and its elements by $b_{(\omega', \mathbf{k}'), (\omega'', \mathbf{k}'')}$ for convenience.

In order to have nonzero solutions, the determinant of the uncountably infinite matrix B has to be zero, which gives the dispersion relations that ϵ and v must be satisfied in the asymptotic region $\epsilon, v \rightarrow 0$.

The ‘‘determinant’’ of B can be formally calculated through Laplace expansion similar to (6.20):

$$\begin{aligned}
\det B &= b_{(0, \mathbf{0}), (0, \mathbf{0})} M_{(0, \mathbf{0}), (0, \mathbf{0})} \\
&+ \int_{\substack{\omega'' \neq 0 \\ \mathbf{k}'' \neq \mathbf{0}}} d\omega'' d^3 k'' (-1)^{(\omega'', \mathbf{k}'')} b_{(0, \mathbf{0}), (\omega'', \mathbf{k}'')} M_{(0, \mathbf{0}), (\omega'', \mathbf{k}'')},
\end{aligned} \tag{6.62}$$

6.2. General case

where $M_{(0,0),(\omega'',\mathbf{k}'')}$ is the $(0, \mathbf{0}), (\omega'', \mathbf{k}'')$ minor of B , i.e. the ‘determinant’ resulting from deleting the $(0, \mathbf{0})$ th row and (ω'', \mathbf{k}'') th column of B .

Notice that since $f_1(t, \mathbf{x})$, $f_2(t, \mathbf{x})$ and $\mathbf{f}_3(t, \mathbf{x})$ are all real, their Fourier transforms $f_1(\omega, \mathbf{k})$, $f_2(\omega, \mathbf{k})$ and $\mathbf{f}_3(\omega, \mathbf{k})$ defined by (6.48), (6.49) and (6.50) must satisfy the following relations:

$$\begin{aligned} f_1(\omega, \mathbf{k}) &= f_1(-\omega, -\mathbf{k})^*, \\ f_2(\omega, \mathbf{k}) &= f_2(-\omega, -\mathbf{k})^*, \\ \mathbf{f}_3(\omega, \mathbf{k}) &= \mathbf{f}_3(-\omega, -\mathbf{k})^*, \end{aligned} \tag{6.63}$$

where the $*$ means complex conjugate.

The above symmetry property (6.63) leads to

$$\begin{aligned} b_{(0,0),(\omega'',\mathbf{k}'')} &= b_{(0,0),(-\omega'',-\mathbf{k}'')}, \\ M_{(0,0),(\omega'',\mathbf{k}'')} &= -M_{(0,0),(-\omega'',-\mathbf{k}'')}, \quad \text{if } (-\omega'', -\mathbf{k}'') \neq (0, \mathbf{0}), \end{aligned} \tag{6.64}$$

which implies that all the terms inside the integral symbol \int of (6.62) exactly cancel. Therefore, only the first term in (6.62) survives and thus we have

$$\det B = M_{(0,0),(0,0)}(\epsilon^2 - v^2) = 0, \tag{6.65}$$

which gives again the usual dispersion relation

$$\epsilon^2 = v^2 \quad \text{or} \quad \omega^2 = \mathbf{k}^2. \tag{6.66}$$

After setting the dispersion relation (6.66), we only need to solve the $(\omega', \mathbf{k}') \neq (0, \mathbf{0})$ th equations in (6.61) since $\det B = 0$ implies that the $(\omega', \mathbf{k}') = (0, \mathbf{0})$ th equation is redundant.

For convenience, we define new variables $x_{\mathbf{k}}(\omega', \mathbf{k}')$ similar to the x_n defined in (6.29):

$$u_{\mathbf{k}}(\omega', \mathbf{k}') = \epsilon c_0 x_{\mathbf{k}}(\omega', \mathbf{k}'), \quad (\omega', \mathbf{k}') \neq (0, \mathbf{0}). \tag{6.67}$$

Then (6.61) can be rewritten as

$$\begin{aligned} &\text{if } (\omega', \mathbf{k}') \neq (0, \mathbf{0}) : \\ &\left[\left(\frac{\omega'}{\Omega_0} \right)^2 - \left(\frac{\mathbf{k}'}{\Omega_0} \right)^2 \right] x_{\mathbf{k}}(\omega', \mathbf{k}') \\ &+ \int_{\substack{\omega'' \neq \omega' \\ \mathbf{k}'' \neq \mathbf{k}'}} d\omega'' d^3 k'' \left[\left(\frac{\omega'}{\Omega_0} - \frac{\omega''}{\Omega_0} \right)^2 f_1(\omega'', \mathbf{k}'') + i \left(\frac{\omega'}{\Omega_0} - \frac{\omega''}{\Omega_0} \right) f_2(\omega'', \mathbf{k}'') \right. \\ &\left. - i\delta \left(\frac{|\mathbf{k}'|}{\Omega_0} \cos \mu' - \frac{|\mathbf{k}''|}{\Omega_0} \cos \mu'' \right) |\mathbf{f}_3(\omega'', \mathbf{k}'')| \right] x_{\mathbf{k}}(\omega' - \omega'', \mathbf{k}' - \mathbf{k}'') \\ &= i f_2(\omega', \mathbf{k}') + i\delta \cos \mu |\mathbf{f}_3(\omega', \mathbf{k}')|. \end{aligned} \tag{6.68}$$

6.2. General case

Replacing the $u_{\mathbf{k}}(\omega', \mathbf{k}')$ in (6.58) by $x_{\mathbf{k}}(\omega', \mathbf{k}')$ through (6.67) we obtain that, as $\epsilon \rightarrow 0$, the mode solution $u_{\mathbf{k}}(t, \mathbf{x})$ is asymptotic to

$$u_{\mathbf{k}}(t, \mathbf{x}) = c_0 e^{-i(\omega t - \mathbf{k} \cdot \mathbf{x})} \left(1 + \epsilon \int_{\substack{\omega' \neq 0 \\ \mathbf{k}' \neq 0}} d\omega' d^3 k' x_{\mathbf{k}}(\omega', \mathbf{k}') e^{i(\omega' t + \mathbf{k}' \cdot \mathbf{x})} \right), \quad (6.69)$$

where $x_{\mathbf{k}}(\omega', \mathbf{k}')$ is determined by (6.68).

Analogous to (6.37) in the simplified toy model, $x_{\mathbf{k}}(\omega', \mathbf{k}')$ would also go as

$$x_{\mathbf{k}}(\omega', \mathbf{k}') \sim \frac{1}{m}, \quad (6.70)$$

when ω', \mathbf{k}' taking values around the centers

$$\omega' \sim \pm 2m\Omega_0, \quad |\mathbf{k}'| \sim 2mK_0, \quad m = 1, 2, 3, \dots \quad (6.71)$$

($x_{\mathbf{k}}(\omega', \mathbf{k}')$ is negligible if ω', \mathbf{k}' is far away from these centers).

Due to Parseval's theorem, (6.70) implies that the integral inside the bracket of (6.69) converges which is similar to (6.39) and thus the correction to $u_{\mathbf{k}}(t, \mathbf{x})$ also goes as ϵ .

Therefore, when we quantize the scalar field ϕ in our wildly fluctuating spacetime by expanding it in terms of the annihilation and creation operators according to (6.5), the leading order would still be the form of the Minkowski quantum field expansion (3.1). The correction to the dispersion relation $\omega^2 = \mathbf{k}^2$ and the plane wave mode $e^{-i(\omega t - \mathbf{k} \cdot \mathbf{x})}$ are on the order $\sim \epsilon$. In addition, the extra wave modes which mixing in (6.38) or (6.69) are all modes with frequencies higher than $\Omega_0 \sim \sqrt{G}\Lambda^2$, which is much larger than our effective QFT's cutoff Λ . These extremely high frequency modes beyond the cutoff are irrelevant to our low energy physics. This also explains why the ordinary QFT works by assuming fixed Minkowski spacetime. The small scale structure averages out in its effect on the long wavelength low energy fields.

In summary, we have argued that although our spacetime sourced by the quantum vacuum is highly curved and wildly fluctuating, the back reaction of the resulting spacetime on the quantum field sitting on it is small. This justifies our method of neglecting back reaction and using the quantum field expansion (3.1) in Minkowski spacetime at the beginning.

Chapter 7

The more general metrics

In previous chapters we assume the simplest inhomogeneous metric (4.1) to describe the spacetime resulting from the inhomogeneous vacuum. In this chapter, we try to generalize the result to more general inhomogeneous metrics.

7.1 The full metric and Einstein equations

We can always choose a spacelike hypersurface and construct the following general synchronous coordinate (at least locally) (see pages 42-43 of [4]):

$$ds^2 = -dt^2 + h_{ab}(t, \mathbf{x})dx^a dx^b, \quad a, b = 1, 2, 3. \quad (7.1)$$

For the above metric (7.1), we employ the initial value formulation of general relativity. In this formulation, the Einstein equation is equivalent to six equations for the evolution of the second fundamental form

$$\begin{aligned} \dot{k}_{ab} = & -R_{ab}^{(3)} - (trk)k_{ab} + 2k_{ac}k_b^c \\ & + 4\pi G\rho h_{ab} + 8\pi G \left(T_{ab} - \frac{1}{2}h_{ab}trT \right), \end{aligned} \quad (7.2)$$

plus the usual four constraint equations,

$$R^{(3)} + (trk)^2 - k_{ab}k^{ab} = 16\pi G\rho, \quad (7.3)$$

$$D_a k_b^a - D_b(trk) = 8\pi G j_b, \quad (7.4)$$

where $k_{ab} = \frac{1}{2}\dot{h}_{ab}$, $k^{ab} = h^{ac}h^{bd}k_{cd}$, $trk = h^{ab}k_{ab}$, $\rho = T_{00}$, $j_b = h_b^a T_{0a}$, $trT = h^{ab}T_{ab}$, $R^{(3)}$ is the 3-dimensional spatial curvature and D_a is the derivative operator associated with h_{ab} .

Taking trace on both sides of (7.2) and then combining with (7.3) gives:

$$h^{ab}\dot{k}_{ab} - k_{ab}k^{ab} = -4\pi G(\rho + trT). \quad (7.5)$$

It is interesting to notice that there are no spatial derivatives included on the left hand of the above equation (7.5). The key evolution equation (4.19) for $a(t, \mathbf{x})$ we used in previous chapters is just the special case of the above equation (7.5).

Direct calculation using the expression (4.22) shows that, the contribution from a real massless scalar field to the right-hand side of (7.5) is

$$\rho + trT = 2\dot{\phi}^2, \quad (7.6)$$

where all the spatial derivatives of ϕ and all the explicit dependence on the metric $g_{\mu\nu}$ in the definition of stress energy tensor (4.22) are canceled. It is also interesting to notice that the above exact expression (7.6) is exactly the same with the corresponding expression (4.23) for the simplest inhomogeneous metric (4.1) case.

7.2 The Mixmaster-type metric

We first consider the following special case:

$$h_{ab}(t, \mathbf{x}) = \begin{pmatrix} a^2(t, \mathbf{x}) & 0 & 0 \\ 0 & b^2(t, \mathbf{x}) & 0 \\ 0 & 0 & c^2(t, \mathbf{x}) \end{pmatrix}, \quad (7.7)$$

which is similar to the metric of Mixmaster universe [26].

The spacetime described by the above coordinate (7.7) possesses more freedoms than (4.1) and thus would exhibit richer structures. In this case, the expansion rate at the same point becomes directionally dependent. Along the three principle axes \hat{x} , \hat{y} and \hat{z} , which are eigenvectors of the symmetric matrix h_{ab} in (7.7), the expansion rates \dot{a}/a , \dot{b}/b and \dot{c}/c can be different. This means that, at one same point, the space can be expanding in one or two directions and contracting on the other two or one directions.

Under the coordinate system (7.7), equation (7.5) becomes

$$\frac{\ddot{a}}{a} + \frac{\ddot{b}}{b} + \frac{\ddot{c}}{c} = -4\pi G \left(\rho + \sum_{i=1}^3 P_i \right), \quad (7.8)$$

where $P_1 = T_{11}/a^2$, $P_2 = T_{22}/b^2$, $P_3 = T_{33}/c^2$. This equation is a generalization of the key evolution equation (4.19) we used in previous chapters.

Let

$$\frac{\ddot{a}}{a} = -\Omega_1^2(t, \mathbf{x}), \quad \frac{\ddot{b}}{b} = -\Omega_2^2(t, \mathbf{x}), \quad \frac{\ddot{c}}{c} = -\Omega_3^2(t, \mathbf{x}), \quad (7.9)$$

7.2. The Mixmaster-type metric

then (7.8) immediately leads to

$$\Omega_1^2(t, \mathbf{x}) + \Omega_2^2(t, \mathbf{x}) + \Omega_3^2(t, \mathbf{x}) = 4\pi G \left(\rho + \sum_{i=1}^3 P_i \right). \quad (7.10)$$

Unlike equation (4.19), here the time dependent frequencies $\Omega_i^2(t, \mathbf{x}_0)$ do not necessarily go exactly the same as $\Omega^2 = \frac{4\pi G}{3} \left(\rho + \sum_{i=1}^3 P_i \right)$. However, as the functions a , b and c are alternately symmetric, Ω_1^2 , Ω_2^2 and Ω_3^2 must have the same statistical properties. Especially, their expectation values must be equal

$$\langle \Omega_i^2(t, \mathbf{x}_0) \rangle = \frac{4\pi G}{3} \left\langle \left(\rho + \sum_{i=1}^3 P_i \right) \right\rangle, \quad i = 1, 2, 3. \quad (7.11)$$

Moreover, since Ω^2 is slowly varying, Ω_i^2 should also be slowly varying functions, since otherwise we would have three fast varying functions sum together and precisely cancel each other to give a slowly varying function, which is almost impossible in the system with such huge quantum fluctuations (This argument is from probability sense. To prove this, one need to also investigate other Einstein equations. This needs more study in the future.). Thus the evolution of a , b and c are also adiabatic processes that the solutions would be similar to (5.4):

$$a \simeq e^{\int_0^t H_{1\mathbf{x}_0}(t') dt'} \tilde{P}_1(t, \mathbf{x}_0), \quad (7.12)$$

$$b \simeq e^{\int_0^t H_{2\mathbf{x}_0}(t') dt'} \tilde{P}_2(t, \mathbf{x}_0), \quad (7.13)$$

$$c \simeq e^{\int_0^t H_{3\mathbf{x}_0}(t') dt'} \tilde{P}_3(t, \mathbf{x}_0), \quad (7.14)$$

where \tilde{P}_i are quasiperiodic functions with the same quasiperiods as the time dependent frequencies Ω_i .

Also, on average, we have

$$H_i = H = \alpha \Lambda e^{-\beta \sqrt{G} \Lambda}, \quad i = 1, 2, 3, \quad (7.15)$$

where

$$H_i = \frac{1}{t} \int_0^t H_{i\mathbf{x}_0}(t') dt'. \quad (7.16)$$

Therefore, the determinant of h_{ab} goes as

$$h(t, \mathbf{x}_0) = \det h_{ab}(t, \mathbf{x}_0) = a^2 b^2 c^2 \simeq \exp \left(2 \sum_{i=1}^3 H_i t \right) \prod_{i=1}^3 \tilde{P}_i^2, \quad (7.17)$$

and the observable physical volume would be,

$$V(t) = \int \sqrt{h(t, \mathbf{x})} d^3x = V(0)e^{3Ht}, \quad (7.18)$$

which also gives the slow accelerating expansion of the Universe on cosmological scale.

7.3 An alternative derivation from geodesic deviation equation

The dynamic equation (7.8) can also be derived from the geodesic deviation equation. It is easier to understand the physical meaning of (7.8) from this alternative derivation.

We first review the formalism of geodesic deviation equation. We will follow the same notation in [4].

Let $\gamma_s(t)$ denote a smooth one-parameter family of geodesics, that is, for each $s \in \mathbb{R}$, γ_s is a geodesic parameterized by the affine parameter t and the map $(t, s) \rightarrow \gamma_s(t)$ is smooth, one-to-one and has smooth inverse. The collection of these curves defines a smooth two-dimensional surface. We may choose (t, s) as coordinates of this surface.

There are two natural vector fields: the tangent vectors to the geodesics $T^a = \left(\frac{\partial}{\partial t}\right)^a$ and the deviation vectors $X^a = \left(\frac{\partial}{\partial s}\right)^a$ which represent the displacements to infinitesimally nearby geodesics. The quantity

$$v^a = T^b \nabla_b X^a \quad (7.19)$$

gives the rate of change along a geodesic of the displacement to an infinitesimally nearby geodesic and may be interpreted as the relative velocity of an infinitesimally nearby geodesics. The quantity

$$a^a = T^c \nabla_c v^a = T^c \nabla_c \left(T^b \nabla_b X^a \right) \quad (7.20)$$

may be interpreted as the relative acceleration of an infinitesimally nearby geodesic in the family.

The curvature of spacetime tells how the geodesics move. It is easy to derive the following geodesic deviation equation from the definition of Riemann curvature tensor (see derivation of Eq.(3.3.18) in page 47 of [4])

$$a^a = -R_{cbd}^a X^b T^c T^d, \quad (7.21)$$

7.3. An alternative derivation from geodesic deviation equation

which shows that the relative acceleration between two neighboring geodesics is proportional to the curvature.

For synchronized coordinates, the curves $\{\gamma_{\mathbf{x}}(t) : \mathbf{x} = \text{Constant}\}$ are all geodesics. This is a three-parameter family of geodesics (parameters x, y, z). To apply the geodesic deviation equation (7.21), we first pick the sub-family of geodesics: $\{\gamma_x(t) : -\infty < x < +\infty, y = y_0, z = z_0\}$. For this one-parameter family of geodesics, we apply (7.21) to the geodesic $\gamma_{\mathbf{x}_0}(t)$ which goes through an arbitrary point $\mathbf{x} = \mathbf{x}_0 = (x_0, y_0, z_0)$.

The tangent vector and the deviation vector of $\gamma_{\mathbf{x}_0}(t)$ expressed in the coordinate (7.7) are

$$T^a = \left(\frac{\partial}{\partial t} \right)^a = (1, 0, 0, 0), \quad (7.22)$$

$$X^a = \left(\frac{\partial}{\partial x} \right)^a = (0, 1, 0, 0). \quad (7.23)$$

The relative velocity is

$$\begin{aligned} v^a &= T^b \nabla_b X^a \\ &= T^b \partial_b X^a + T^b \Gamma_{bc}^a X^c \\ &= \Gamma_{01}^a \\ &= \left(0, \frac{\dot{a}}{a}, 0, 0 \right). \end{aligned} \quad (7.24)$$

The relative acceleration is

$$\begin{aligned} a^a &= T^b \nabla_b v^a \\ &= T^b \partial_b \Gamma_{01}^a + T^b \Gamma_{bc}^a \Gamma_{01}^c \\ &= \partial_0 \Gamma_{01}^a + \Gamma_{01}^a \Gamma_{01}^1 \\ &= \left(0, \frac{\ddot{a}}{a}, 0, 0 \right). \end{aligned} \quad (7.25)$$

Also expressing (7.21) in the coordinate (7.7) gives

$$a^a = -R_{010}^a. \quad (7.26)$$

Comparing (7.25) and (7.26) we obtain that

$$\frac{\ddot{a}}{a} = -R_{010}^1. \quad (7.27)$$

7.3. An alternative derivation from geodesic deviation equation

Picking the other two sub-family of geodesics: $\{\gamma_{y'}(t') : x' = x_0, y' = \text{Constant}, z' = z_0\}$ and $\{\gamma_{z'}(t') : x' = x_0, y' = y_0, z' = \text{Constant}\}$, and following the same procedures we obtain that

$$\frac{\ddot{b}}{b} = -R_{020}^2, \quad (7.28)$$

$$\frac{\ddot{c}}{c} = -R_{030}^3. \quad (7.29)$$

Summing (7.27), (7.28) and (7.29) together we obtain that

$$\frac{\ddot{a}}{a} + \frac{\ddot{b}}{b} + \frac{\ddot{c}}{c} = -R_{0\mu 0}^\mu, \quad (7.30)$$

where the sum over μ can range over all four coordinates, not just the three spatial ones, since the symmetries of the Riemann tensor requires that $R_{000}^0 = 0$.

The right-hand side of the above equation is just minus the time-time component of the Ricci tensor

$$R_{00} = R_{0\mu 0}^\mu. \quad (7.31)$$

Einstein equation has an equivalent form which directly relates the Ricci tensor with matter field stress energy tensor (see e.g. Eq. (4.3.23) in page 72 of [4]):

$$R_{\mu\nu} = 8\pi G \left(T_{\mu\nu} - \frac{1}{2} g_{\mu\nu} T \right), \quad (7.32)$$

where $T = g^{\mu\nu} T_{\mu\nu}$ is the trace of the stress energy tensor. Specially, the time-time component of (7.32) expressed in the coordinate (7.7) is just

$$R_{00} = 4\pi G \left(\rho + \sum_{i=1}^3 P_i \right). \quad (7.33)$$

Therefore, replacing the $R_{0\mu 0}^\mu$ in the right-hand side of (7.30) by (7.33) we obtain the same equation as (7.8):

$$\frac{\ddot{a}}{a} + \frac{\ddot{b}}{b} + \frac{\ddot{c}}{c} = -4\pi G \left(\rho + \sum_{i=1}^3 P_i \right). \quad (7.34)$$

An interesting fact that needs to be pointed out is that the key dynamic equations (4.19), (7.5), (7.8) are all just the time-time component of Eq.(7.32) expressed in the corresponding coordinates.

7.4 The physical picture

It is easy to understand the physical meaning of our key dynamic equation (7.8) from the last section's derivation. (7.8) describes how the geodesics $\gamma_{\mathbf{x}}(t)$ which are infinitesimally close to $\gamma_{\mathbf{x}_0}(t)$ move in the wildly fluctuating spacetime. It shows that the sum of the relative accelerations $\ddot{a}/a, \ddot{b}/b, \ddot{c}/c$ is proportional to the energy density ρ plus the pressures P_1, P_2, P_3 of the matter fields.

Geometrically, the geodesics $\gamma_{\mathbf{x}}(t)$ with $|\mathbf{x} - \mathbf{x}_0|$ sufficiently small form an infinitesimally small ellipsoid of test particles around \mathbf{x}_0 . The solutions (7.12), (7.13), (7.14) for a, b, c show that the ellipsoid is alternatively expanding and contracting in the three principal directions $\hat{x}, \hat{y}, \hat{z}$. Moreover, due to the weak parametric resonance effect, the expansion wins out a little bit that the average volume of the ellipsoid would gradually increase. This effect accumulates on the cosmological scale, which gives the slow accelerating expansion of the Universe.

7.5 The Raychaudhuri equation

If h_{ab} take the most general form

$$h_{ab}(t, \mathbf{x}) = \begin{pmatrix} a^2(t, \mathbf{x}) & d(t, \mathbf{x}) & e(t, \mathbf{x}) \\ d(t, \mathbf{x}) & b^2(t, \mathbf{x}) & f(t, \mathbf{x}) \\ e(t, \mathbf{x}) & f(t, \mathbf{x}) & c^2(t, \mathbf{x}) \end{pmatrix}, \quad (7.35)$$

then the dynamic equation (7.5) becomes

$$\begin{aligned} & \frac{a^2 h_{11}^*}{h} \frac{\ddot{a}}{a} + \frac{b^2 h_{22}^*}{h} \frac{\ddot{b}}{b} + \frac{c^2 h_{33}^*}{h} \frac{\ddot{c}}{c} \\ & + \frac{d h_{12}^*}{h} \frac{\ddot{d}}{d} + \frac{e h_{13}^*}{h} \frac{\ddot{e}}{e} + \frac{f h_{23}^*}{h} \frac{\ddot{f}}{f} + F(h_{ab}, \dot{h}_{ab}) = -4\pi G(\rho + trT), \end{aligned} \quad (7.36)$$

where $h = \det(h_{ab})$ is the determinant of the matrix (7.35), h_{ab}^* is the matrix's (a, b) cofactor and F is a nonlinear function of the metric components h_{ab} and their first time derivatives \dot{h}_{ab} .

(7.36) is very difficult to handle. However, it is in fact equivalent to the well known Raychaudhuri equation. Its physical meaning is easier to understand in this way. In the following we will first review some basics about Raychaudhuri's equation (see Section 9.2 of [4] for details).

Consider a general spacetime g_{ab} and a smooth congruence of timelike geodesics which are parameterized by proper time τ . So the vector field, ξ^a ,

7.5. The Raychaudhuri equation

of tangents is normalized to unit length, $\xi^a \xi_a = -1$. One then define the tensor field B_{ab} , the expansion θ , shear σ_{ab} , and twist ω_{ab} by

$$B_{ab} = \nabla_b \xi_a, \quad (7.37)$$

$$\theta = B^{ab} h_{ab}, \quad (7.38)$$

$$\sigma_{ab} = B_{(ab)} - \frac{1}{3} \theta h_{ab}, \quad (7.39)$$

$$\omega_{ab} = B_{[ab]}, \quad (7.40)$$

where the spatial metric h_{ab} is defined by

$$h_{ab} = g_{ab} + \xi_a \xi_b. \quad (7.41)$$

Along any geodesic in the congruence, θ measures the average rate of expansion of the infinitesimally nearby surrounding geodesics; ω_{ab} measures their rotation; and σ_{ab} measures their shear, i.e. an initial sphere in the tangent space which is Lie transported along ξ^a will distort toward an ellipsoid with principle axes by the eigenvectors of σ_b^a , with rate given by the eigenvalues of σ_b^a .

Raychaudhuri's equation is a differential equation for the expansion θ :

$$\xi^c \nabla_c \theta + \frac{1}{3} \theta^2 + \sigma_{ab} \sigma^{ab} - \omega_{ab} \omega^{ab} = -R_{ab} \xi^a \xi^b. \quad (7.42)$$

If the congruence is hypersurface orthogonal, we have $\omega_{ab} = 0$ that the above equation (7.42) becomes

$$\xi^c \nabla_c \theta + \frac{1}{3} \theta^2 + \sigma_{ab} \sigma^{ab} = -8\pi \left(T_{ab} - \frac{1}{2} T g_{ab} \right) \xi^a \xi^b, \quad (7.43)$$

where we have used the equivalent version of Einstein equation (7.32) to replace the Ricci tensor R_{ab} .

For synchronized coordinate (4.1) or (7.7) or (7.1), the curves $\{\gamma_{\mathbf{x}}(t) : \mathbf{x} = \text{Constant}\}$ are all geodesics and they also form a congruence. Let ξ^a be the tangent vectors of them, i.e.

$$\xi^a = \left(\frac{\partial}{\partial t} \right)^a, \quad (7.44)$$

then (7.43) can be expressed in the coordinate (4.1) or (7.7) or (7.1) as

$$\ddot{\theta} + \frac{1}{3} \theta^2 + \sigma_{ab} \sigma^{ab} = -4\pi G (\rho + trT). \quad (7.45)$$

7.5. The Raychaudhuri equation

For the simplest inhomogeneous metric (4.1), we have

$$\sigma_{ab} = 0, \quad (7.46)$$

and

$$\theta = 3\frac{\dot{a}}{a}, \quad (7.47)$$

i.e. the average expansion θ is just 3 times the local Hubble expansion rate \dot{a}/a ; Then (7.45) becomes

$$\ddot{\theta} + \frac{1}{3}\theta^2 = 3\frac{\ddot{a}}{a} = -4\pi G \left(\rho + \sum_{i=1}^3 P_i \right), \quad (7.48)$$

which is just the key equation (4.19) for a time dependent harmonic oscillator we used in previous chapters.

For the mixmaster-type metric (7.7), we have

$$\theta = \frac{\dot{a}}{a} + \frac{\dot{b}}{b} + \frac{\dot{c}}{c} \quad (7.49)$$

and

$$\ddot{\theta} + \frac{1}{3}\theta^2 + \sigma_{ab}\sigma^{ab} = \frac{\ddot{a}}{a} + \frac{\ddot{b}}{b} + \frac{\ddot{c}}{c}. \quad (7.50)$$

Then (7.45) becomes

$$\frac{\ddot{a}}{a} + \frac{\ddot{b}}{b} + \frac{\ddot{c}}{c} = -4\pi G \left(\rho + \sum_{i=1}^3 P_i \right), \quad (7.51)$$

which is just equation (7.8).

For the most general metric (7.1), (7.45) just becomes (7.36). This case is difficult to handle. Further investigations are needed in the future.

However, the results we obtained for the mixmaster-type metric (7.7) suggest that, for the most general case (7.35), the eigenvalues $\lambda_i^2(t, \mathbf{x})$ of the matrix h_{ab} should also evolve adiabatically similar to a^2 , b^2 and c^2 . In other words, we expect that the results (7.12), (7.13), (7.14) and (7.15) can be generalized to λ_i in the most general case and the physical volume of space would expand as

$$\begin{aligned} V(t) &= \int \sqrt{h(t, \mathbf{x})} d^3x \\ &= \int \sqrt{\lambda_1^2 \lambda_2^2 \lambda_3^2} d^3x \\ &= V(0)e^{3Ht}, \end{aligned} \quad (7.52)$$

where H is determined by (5.25).

Chapter 8

Similarity of effects of vacuum energy in non-gravitational system and gravitational system

Vacuum fluctuations and their associated vacuum energies are direct consequences of the Heisenberg's uncertainty principle of quantum mechanics. Although it is still controversial [27], various observable effects are often ascribed to the existence of vacuum energies and have been experimentally verified, which strongly suggests the reality of vacuum fluctuations. These vacuum fluctuation effects include the spontaneous emission [28], the Lamb shift [29], the anomalous magnetic moment of the electron [30, 31] and the Casimir effect [32–35]. The reality of the vacuum energy associated to the spontaneous symmetry breaking of electroweak theory has also been confirmed by the discovery of the Higgs boson at the LHC [36, 37].

If we assume that the vacuum fluctuations do exist as evidenced by the above listed observable effects, then according to the equivalence principle, the associated vacuum energies would gravitate as well as all other forms of energy. This has been experimentally demonstrated by, for example, the gravitational test of Lamb shift energy [38–40]. The gravitational property of Casimir energy has not been tested experimentally, but has been demonstrated theoretically with the conclusion that it does gravitate according to equivalence principle [41–44].

However, in the literature, the value of vacuum energy density is usually thought to play a different role in non-gravitational systems and in gravitational systems. The actual value of the vacuum energy density is generally regarded as irrelevant in non-gravitational contexts based on the argument that only energy differences from the vacuum are measurable; while when gravity is present, the actual value of the energy matters, not just the differences, since the source for the gravitational field is the entire

energy momentum tensor that its large value may be potentially disastrous.

We argue differently in this section with the following points: (i) the value of vacuum energy density can also be relevant in non-gravitational contexts; (ii) the huge value of vacuum energy density is not a direct observable and that it is not disastrous in a theory of gravity. Moreover, there is essentially no difference between the roles played by vacuum energy in non-gravitational systems and in gravitational systems. In other words, although technically more complicated when gravity is included, the gravitational effect of the vacuum energy on spacetime metric is intrinsically the same as its effect on material bodies when gravity is excluded.

8.1 Value of vacuum energy is relevant in Casimir effect

Let us first consider the Casimir effect. The Casimir force is usually derived by calculating the change in vacuum energy due to the presence of the conducting plates, which acts as mirrors to reflect electromagnetic waves (We will call them mirrors in the following). This derivation is straightforward, but loses some important physical details about what is going on in the system [45, 46]. Due to quantum fluctuations, the zero point fields constantly impinge on both sides of the mirror and then reflect back, which transmit momentum to the mirror and thus result in forces on both sides of the mirror. The Casimir stress (force per unit area) is just the difference between the pressure exerted by the electromagnetic field vacuum from inside and outside

$$S(t, x, y) = T_{zz}^{\text{inside}} - T_{zz}^{\text{outside}}, \quad (8.1)$$

where we have set that the two parallel mirrors are normal to the z axis. Since the vacuum fluctuations between the two mirrors are different from the vacuum fluctuations outside, the expectation values of T_{zz}^{inside} and T_{zz}^{outside} would be different and thus gives a net average force. Although both T_{zz}^{inside} and T_{zz}^{outside} are divergent, this average force is finite since the quartic divergent Minkowski zero point fluctuations are canceled after the subtraction in (8.1) and one obtains the well known Casimir stress [46]

$$\langle S \rangle = -\frac{\pi^2}{240d^4}. \quad (8.2)$$

Thus the effect of the value of zero point energy disappears in the calculations. It is for this reason that although the Casimir effect is usually

regarded as evidence of the reality of zero point energy, the actual value of its energy density is thought to be irrelevant in this effect.

However, the value of zero point energy density does have an effect. Note that (8.2) only gives the expectation value of the Casimir stress S , but S is never a constant, it fluctuates. That's because the amount of momentum carried by the zero point fields which impinge on both sides of the mirror is constantly fluctuating due to the fact that the vacuum is not an eigenstate of the zz component of the stress energy tensor T_{zz} . The magnitude of the fluctuation of each T_{zz} is large and diverges as the same order of the vacuum energy density $\langle T_{00} \rangle$. For a perfect mirror, since the fields on the two sides fluctuate independently of each other, the mean-squared stresses on the two sides simply add, resulting in the magnitude of the fluctuation of the net stress also diverges as

$$\langle \Delta S^2 \rangle = \langle (S - \langle S \rangle)^2 \rangle \sim \langle T_{00} \rangle^2 \rightarrow \infty. \quad (8.3)$$

For more realistic imperfect mirrors which become transparent for frequencies higher than its plasma frequency Λ , the $\langle T_{00} \rangle$ in (8.3) contains contributions only from field modes of frequencies lower than Λ and the mean squared value of the net stress S goes as

$$\langle \Delta S^2 \rangle \sim \langle T_{00} \rangle^2 \sim \Lambda^8. \quad (8.4)$$

The plasma frequency Λ in (8.4) acts as an effective cutoff which depends on the microstructure of the mirror. It is similar but distinct from the effective QFT's cutoff Λ in (5.25), which depends on the microstructure of spacetime.

Therefore, the value of zero point energy density is still physically significant even in non-gravitational system. Its value appears in (8.3) and (8.4) to characterize the strength of Casimir stress fluctuation, which implies that the net Casimir stress is constantly fluctuating with huge magnitudes around its small mean value (8.2). Due to this huge fluctuation, at almost any instant, the magnitude of the stress at each single point of the mirror is as large as the value of the zero point energy density.

However, this effect is strong only at small scales. Its measurable effect becomes small at larger scales. In practice, the measurements must be taken over some finite time interval T and some finite surface area of order l^2 . More precisely, what the force detector measures is the time and surface average

$$\bar{S} = \int dt dx dy f(t, x, y) S(t, x, y), \quad (8.5)$$

where the averaging function f satisfies

$$\int dt dx dy f(t, x, y) = 1. \quad (8.6)$$

The exact shape of the averaging function depends on the measuring apparatus. On physical grounds one can choose f to be a single peak over a time interval T comparable to the experimental resolving time and over a spatial region of area l^2 comparable to the resolution of the measuring device. Although the magnitude of the fluctuations of the net stress S is formally infinite as shown in (8.3), the magnitude of the measurable fluctuations of its average \bar{S} is finite. This is because the effect of the vacuum fluctuations at small scales is significantly weakened when averaging over larger scales. The calculations have been done by G Barton in [47] with the conclusion that, for the realistic case where $l \ll cT$, the mean squared deviation

$$\langle \Delta \bar{S}^2 \rangle = \langle (\bar{S} - \langle \bar{S} \rangle)^2 \rangle = \frac{\text{constant}}{T^8}, \quad (8.7)$$

where the “constant” here is a pure number as could have been foreseen on dimensional grounds. The above equation (8.7) shows that $\langle \Delta \bar{S}^2 \rangle$ increases as T decreases, which means that the better the measuring device, the stronger fluctuation due to the effect of the value of the zero point energy density can be measured. And in principle, using a perfect instantaneous measuring device ($T \rightarrow 0$), one can measure the infinite fluctuations of the Casimir stress on a perfect mirror due to the infinite value of zero point energy density. In practice, however, $\langle \Delta \bar{S}^2 \rangle$ is too small to be measured for a real force detector whose resolving time T is too large [47].

8.2 Effect of vacuum energy on the motion of mirrors

The value of zero point energy density also has effects on the dynamic motion of small material bodies. Imagine that we place a single mirror of very small size in the vacuum and then release it. The mirror would experience a fluctuating force exerted by the quantum field vacuum and starts to move. The equation of motion of the mirror, which is called quantum Langevin equation, can be generally described by

$$\ddot{X} = F(t, X, \dot{X}, \phi, \dot{\phi}, \dots), \quad (8.8)$$

where X is the mirror’s position, ϕ represents the field interacting with the mirror which is usually taken to be a scalar field for simplicity and we have set the mirror’s mass $M = 1$ for convenience. The average force in this case would be zero because of symmetry

$$\langle F \rangle = 0, \quad (8.9)$$

8.3. Analogies between the motion of mirror and the motion of $a(t, \mathbf{x})$

and similar to the Casimir stress fluctuation (8.3), the force here also undergoes wild fluctuations with a magnitude

$$\langle F^2 \rangle \propto \langle T_{00} \rangle^2 \rightarrow \infty. \quad (8.10)$$

The mathematically infinite fluctuating force F gives infinite instantaneous accelerations of the mirror through (8.8). Similar to the case of infinite Casimir stress fluctuation (8.3), this infinite fluctuating force and infinite instantaneous acceleration make sense since they are also only significant at very small scales and will not result in infinite fluctuation of the mirror's position at observable larger scales. In fact, the mirror would oscillate back and forth with very high speeds, but its range of motion is still small [48–52].

More precisely, suppose that the mirror is initially located at $X(0) = 0$ with velocity $\dot{X}(0) = 0$ and is then released at $t = 0$. The magnitude of its acceleration $\ddot{X}(t)$ and velocity $\dot{X}(t)$, which can be characterized by the quantity $\langle \ddot{X}^2(t) \rangle$ and $\langle \dot{X}^2(t) \rangle$, is large. But, the magnitude of the range of the mirror's fluctuating motion, which can be characterized by the observable mean squared displacement $\langle X^2(t) \rangle$, is still small.

In this sense, the value of vacuum energy density is still relevant even in non-gravitational physics. This value appears in the equation (8.10) to characterize the strength of the force fluctuations acting on the mirror at small scales and it may have small observable effects at larger scales such as diffusions predicted in [50–52].

8.3 Analogies between the motion of mirror and the motion of $a(t, \mathbf{x})$

Although technically more complicated in gravity, the basic dynamic equation of motion (4.19) satisfied by the scale factor $a(t, \mathbf{x})$ is in fact very similar to the equation of motion (8.8) satisfied by the mirror's position $X(t)$. Consider only the contribution from the massless scalar field ϕ , (4.19) is just the following same form as the equation (8.8)

$$\ddot{a} = F(a, \dot{\phi}), \quad (8.11)$$

where

$$F(a, \dot{\phi}) = -\frac{8\pi G}{3}\dot{\phi}^2 a. \quad (8.12)$$

Also, the average of the fluctuating force $F(a, \dot{\phi})$ is zero due to symmetry

$$\langle F(a, \dot{\phi}) \rangle = 0, \quad (8.13)$$

8.3. Analogies between the motion of mirror and the motion of $a(t, \mathbf{x})$

and its magnitude of fluctuation

$$\langle F^2(a, \dot{\phi}) \rangle \propto \langle T_{00} \rangle^2 \rightarrow \infty. \quad (8.14)$$

The above two statistical properties (8.13) and (8.14) satisfied by the “force” driving the “motion” of the scale factor a are the same with the statistical properties (8.9) and (8.10) satisfied by the force driving the motion of the mirror. In this sense, the role played by the value of the vacuum energy density in gravitational system is similar to its role in non-gravitational system.

Concretely speaking, the vacuum energy density results in large instantaneous acceleration \ddot{X} and velocity \dot{X} of the mirror, but the observable position fluctuations of the mirror, which can be characterized by the quantity $\langle X^2 \rangle$, is not large. Analogously, the vacuum energy density results in the large instantaneous “acceleration” \ddot{a} and “velocity” \dot{a} of the scale factor, but the observable physical distance defined by (4.8), whose value is determined by the quantity $\langle a^2 \rangle$, is also not large. These properties about $a(t, \mathbf{x})$ are evident from the solutions (5.4), (5.8) and (5.25), from which we can see that the quantities $\langle \ddot{a}^2 \rangle$ and $\langle \dot{a}^2 \rangle$ are as large as $\langle T_{00} \rangle^2$ and $\langle T_{00} \rangle$ respectively, while the magnitude of the quantity $\langle a^2 \rangle$ is on the order 1.

In this sense, the role played by vacuum energy in gravitational system is similar to its role in the non-gravitational mirror systems—it appears both at (8.10) and (8.14) to show the strongness of vacuum fluctuations at microscopic scales (for mirrors, microscopic means atomic scale; for gravity, microscopic means Planck scale) and their observable effects are both small at macroscopic scales.

By this same kind of mechanism, the violent gravitational effect produced by the vacuum energy density is confined to Planck scales, and its effect at macroscopic scales—the accelerating expansion of the Universe, due to the weak parametric resonance is so small that, it is only observable after accumulations on the largest scale—the cosmological scale.

Chapter 9

The singularities at $a(t, \mathbf{x}) = 0$

In our way of vacuum gravitating, the space is alternatively expanding and contracting at each spatial point, and, during each such cycle, the expansion outweighs the contraction a little bit due to the weak parametric resonance effect. This process gives a slowly increasing amplitude $A(t, \mathbf{x})$ of the scale factor $a(t, \mathbf{x})$, whose observable effect is just the accelerating expansion of our Universe.

Probably one of the biggest concerns about this physical picture is the appearance of singularities at points $a(t, \mathbf{x}) = 0$ —according to the solution (5.8), the scale factor $a(t, \mathbf{x})$ must go through zero whenever the space at \mathbf{x} switches from contraction phase to expansion phase. In this section, we are going to discuss this issue of singularities.

9.1 Is singularity an end or a new beginning?

Singularities are a generic feature of the solution of Einstein field equations under rather general energy conditions (e.g. strong, weak, dominant etc.), which is guaranteed by Penrose-Hawking singularity theorems [53–58]. In this paper, since we investigate the gravitational property of quantum vacuum without modifying either QFT or GR, the appearance of singularities is inevitable—QFT predicts a huge vacuum energy, and according to GR, huge energy must collapse to form singularity.

The Raychaudhuri equation (7.42) serves as a fundamental lemma for the Penrose-Hawking singularity theorems. This lemma says that if the strong energy condition is satisfied, the expansion θ , which is defined by (7.38), must satisfy the following inequality:

$$\frac{1}{\theta} \geq \frac{1}{\theta_0} + \frac{\tau}{3}, \quad (9.1)$$

where θ_0 is the initial value of θ . If θ_0 is negative, then (9.1) implies that $1/\theta$ must pass through zero, i.e. $\theta \rightarrow -\infty$, within a proper time $\tau \leq 3/|\theta_0|$. This usually signals an encounter with a curvature singularity (although not necessarily) and in our case it is indeed a singularity.

It is usually thought that the Einstein field equations break down at singularities and thus the spacetime evolution will stop once the singularity is formed. However, it is not the case for our solution to the key dynamic evolution equation (4.19), which describes the oscillating motion of a harmonic oscillator. It is natural for a harmonic oscillator to pass its equilibrium point $a(t, \mathbf{x}) = 0$ at maximum speed without stopping. From the calculation (7.47) we know that θ is just $3\dot{a}/a$ that as $a \rightarrow 0^+$, $\theta \rightarrow -\infty$ and as time goes on, a quickly passes 0 and θ jumps discontinuously from $-\infty$ to $+\infty$ and the spacetime evolution start again. In this process, the metric a is still continuous, although the expansion θ is not.

So in our solution, the singularity immediately disappears after it forms and the spacetime continues to evolve without stopping. Singularities are not endings but new beginnings. They serve as the turning points at which the space switches from contraction phase to expansion phase.

9.2 Resolving singularity by multiplying a

In order to understand better why in our solution the singularity is not the end of spacetime evolution, it is helpful to review one crucial step in deriving (4.19) from (4.18). Rigorously speaking, we can only obtain the following equation from (4.18):

$$-\frac{\ddot{a}}{a} = \Omega^2(t, \mathbf{x}), \quad (9.2)$$

which is not equivalent to (4.19). To get (4.19), we need one more step—multiply both sides of (9.2) by a .

Mathematically, a is not allowed to be zero in (9.2) since it is in the denominator. In fact, when writing down the Einstein field equations (4.2), (4.3), (4.4) and (4.5), it has been presumed that $a \neq 0$ since if $a = 0$, the metric would become degenerate ($g = \det(g_{\mu\nu}) = -a^6 = 0$), the curvature would become infinite and the Einstein tensor are simply not defined there.

But, after the inequivalent algebraic manipulation of multiplying both sides of (9.2) by a , a is allowed to evolve to zero in the resulting equation (4.19) since there is nothing wrong for a harmonic oscillator to go through its equilibrium point. In this sense, we have smoothly extended the solution beyond the singularity by the mathematical operation of multiplying both sides of (9.2) by a (or more generally by some power of the metric determinant).

The idea of resolving a singularity by multiplying Einstein equations with some power of the determinant of the metric is not new. Einstein him-

self had proposed this idea with his collaborator Rosen in 1935 (for which they credited this idea to Mayer) [59]. Ashtekar used a similar trick in his method of “new variables” to develop an equivalent Hamiltonian formulation of GR [60]. It is also proposed by Stoica that the equations obtained after multiplying the usual Einstein equations by some power of the metric determinant are actually more fundamental than the usual Einstein equations [61–69]. In this sense, we argue that our spacetime with singularities due to the metric becoming degenerate ($a = 0$) is a legitimate solution of GR.

9.3 Singularities do not cause problems

While singularities are natural and inevitable in solutions to Einstein’s equations, we must discuss the consequences they bring to this calculation.

Will the singularities cause serious problems? At least in our case we do not feel they cause problems.

To see this, we investigate how the singularities affect the propagation of the field modes in our toy model (6.12).

In this toy model, the spacetime have singularities at the hypersurfaces

$$\Theta = \Omega t + \mathbf{K} \cdot \mathbf{x} = \left(n + \frac{1}{2}\right)\pi, \quad n = 0, \pm 1, \pm 2, \pm 3, \dots \quad (9.3)$$

Using the relation $x_m = -x_{-m}$, which is evident from (6.28) and (6.29), the asymptotic mode solution (6.38) becomes

$$u_{\mathbf{k}}(t, \mathbf{x}) = c_0 e^{-i(\omega t - \mathbf{k} \cdot \mathbf{x})} \left(1 + 2i\epsilon \sum_{m=1}^{+\infty} x_m \sin 2m\Theta \right). \quad (9.4)$$

At the singularities (9.3), the correction terms $\sin 2m\Theta$ of (9.4) are all zero and thus we have

$$u_{\mathbf{k}}(t, \mathbf{x}) = c_0 e^{-i(\omega t - \mathbf{k} \cdot \mathbf{x})} \quad (9.5)$$

So the value of $u_{\mathbf{k}}$ is normal at singularities.

However, the stress energy tensor (4.22) for the field ϕ , which sources the Einstein field equations (4.2), (4.3), (4.4) and (4.5), mainly contains time

9.3. Singularities do not cause problems

and spatial derivatives of ϕ :

$$3 \left(\frac{\dot{a}}{a} \right)^2 + \frac{1}{a^2} \left(\frac{\nabla a}{a} \right)^2 - \frac{2}{a^2} \left(\frac{\nabla^2 a}{a} \right) = 4\pi G \left(\dot{\phi}^2 + \frac{1}{a^2} (\nabla \phi)^2 \right) \quad (9.6)$$

$$\begin{aligned} & -2a\ddot{a} - \dot{a}^2 - \left(\frac{\nabla a}{a} \right)^2 + \frac{\nabla^2 a}{a} + 2 \left(\frac{\partial_i a}{a} \right)^2 - \frac{\partial_i^2 a}{a} \\ & = 8\pi G \left((\partial_i \phi)^2 + \frac{1}{2} (a^2 \dot{\phi}^2 - (\nabla \phi)^2) \right), \end{aligned} \quad (9.7)$$

$$2 \frac{\dot{a}}{a} \frac{\partial_i a}{a} - 2 \frac{\partial_i \dot{a}}{a} = 8\pi G \dot{\phi} \partial_i \phi, \quad (9.8)$$

$$2 \frac{\partial_i a}{a} \frac{\partial_j a}{a} - \frac{\partial_i \partial_j a}{a} = 8\pi G \partial_i \phi \partial_j \phi, \quad i, j = 1, 2, 3, \quad i \neq j. \quad (9.9)$$

Especially, the Ω^2 in our key dynamic equation (4.19) is (see Eq.(4.24))

$$\Omega^2 = \frac{8\pi G}{3} \dot{\phi}^2. \quad (9.10)$$

Therefore, one has to investigate how the derivatives of ϕ behave at the singularities to assess the influence of the singularities on our calculations. To do this, we plot the correction function

$$f(\Theta) = \sum_{m=1}^{+\infty} x_m \sin 2m\Theta \quad (9.11)$$

to the mode solution $u_{\mathbf{k}}$ defined by (9.4) and its derivative around the singularity at $\Theta = \pi/2$. The sum in the plots are from $m = 1$ to $m = 20000$. The result are shown in FIG. 9.1 and FIG. 9.2.

It can be seen from FIG. 9.1 and FIG. 9.2 that the derivative of $f(\Theta)$ is almost constant except suddenly goes to infinity when approaching the spacetime singularity at $\Theta = \pi/2$. Therefore, the property of Ω^2 does not change beyond the singularity. It suddenly goes to infinity as $a \rightarrow 0$.

This sudden change at the singularity should not alter the dynamics of our key equation (4.19) for the two following reasons: i) a passes through 0 within an extremely short period Δt since a harmonic oscillator reaches maximum speed at the equilibrium point. So the change in the momentum of the oscillator due to the singularity $\Delta P = F \Delta t = -\Omega^2 a \Delta t$ as $a \rightarrow 0$ will be small ($\Omega^2 \rightarrow +\infty$ but $a \rightarrow 0$ so F does not necessarily blow up); ii) From FIG. 9.1 we see that the correction to Ω^2 around $a = 0$ is symmetric that the effect of F should be canceled that $\Delta P \rightarrow 0$.

9.3. Singularities do not cause problems

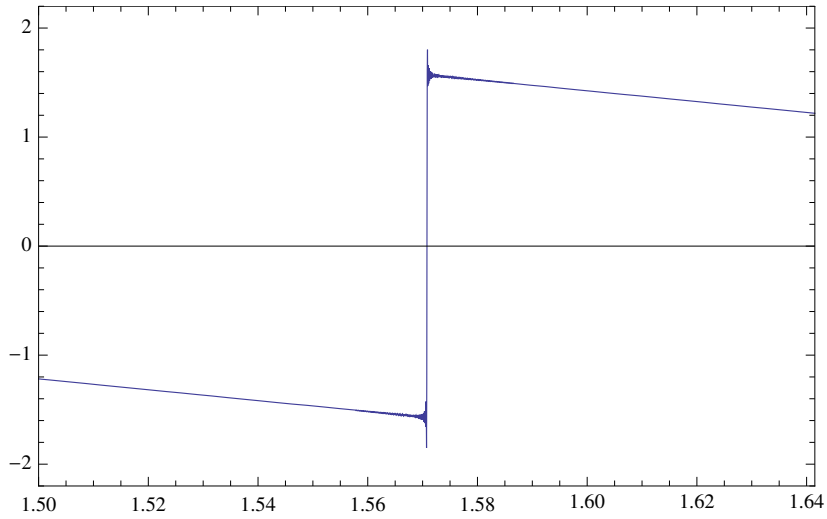


Figure 9.1: Plot of the correction function $f(\Theta) = \sum_{m=1}^{+\infty} x_m \sin 2m\Theta$ around the spacetime singularity at $\Theta = \Omega t + \mathbf{K} \cdot \mathbf{k} = \pi/2$, where the sum in the plot is from $m = 1$ to $m = 20000$.

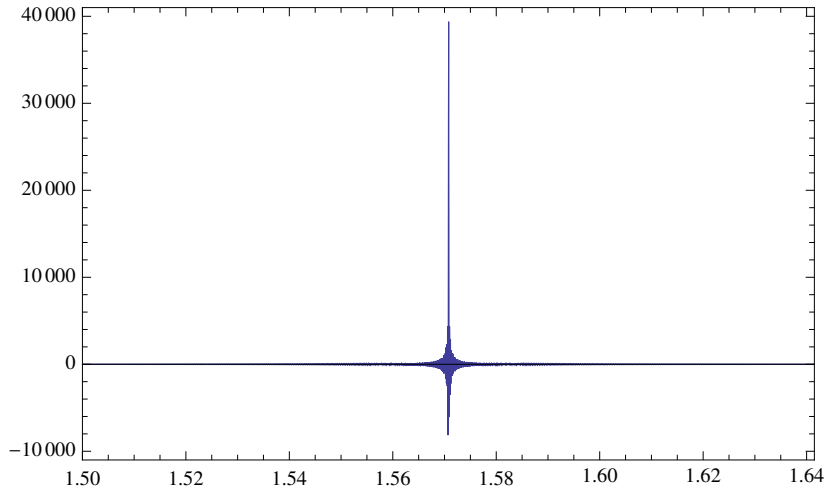


Figure 9.2: Plot of the derivative of the correction function $\frac{df(\Theta)}{d\Theta} = \sum_{m=1}^{+\infty} 2mx_m \cos 2m\Theta$ around the spacetime singularity at $\Theta = \Omega t + \mathbf{K} \cdot \mathbf{k} = \pi/2$, where the sum in the plot is from $m = 1$ to $m = 20000$.

9.3. Singularities do not cause problems

So we have argued that a goes through 0 is not a problem for the key equation (4.19) we used. But is it a problem for other Einstein equations (9.6), (9.7), (9.8) and (9.9)? If we stick the solution (5.8) for a into these equations, the left-hand side would blow up at $a = 0$, which requires that the time and spatial derivatives of ϕ on the right-hand side must also blow up (see eq. (9.8), (9.9)). As we can see from the plot of the correction to the mode solution $u_{\mathbf{k}}$ of ϕ in FIG. 9.1, $\dot{\phi}$ and $\nabla\phi$ do blow up at $a = 0$, so our solution (5.8) for a is also consistent with these other Einstein equations.

The blow up of $\dot{\phi}$ at $a = 0$ seems invalidated our calculation at first glance since we have implicitly assumed that Ω^2 behaves normal all the time to be able to vary slowly, which is the key property we used to solve (4.19). However, because of the two reasons we have argued, this should not alter the dynamics of (4.19).

Chapter 10

A different model with a large bare cosmological constant (unsuccessful)

In this chapter we introduce a different model with a large negative bare cosmological constant. This model was motivated to cure the original model published in [1] after the mistakes in the numerical calculation were found. In this model, instead of discarding the bare cosmological constant λ_b and taking the high energy cutoff Λ to infinity, we keep the bare constant λ_b and take it to negative infinity with Λ fixed. This model does have some advantages over the original one, but unfortunately a fatal flaw was founded. We include this model here since even unsuccessful attempt could still be valuable in scientific research.

10.1 The formulation of the cosmological constant problem is destroyed by density fluctuations of quantum vacuum

Consider a new model⁶ in which we keep the bare cosmological constant λ_b :

$$ds^2 = -dt^2 + a^2(t, \mathbf{x})(dx^2 + dy^2 + dz^2). \quad (10.1)$$

⁶See chapter 4 for more details about this model.

10.1. *The formulation of the cosmological constant problem is destroyed by density fluctuations of quantum vacuum*

$$G_{00} = 3 \left(\frac{\dot{a}}{a} \right)^2 + \frac{1}{a^2} \left(\frac{\nabla a}{a} \right)^2 - \frac{2}{a^2} \left(\frac{\nabla^2 a}{a} \right) = 8\pi GT_{00} + \lambda_b, \quad (10.2)$$

$$\begin{aligned} G_{ii} &= -2a\ddot{a} - \dot{a}^2 - \left(\frac{\nabla a}{a} \right)^2 + \frac{\nabla^2 a}{a} + 2 \left(\frac{\partial_i a}{a} \right)^2 - \frac{\partial_i^2 a}{a} \\ &= 8\pi GT_{ii} - \lambda_b a^2, \end{aligned} \quad (10.3)$$

$$G_{0i} = 2 \frac{\dot{a}}{a} \frac{\partial_i a}{a} - 2 \frac{\partial_i \dot{a}}{a} = 8\pi GT_{0i}, \quad (10.4)$$

$$G_{ij} = 2 \frac{\partial_i a}{a} \frac{\partial_j a}{a} - \frac{\partial_i \partial_j a}{a} = 8\pi GT_{ij}, \quad i, j = 1, 2, 3, \quad i \neq j, \quad (10.5)$$

where $\nabla = (\partial_1, \partial_2, \partial_3)$ is the ordinary gradient operator with respect to the spatial coordinates x, y, z .

A linear combination of equations (10.2) and (10.3) gives,

$$G_{00} + \frac{1}{a^2} (G_{11} + G_{22} + G_{33}) = -\frac{6\ddot{a}}{a}, \quad (10.6)$$

where all the spatial derivatives of a cancel and only the second order time derivative left. Therefore we reach the following dynamic evolution equation for $a(t, \mathbf{x})$:

$$\ddot{a} + \Omega^2(t, \mathbf{x})a = 0, \quad (10.7)$$

where

$$\Omega^2 = \frac{4\pi G}{3} \left(\rho + \sum_{i=1}^3 P_i \right) - \frac{\lambda_b}{3}, \quad \rho = T_{00}, P_i = \frac{1}{a^2} T_{ii}. \quad (10.8)$$

(10.7) is just a generalization of the second Friedman equation (2.12). In the usual renormalization approach, λ_b is chosen very precisely to cancel the expectation value of the first term $\rho + \sum_{i=1}^3 P_i$ in (10.8). Suppose that we have successfully fine-tuned λ_b to an accuracy of 10^{-122} that the expectation value of the Ω^2 in (10.8)

$$\langle \Omega^2 \rangle = -\lambda_{\text{eff}}/3 = -1.86 \times 10^{-122} \quad (10.9)$$

in Planck units. Because of the huge fluctuations in $\rho + \sum_{i=1}^3 P_i$, Ω^2 would have large chances to fluctuate to both large negative and positive values. When Ω^2 fluctuates to negative values, a roughly grows exponentially

$$a \sim e^{|\Omega|t} \sim e^{\sqrt{G}\Lambda^2 t} \sim e^{E_P t} \gg e^{10^{-61} E_P t}, \quad (10.10)$$

where E_P is Planck energy, the high energy cutoff $\Lambda \sim E_P$ has been taken to be Planck energy in the above estimation and 10^{-61} is the current order of

magnitude of Hubble expansion rate in Planck units. When Ω^2 fluctuates to a positive value, (10.7) becomes a harmonic oscillator with time dependent frequency and parametric resonance ⁷ would happen that a would roughly go as

$$a \sim e^{\tilde{H}t} P, \quad (10.11)$$

where P is a quasiperiodic function oscillating around 0. In this case, $\Omega \sim \sqrt{G}\Lambda^2$ while the varying frequency of Ω itself is roughly Λ . As taking $\Lambda \sim E_P$, the two frequency closes to each other that the parametric resonance would be strong.

Therefore, the density fluctuations would cause large deviations from (2.13) and the universe would still explode even one has successfully fine-tuned λ_b to an accuracy of 10^{-122} . Moreover, the relation (2.7) which describes the dependence of the observed effective cosmological constant λ_{eff} on the bare cosmological constant λ_b is destroyed by these fluctuations. A new relation between λ_{eff} and λ_b is needed.

10.2 New relation between λ_{eff} and λ_b

Since the matter fields ⁸ in (10.8) go as

$$\frac{4\pi G}{3} \left(\rho + \sum_{i=1}^3 P_i \right) \sim (\pm) G\Lambda^4, \quad (10.12)$$

the time dependent frequency Ω^2 would average around

$$\langle \Omega^2 \rangle \sim -\frac{\lambda_b}{3} \pm G\Lambda^4. \quad (10.13)$$

Something interesting happens if $-\lambda_b$ is taken to the range $-\lambda_b \gg \Lambda^2 \geq G\Lambda^4$, assuming $\Lambda \leq E_P$ (see FIG. 10.1). In this limit, i) the probability that Ω^2 fluctuates to negative values goes to zero; ii) the strength of the parametric resonance goes to zero. Thus the Hubble expansion rate $H \rightarrow 0$ and then the effective cosmological constant $\lambda_{\text{eff}} = 3H^2 \rightarrow 0$ as $-\lambda_b \rightarrow +\infty$. In the following we give an expression for the dependence of λ_{eff} on λ_b in this regime.

⁷See chapter 5.1 for more detailed explanation about the parametric resonance effect.

⁸The sign of (10.12) is not known. In principle all known and unknown fundamental fields in nature would contribute. Boson fields give positive signs to ρ but Fermion fields give negative signs to ρ . Since we do not have the knowledge about all of them, the sign can not be determined.

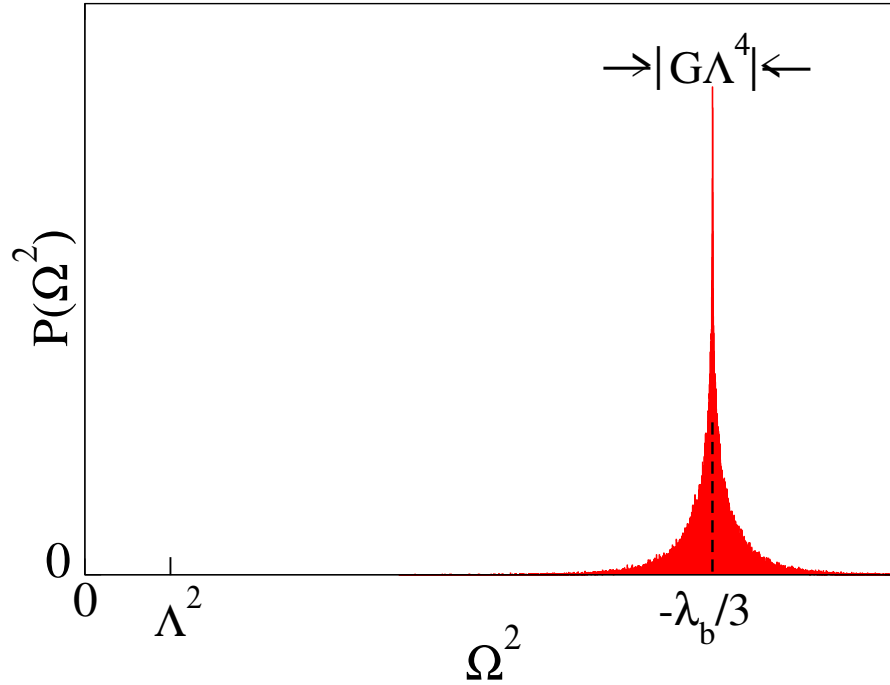


Figure 10.1: An illustration of the probability density distribution $P(\Omega^2)$. The shape of the graph is obtained from the histogram of a sample of $\Omega^2(t)$ we used in the numerical simulation 10.3. This is for one boson and one fermion field. The tails fall as $e^{-\kappa|\Omega^2+\lambda_b/3|}$ (as shown in FIG. 10.2) for large argument where κ is some constant.

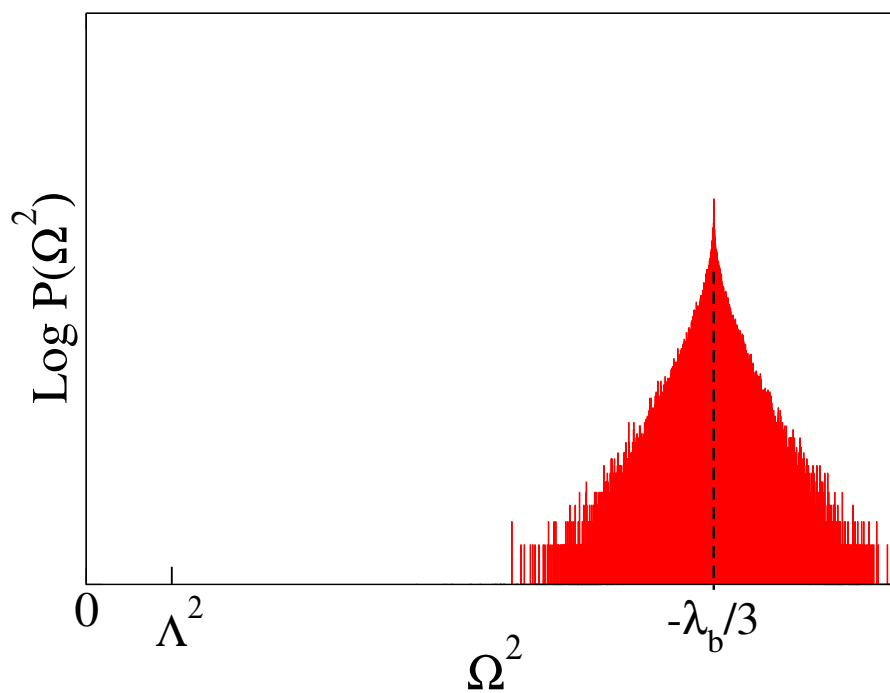


Figure 10.2: Plot of $\log(\Omega^2)$ which shows the tail of $P(\Omega^2)$ falls as $e^{-\kappa|\Omega^2+\lambda_b/3|}$ for large argument where κ is some constant.

Due to quantum fluctuation, we assume that Ω^2 can possibly fluctuate to any values. Different values of Ω^2 give different dynamics of the equation(10.7). All possible values of Ω^2 can be divided into two cases: i) $\Omega^2 < 0$ or $\Omega \sim \Lambda$; ii) $\Omega \gg \Lambda$.

Case I: $\Omega^2 < 0$ or $\Omega \sim \Lambda$. The probability that Ω^2 fluctuates to these values is exponentially suppressed, since $\rho + \sum_{i=1}^3 P_i$ approximately obeys chi-square distributions. In fact, a free quantum field may be viewed as a collection of decoupled, time-independent, harmonic oscillators. At ground state, each oscillator satisfies Gaussian distribution, and the sum of Gaussian distributions are still Gaussian distributions. Since $\rho + \sum_{i=1}^3 P_i$ is in general contains squares of the time and spatial derivatives of the fields, it would approximately obey chi-square distributions. The probability density function $f(x)$ of a chi-square distribution roughly goes as $\sim e^{-\kappa x}$ as x large (as shown in FIG. 10.2), where κ is some constant. Therefore, the contribution to the growth of a from this case is proportional to

$$H \propto e^{-\tilde{\beta}(-\frac{\lambda_b}{3} - \frac{4\pi G}{3}\langle\rho + \sum_{i=1}^3 P_i\rangle)} \propto e^{\tilde{\beta}\lambda_b}, \quad \text{as } -\lambda_b \gg \Lambda^2 \geq G\Lambda^4, \quad (10.14)$$

where we have absorbed the numerical factor $1/3$ into the constant $\tilde{\beta}$. FIG. 10.4 shows that $\tilde{\beta} = 6.09$ for the matter fields used in the numerical simulation 10.3.

Case II: $\Omega \gg \Lambda$. In this case, since Ω itself varies on the time scale $1/\Lambda$, which is much longer than the time scale $1/\Omega$ of the oscillation of a , this process is basically adiabatic⁹. It has been well-established that the error in adiabatic invariant is exponentially small [22, 24]. Thus we would expect that in this case the strength of the parametric resonance would also be exponentially suppressed. To obtain more detailed estimation, we only need to follow exactly the same steps of Chapter 5.3 with $\Omega \sim \sqrt{G}\Lambda^2$ replaced by $\Omega \sim \sqrt{\frac{4\pi G}{3}\langle\rho + \sum_{i=1}^3 P_i\rangle - \lambda_b/3} \sim \sqrt{\pm G\Lambda^4 - \lambda_b/3}$. Then the contribution to the growth of a from this case is proportional to

$$H \propto \Lambda e^{-\beta \frac{\sqrt{\pm G\Lambda^4 - \lambda_b/3}}{\Lambda}} \sim \Lambda e^{-\beta \frac{\sqrt{-\lambda_b}}{\Lambda}}, \quad \text{as } -\lambda_b \gg \Lambda^2 \geq G\Lambda^4, \quad (10.15)$$

where we have absorbed the numerical factor into β .

⁹See chapter 5.2 for detailed analysis about this process.

10.3. Numerical simulation

When $|\lambda_b|$ is large, the contribution to H from (10.14) drops faster than the contribution from (10.15). So (10.15) is dominant:

$$H = \alpha\Lambda e^{-\beta\frac{\sqrt{-\lambda_b}}{\Lambda}}, \quad \text{as } -\lambda_b \gg \Lambda^2 \geq G\Lambda^4, \quad (10.16)$$

where $\alpha, \beta > 0$ are two dimensionless constants. This gives a different relation between the observed effective cosmological constant λ_{eff} and the bare cosmological constant λ_b :

$$\lambda_{\text{eff}} = 3H^2 = \alpha^2\Lambda^2 e^{-2\beta\frac{\sqrt{-\lambda_b}}{\Lambda}}, \quad \text{as } -\lambda_b \gg \Lambda^2 \geq G\Lambda^4. \quad (10.17)$$

10.3 Numerical simulation

We follow the same numerical method as described in chapter 5.7 and appendix B. The difference is that the source of gravity is taken to be one Boson field and one Fermion field. The contribution to $\langle\Omega^2\rangle$ from the Boson field is set to be $G\Lambda^4/6\pi$ and from the Fermion field is set to be $-G\Lambda^4/6\pi$, i.e. we set $\langle\rho + \sum_{i=1}^3 P_i\rangle = 0$ in the simulation.

The numerical simulation for the regime $|\lambda_b|$ is small is shown in FIG. 10.3 and FIG. 10.4. FIG. 10.3 shows that the Hubble expansion rate H decreases as $-\lambda_b$ increases. FIG. 10.4 shows that this decrease is exponential as predicted by (10.14) and the parameter $\tilde{\beta}$ there is around 6 in this setting. Note that the red line ($\lambda_b = 0$) in FIG 10.3 represents the case $\langle\rho^{\text{vac}}\rangle = 0$ (or λ_{eff} has been tuned to zero in the usual sense). It clearly shows that the universe is exploding instead of stay still because of the density fluctuation of quantum vacuum, i.e. even if one has successfully fine-tuned the cosmological constant to the usually required accuracy of 10^{-122} , the problem of rapid exponential expansion of the universe driven by the large vacuum energy is still not resolved.

The numerical simulation for the regime $|\lambda_b|$ is large is shown in FIG. 10.5 and FIG. 10.6. FIG. 10.5 shows that the Hubble expansion rate H decreases as $-\lambda_b$ increases. FIG. 10.6 shows that this decrease is exponential as predicted by (10.16) and the parameters $\alpha \sim e^{18}$, $\beta \sim 14$ in this setting. The error bar for the slope of the lines in FIG. 10.5 is big that the fitting parameters α and β obtained in FIG. 10.6 may not be accurate. These parameters would also depend on the matter fields we used. But FIG. 10.6 at least gives an estimation that α is somewhere between e^{10} to e^{20} and β is somewhere between 10 to 20. These values are not accurate but it is not important for our model to work as explained in the next subsection.

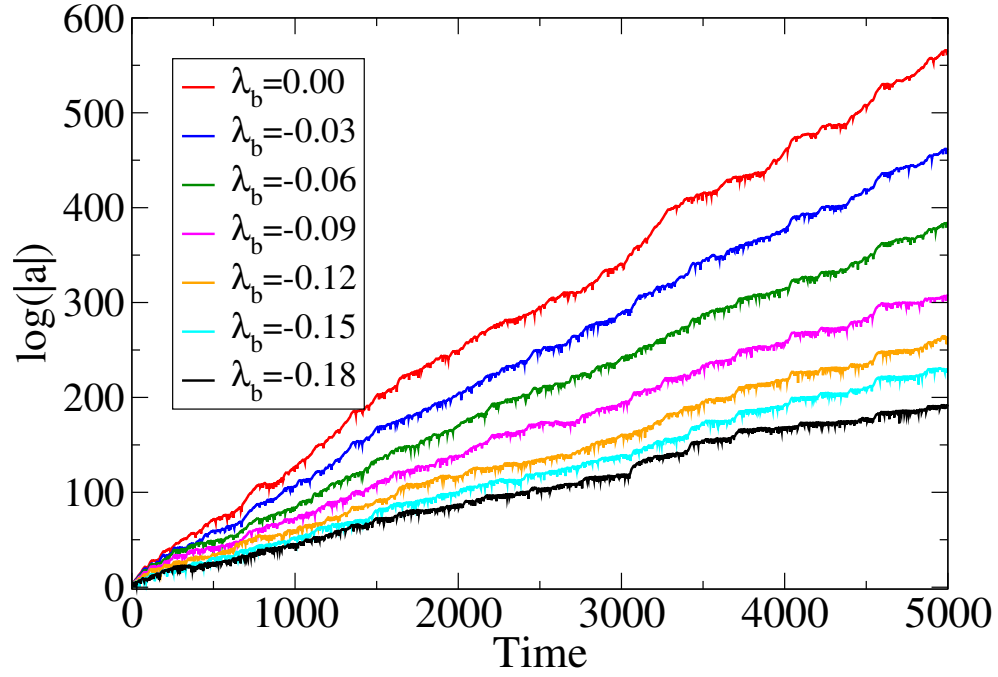


Figure 10.3: Numerical result for the dependence of $\log|a|$ on the bare cosmological constant λ_b as $|\lambda_b|$ is small. The cutoff $\Lambda = 1$. 100 samples are averaged for each line. Planck units are used for convenience. The matter fields are one Boson field and one Fermion field. The magnitude of $\langle \rho + \sum_{i=1}^3 P_i \rangle$ for both fields are set equal but with opposite sign, i.e. we set $\langle \rho + \sum_{i=1}^3 P_i \rangle = 0$ in the simulation. It shows that the Hubble expansion rate decreases as $-\lambda_b$ increases.

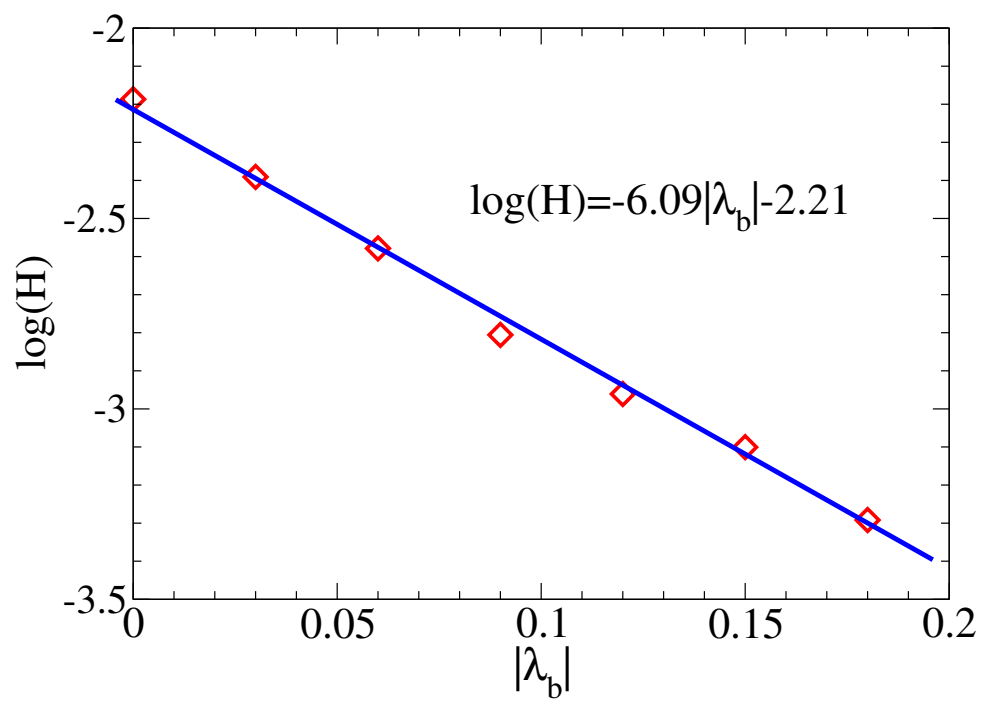


Figure 10.4: Plot of $\log H$ over $|\lambda_b|$ when $|\lambda_b|$ is small. The fitting result shows that $\tilde{\beta} \sim 6$. Planck units are used for convenience.

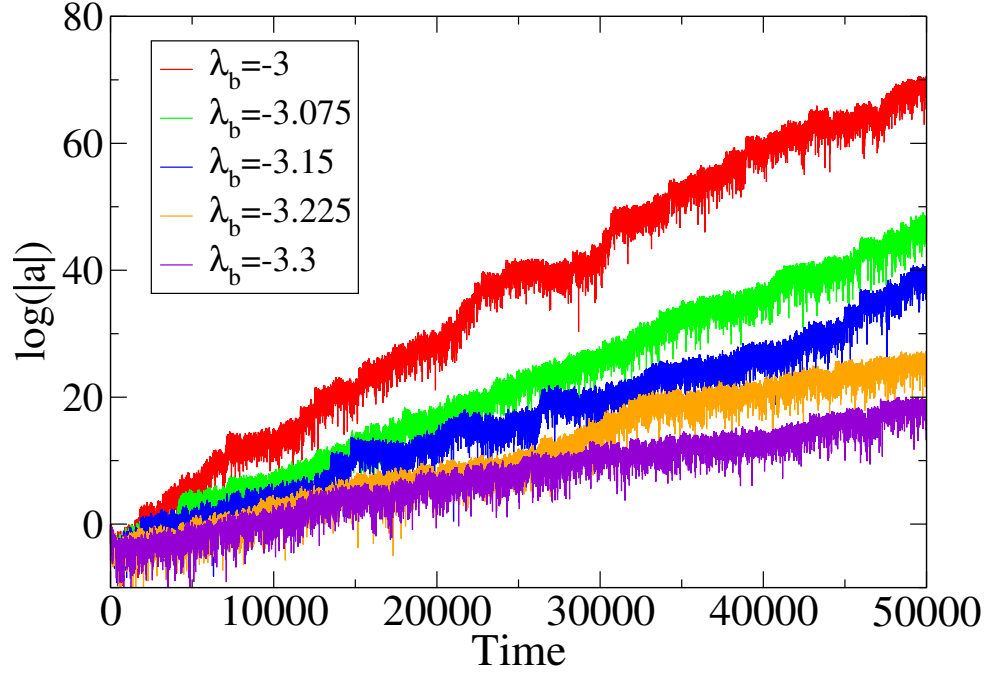


Figure 10.5: Numerical result for the dependence of $\log |a|$ on the bare cosmological constant λ_b as $|\lambda_b|$ is large. The cutoff $\Lambda = 1$. 400 samples are averaged for each line. Planck units are used for convenience. The matter fields are one Boson field and one Fermion field. The magnitude of $\langle \rho + \sum_{i=1}^3 P_i \rangle$ for both fields are set equal but with opposite sign, i.e. we set $\langle \rho + \sum_{i=1}^3 P_i \rangle = 0$ in the simulation. It shows that the Hubble expansion rate decreases as $-\lambda_b$ increases. For larger $-\lambda_b$ the slope of $\log |a|$ grows too slow that the numerical rounding errors seem to dominant.

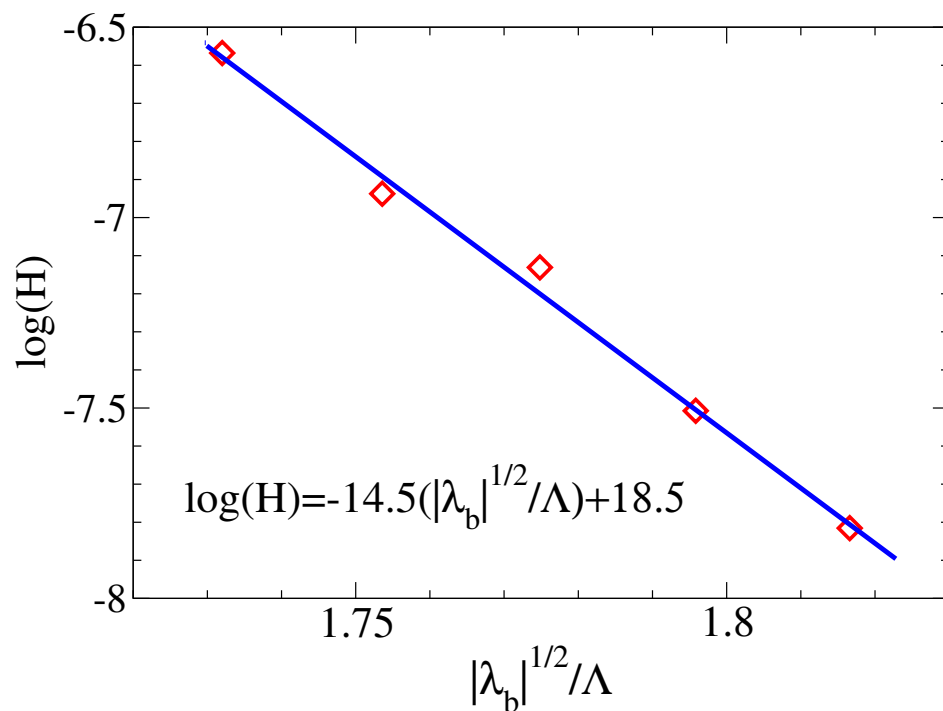


Figure 10.6: Plot of $\log H$ over $\sqrt{|\lambda_b|}$ when $|\lambda_b|$ is large. The fitting result shows that $\alpha \sim e^{18}, \beta \sim 14$. Planck units are used for convenience. The cutoff $\Lambda = 1$.

10.4 Meaning of the results

In this section we use Planck units for convenience.

The usual relation between λ_{eff} and λ_b which missed the important effect from the large density fluctuation of quantum vacuum is given by

$$\lambda_{\text{eff}} = \lambda_b + 8\pi\rho^{\text{vac}}, \quad (10.18)$$

Since ρ^{vac} (~ 1 if take the cutoff $\Lambda = 1$) is larger than $\lambda_{\text{eff}} = 5.6 \times 10^{-122}$ (Planck units is used here) by 50 to 122 orders of magnitude depending on the cutoff energy scale Λ , λ_b has to be extremely fine-tuned to a precision of at least 50 decimal places.

However, once the effect of the density fluctuation is included, the quantum vacuum gravitates in a different way that the relation between λ_{eff} and λ_b becomes the equation (10.17). Rewrite (10.17) as

$$-\frac{\Lambda}{2\beta} \log(\lambda_{\text{eff}}) = \sqrt{-\lambda_b} - \frac{\Lambda}{2\beta} \log(\alpha^2 \Lambda). \quad (10.19)$$

The numerical simulation in 10.3 gives an estimation that α is somewhere between e^{10} to e^{20} and β is somewhere between 10 to 20, for one Boson field and one Fermion field. If we take $\Lambda = 1$, i.e. the Planck energy, we would have

$$-\frac{\Lambda}{2\beta} \log(\lambda_{\text{eff}}) \sim 10, \quad \frac{\Lambda}{2\beta} \log(\alpha^2 \Lambda) \sim 1. \quad (10.20)$$

In this case, since the term $-\frac{\Lambda}{2\beta} \log(\lambda_{\text{eff}})$ is only different from the term $\frac{\Lambda}{2\beta} \log(\alpha^2 \Lambda)$ by 1 order of magnitude, the term $\sqrt{-\lambda_b}$ only need to be tuned to an accuracy of 10^{-1} or λ_b only need to be tuned to an accuracy of 10^{-2} to satisfy (10.19).

In general, the difference in the order of magnitude between the two terms $-\frac{\Lambda}{2\beta} \log(\lambda_{\text{eff}})$ and $\frac{\Lambda}{2\beta} \log(\alpha^2 \Lambda)$ in (10.19) is mainly determined by the value of α . α cannot be precisely determined because of the limitation of numerical simulation and the lack of the knowledge about the contribution to $\rho + \sum_{i=1}^3 P_i$ from all fundamental fields in nature. But this does not matter. Even if α could take values in the range from 1 to e^{100} , we would have $\log(\alpha^2)$ in the range from 0 to 200. This is different from the term $-\log(\lambda_{\text{eff}}) = 279$ by at most the order of 10^2 . Then $\sqrt{-\lambda_b}$ at most needs to be tuned to an accuracy of 10^{-2} and λ_b at most needs to be tuned to an accuracy of 10^{-4} . Therefore, the extreme fine-tuning of the bare cosmological constant to match the observation is no long needed.

10.5 Problem of this model

In this model, we still presumed that the inhomogeneous “spatially flat” FLRW metric of the form (10.1). Unfortunately, it turns out that Einstein equations with a large negative bare cosmological constant cannot be fitted in this metric.

In fact, since we require that $-\lambda_b \gg \Lambda^2 \geq G\Lambda^4$, i.e. the cosmological constant is dominant over the zero point fluctuations. Therefore, the solution to the Einstein equations must be a small perturbation from the solution of vacuum Einstein equations in which the only term in the stress-energy tensor is a negative cosmological constant term, which is well known to be the anti-de Sitter space.

Let us derive the solution in detail. We start with the Einstein field equations without matter fields but with a bare cosmological constant:

$$G_{\mu\nu} + \lambda_b g_{\mu\nu} = 0. \quad (10.21)$$

Then we have the homogeneous FLRW metric

$$ds^2 = -dt^2 + a^2(t)d\Sigma^2, \quad (10.22)$$

where

$$d\Sigma^2 = \frac{1}{1 - kr^2} dr^2 + r^2(d\theta^2 + \sin^2\theta d\varphi^2), \quad (10.23)$$

where k is a constant representing the curvature of the space.

The Einstein equations are

$$G_{00} = 3\left(\frac{\dot{a}}{a}\right)^2 + \frac{3k}{a^2} = \lambda_b, \quad (10.24)$$

$$G_{11} = \frac{1}{1 - kr^2} (-2a\ddot{a} - \dot{a}^2 - k) = -\frac{\lambda_b a^2}{1 - kr^2}, \quad (10.25)$$

$$G_{22} = r^2 (-2a\ddot{a} - \dot{a}^2 - k) = -r^2 \lambda_b a^2, \quad (10.26)$$

$$G_{33} = r^2 \sin^2\theta (-2a\ddot{a} - \dot{a}^2 - k) = -r^2 \sin^2\theta \lambda_b a^2, \quad (10.27)$$

$$G_{0i} = G_{ij} = 0, \quad i, j = 1, 2, 3 = r, \theta, \varphi, i \neq j. \quad (10.28)$$

Since λ_b is negative, k must also be negative according to (10.24).

Equations (10.25), (10.26) and (10.27) are the same. A Linear combination of (10.24), (10.25), (10.26) and (10.27) gives

$$G_{00} + \sum_{i=1}^3 g^{ii} G_{ii} = -\frac{6\ddot{a}}{a} = -2\lambda_b. \quad (10.29)$$

10.5. Problem of this model

Therefore, we have

$$\ddot{a} - \frac{\lambda_b}{3}a = 0. \quad (10.30)$$

For a negative bare cosmological constant λ_b , the solution to (10.30) under the constraint equation (10.24) are

$$a(t) = \sqrt{\frac{3k}{\lambda_b}} \cos \left(\sqrt{-\frac{\lambda_b}{3}}t + \gamma \right), \quad (10.31)$$

where $\lambda_b, k < 0$, γ is an arbitrary phase constant. This gives the solution to the full Einstein equations (10.24), (10.25), (10.26), (10.27) and (10.28).

Next let us add fluctuating matter fields to the Einstein equations:

$$G_{\mu\nu} + \lambda_b g_{\mu\nu} = 8\pi G T_{\mu\nu}. \quad (10.32)$$

Assuming the metric takes the following form to account for the inhomogeneities produced by quantum fluctuations:

$$ds^2 = -dt^2 + a^2(t, r, \theta, \varphi)d\Sigma^2, \quad (10.33)$$

Then the Einstein equations becomes

$$G_{00} = 3 \left(\frac{\dot{a}}{a} \right)^2 + \frac{3k}{a^2} + \frac{4kr\partial_r a}{a^3} + \frac{(\nabla a)^2}{a^4} - \frac{2\nabla^2 a}{a^3} = \lambda_b + 8\pi G T_{00}, \quad (10.34)$$

$$\begin{aligned} G_{11} &= \frac{1}{1-kr^2} \left(-2a\ddot{a} - \dot{a}^2 - k - \frac{(\nabla a)^2}{a^2} + \frac{\nabla^2 a}{a} + 2(1-kr^2)\frac{(\partial_r a)^2}{a^2} \right. \\ &\quad \left. - (1-kr^2)\frac{\partial_r^2 a}{a} - kr\frac{\partial_r a}{a} \right) \\ &= -\frac{\lambda_b a^2}{1-kr^2} + 8\pi G T_{11}, \end{aligned} \quad (10.35)$$

$$\begin{aligned} G_{22} &= r^2 \left(-2a\ddot{a} - \dot{a}^2 - k - \frac{(\nabla a)^2}{a^2} + \frac{\nabla^2 a}{a} + \frac{2(\partial_\theta a)^2}{r^2 a^2} - \frac{\partial_\theta^2 a}{r^2 a} - \left(\frac{1}{r} + kr \right) \frac{\partial_r a}{a} \right) \\ &= -r^2 \lambda_b a^2 + 8\pi G T_{22}, \end{aligned} \quad (10.36)$$

$$\begin{aligned} G_{33} &= r^2 \sin^2 \theta \left(-2a\ddot{a} - \dot{a}^2 - k - \frac{(\nabla a)^2}{a^2} + \frac{\nabla^2 a}{a} + \frac{2(\partial_\varphi a)^2}{r^2 \sin^2 \theta a^2} \right. \\ &\quad \left. - \frac{\partial_\varphi^2 a}{r^2 \sin^2 \theta a} - \frac{\partial_\theta a}{r^2 \tan \theta a} - \frac{\partial_r a}{ra} - \frac{kr\partial_r a}{a} \right) \\ &= -r^2 \sin^2 \theta \lambda_b a^2 + 8\pi G T_{33}, \end{aligned} \quad (10.37)$$

10.5. Problem of this model

$$G_{0i} = -2\partial_i \left(\frac{\dot{a}}{a} \right) = 8\pi GT_{0i}, \quad i = 1, 2, 3 = r, \theta, \varphi, \quad (10.38)$$

$$G_{12} = \frac{\partial_\theta a}{ra} + \frac{2\partial_\theta a \partial_r a}{a^2} - \frac{\partial_r \partial_\theta a}{a} = 8\pi GT_{12}, \quad (10.39)$$

$$G_{13} = \frac{\partial_\varphi a}{ra} + \frac{2\partial_\varphi a \partial_r a}{a^2} - \frac{\partial_r \partial_\varphi a}{a} = 8\pi GT_{13}, \quad (10.40)$$

$$G_{23} = \frac{\partial_\varphi a}{\tan \theta a} + \frac{2\partial_\varphi a \partial_\theta a}{a^2} - \frac{\partial_\theta \partial_\varphi a}{a} = 8\pi GT_{23}, \quad (10.41)$$

where

$$\begin{aligned} (\nabla a)^2 &= \tilde{g}^{ij} \partial_i a \partial_j a \\ &= (1 - kr^2)(\partial_r a)^2 + \frac{1}{r^2}(\partial_\theta a)^2 + \frac{1}{r^2 \sin^2 \theta}(\partial_\varphi a)^2, \end{aligned} \quad (10.42)$$

$$\begin{aligned} \nabla^2 a &= \frac{1}{\sqrt{|\tilde{g}|}} \partial_i \left(\sqrt{|\tilde{g}|} \tilde{g}^{ij} \partial_j a \right) \\ &= (1 - kr^2) \partial_r^2 a + \left(\frac{2}{r} - kr \right) \partial_r a + \frac{1}{r^2} \partial_\theta^2 a \\ &\quad + \frac{1}{r^2 \tan \theta} \partial_\theta a + \frac{1}{r^2 \sin^2 \theta} \partial_\varphi^2 a, \end{aligned} \quad (10.43)$$

and \tilde{g} is the metric components of $d\Sigma^2$ defined by (10.23). The linear combination like (10.29) also gives

$$\begin{aligned} G_{00} + \sum_{i=1}^3 g^{ii} G_{ii} &= -\frac{6\ddot{a}}{a} \\ &= -2\lambda_b + 8\pi G \left(\rho + \sum_{i=1}^3 P_i \right), \end{aligned} \quad (10.44)$$

where all the spatial derivatives of a cancel and $\rho = T_{00}$, $P_i = g^{ii} T_{ii}$ (no summation for i here). Therefore we obtain

$$\ddot{a} + \Omega^2(t, r, \theta, \varphi) a = 0, \quad (10.45)$$

where

$$\Omega^2 = \frac{4\pi G}{3} \left(\rho + \sum_{i=1}^3 P_i \right) - \frac{\lambda_b}{3}. \quad (10.46)$$

Since we have $-\lambda_b \gg \Lambda^2 \geq G\Lambda^4 \sim T_{\mu\nu}$ (assuming $\Lambda \leq E_P$), the solution to the new inhomogeneous Einstein equations would just be a small perturbation around (10.31), which can be obtained by WKB approximation and

the weak parametric resonance effect described in section 5.1:

$$a(t, r, \theta, \varphi) = e^{\int_0^t H(t', r, \theta, \varphi) dt'} \sqrt{\frac{3k\Omega(0, r, \theta, \varphi)}{\lambda_b \Omega(t, r, \theta, \varphi)}} \cdot \cos\left(\int_0^t \Omega(t', r, \theta, \varphi) dt' + \gamma(r, \theta, \varphi)\right). \quad (10.47)$$

The phase $\gamma(r, \theta, \varphi)$ is different from point to point. In fact, plugging (10.47) into (10.38) gives

$$\begin{aligned} \Omega(0, r, \theta, \varphi) \tan \gamma(r, \theta, \varphi) &= \Omega(0, r_0, \theta_0, \varphi_0) \tan \gamma(r_0, \theta_0, \varphi_0) \\ &+ 4\pi G \int_{r_0, \theta_0, \varphi_0}^{r, \theta, \varphi} \mathbf{J}(0, r', \theta', \varphi') \cdot d\mathbf{l}', \end{aligned} \quad (10.48)$$

where $\mathbf{J} = (T_{01}, T_{02}, T_{03})$ is the energy flux and we have neglected the small exponential factor and the relatively small time derivative terms of the slowly varying frequency Ω in the calculation.

Solution (10.47) for a looks good but unfortunately the large negative λ_b actually requires large negative k , which means that the spatial curvatures have to become large everywhere. Then the spatial slice would have hyperboloid geometry with large curvature, which can not be average out to get flat space. This destroys the argument that the spatial averaging done by long wavelength fields would produce a flat spatial spacetime which has been shown in chapter 6. For this reason, this model does not work well.

Chapter 11

Conclusions

Starting from two fundamental principles of modern physics — the uncertainty principle of quantum mechanics and the equivalence principle of general relativity, we have shown that quantum vacuum would gravitate in a completely different way from what people previously thought. The gravitational effect produced by the huge vacuum stress energy is still huge, but confined to Planck scales. At each Planck size region, the spacetime oscillates between expansion and contraction. As it swings back and forth, the two almost cancel each other but the expansion wins out a little bit.

This physical picture might look crazy at first glance, but it is just the prediction of applying quantum mechanics and general relativity together to the quantum vacuum. In fact, this physical picture should be natural. Our approach is very much along Wheeler’s idea of spacetime foam—metric on small (Planck) scale is all higgledy-piggledy.

Due to this mechanism, the universe would expand with a small Hubble expansion rate $H \propto \Lambda e^{-\beta\sqrt{G}\Lambda} \rightarrow 0$ instead of the previous prediction $H = \sqrt{8\pi G\rho^{vac}/3} \propto \sqrt{G}\Lambda^2 \rightarrow \infty$ which was unbounded, as the high energy cutoff Λ is taken to infinity. In this sense, at least the “old” cosmological constant problem would be resolved. Moreover, it gives the observed slow rate of the accelerating expansion as Λ is taken to be some large value of the order of Planck energy or higher. This result suggests that there is no necessity to introduce the cosmological constant, which is required to be fine tuned to an accuracy of 10^{-120} , or other forms of dark energy, which are required to have peculiar negative pressure, to explain the observed accelerating expansion of the Universe.

Bibliography

- [1] Qingdi Wang, Zhen Zhu, and William G. Unruh. How the huge energy of quantum vacuum gravitates to drive the slow accelerating expansion of the universe. *Phys. Rev. D*, 95:103504, May 2017.
- [2] Clifford M. Will. The confrontation between general relativity and experiment. *Living Reviews in Relativity*, 9(3), 2006.
- [3] B. P Abbott et al. Observation of Gravitational Waves from a Binary Black Hole Merger. *Phys. Rev. Lett.*, 116(6):061102, 2016.
- [4] Robert M. Wald. *General Relativity*. 1984.
- [5] Steven Weinberg. The cosmological constant problem. *Rev. Mod. Phys.*, 61:1–23, Jan 1989.
- [6] Antonio Padilla. Lectures on the Cosmological Constant Problem. 2015.
- [7] Adam G. Riess, Alexei V. Filippenko, Peter Challis, Alejandro Clocchiatti, Alan Diercks, Peter M. Garnavich, Ron L. Gilliland, Craig J. Hogan, Saurabh Jha, Robert P. Kirshner, B. Leibundgut, M. M. Phillips, David Reiss, Brian P. Schmidt, Robert A. Schommer, R. Chris Smith, J. Spyromilio, Christopher Stubbs, Nicholas B. Suntzeff, and John Tonry. Observational evidence from supernovae for an accelerating universe and a cosmological constant. *The Astronomical Journal*, 116(3):1009, 1998.
- [8] S. Perlmutter, G. Aldering, G. Goldhaber, R. A. Knop, P. Nugent, P. G. Castro, S. Deustua, S. Fabbro, A. Goobar, D. E. Groom, I. M. Hook, A. G. Kim, M. Y. Kim, J. C. Lee, N. J. Nunes, R. Pain, C. R. Pennyacker, R. Quimby, C. Lidman, R. S. Ellis, M. Irwin, R. G. McMahon, P. Ruiz-Lapuente, N. Walton, B. Schaefer, B. J. Boyle, A. V. Filippenko, T. Matheson, A. S. Fruchter, N. Panagia, H. J. M. Newberg, W. J. Couch, and The Supernova Cosmology Project. Measurements of and from 42 high-redshift supernovae. *The Astrophysical Journal*, 517(2):565, 1999.

Bibliography

- [9] Edward Witten. The cosmological constant from the viewpoint of string theory. In David B. Cline, editor, *Sources and Detection of Dark Matter and Dark Energy in the Universe*, pages 27–36. Springer Berlin Heidelberg, 2001.
- [10] Edward Kolb and Michael Turner. *The Early Universe*. 1993.
- [11] A. D. Dolgov. The Problem of vacuum energy and cosmology. In *Phase transitions in cosmology. Proceedings, 4th Cosmology Colloquium, Euroconference, Paris, France, June 4-9, 1997*, 1997.
- [12] Leonard Susskind. *The Cosmic Landscape : String Theory and the Illusion of Intelligent Design*. Little, Brown, December 2005.
- [13] Svend E. Rugh and Henrik Zinkernagel. The quantum vacuum and the cosmological constant problem, 2001.
- [14] John A. Wheeler. On the Nature of quantum geometrodynamics. *Annals Phys.*, 2:604–614, 1957.
- [15] C.W. Misner, K.S. Thorne, and J.A. Wheeler. *Gravitation*. W. H. Freeman, 1973.
- [16] S.M. Carroll. *Spacetime and Geometry: An Introduction to General Relativity*. Addison Wesley, 2004.
- [17] P. A. R. Ade et al. Planck 2015 results. XIII. Cosmological parameters. 2015.
- [18] Sean M. Carroll. The Cosmological constant. *Living Rev. Rel.*, 4:1, 2001.
- [19] B. L. Hu and E. Verdaguer. Stochastic Gravity: Theory and Applications. *Living Rev. Rel.*, 11:3, 2008.
- [20] G. Teschl. *Ordinary Differential Equations and Dynamical Systems*. Graduate studies in mathematics. American Mathematical Soc.
- [21] L.D. LANDAU and E.M. LIFSHITZ. {CHAPTER} v - {SMALL} {OSCILLATIONS}. In L.D. LANDAU and E.M. LIFSHITZ, editors, *Mechanics (Third Edition)*, pages 58 – 95. Butterworth-Heinemann, Oxford, third edition edition, 1976.

Bibliography

- [22] Marko Robnik and Valery G. Romanovski. Energy evolution in time-dependent harmonic oscillator. *Open Systems and Information Dynamics*, 13(02):197–222, 2006.
- [23] Marko Robnik and Valery G Romanovski. Exact analysis of adiabatic invariants in the time-dependent harmonic oscillator. *Journal of Physics A: Mathematical and General*, 39(1):L35, 2006.
- [24] L.D. LANDAU and E.M. LIFSHITZ. {CHAPTER} {VII} - {THE} {CANONICAL} equations. In L.D. LANDAU and E.M. LIFSHITZ, editors, *Mechanics (Third Edition)*, pages 131 – 167. Butterworth-Heinemann, Oxford, third edition edition, 1976.
- [25] N. D. Birrell and P. C. W. Davies. *Quantum Fields in Curved Space*. Cambridge University Press, 1982. Cambridge Books Online.
- [26] Charles W. Misner. Mixmaster universe. *Phys. Rev. Lett.*, 22:1071–1074, May 1969.
- [27] R. L. Jaffe. Casimir effect and the quantum vacuum. *Phys. Rev. D*, 72:021301, Jul 2005.
- [28] M.O. Scully and M.S. Zubairy. *Quantum Optics*. Cambridge University Press, 1997.
- [29] Willis E. Lamb and Robert C. Retherford. Fine structure of the hydrogen atom by a microwave method. *Phys. Rev.*, 72:241–243, Aug 1947.
- [30] Julian Schwinger. On quantum-electrodynamics and the magnetic moment of the electron. *Phys. Rev.*, 73:416–417, Feb 1948.
- [31] D. Hanneke, S. Fogwell Hoogerheide, and G. Gabrielse. Cavity control of a single-electron quantum cyclotron: Measuring the electron magnetic moment. *Phys. Rev. A*, 83:052122, May 2011.
- [32] H.B.G. Casimir. On the Attraction Between Two Perfectly Conducting Plates. *Indag.Math.*, 10:261–263, 1948.
- [33] S. K. Lamoreaux. Demonstration of the casimir force in the 0.6 to $6\mu\text{m}$ range. *Phys. Rev. Lett.*, 78:5–8, Jan 1997.
- [34] U. Mohideen and Anushree Roy. Precision measurement of the casimir force from 0.1 to $0.9\mu\text{m}$. *Phys. Rev. Lett.*, 81:4549–4552, Nov 1998.

- [35] G. Bressi, G. Carugno, R. Onofrio, and G. Ruoso. Measurement of the casimir force between parallel metallic surfaces. *Phys. Rev. Lett.*, 88:041804, Jan 2002.
- [36] G. Aad et al. Observation of a new particle in the search for the standard model higgs boson with the {ATLAS} detector at the {LHC}. *Physics Letters B*, 716(1):1 – 29, 2012.
- [37] S. Chatrchyan et al. Observation of a new boson at a mass of 125 gev with the {CMS} experiment at the {LHC}. *Physics Letters B*, 716(1):30 – 61, 2012.
- [38] Joseph Polchinski. The Cosmological Constant and the String Landscape. In *The Quantum Structure of Space and Time*, pages 216–236, 2006.
- [39] Eduard Masso. The Weight of Vacuum Fluctuations. *Phys. Lett.*, B679:433–435, 2009.
- [40] V. B. Braginskii and V. I. Panov. Verification of equivalence of inertial and gravitational masses. *Sov. Phys. JETP*, 34:463–466, 1972. [Zh. Eksp. Teor. Fiz.61,873(1971)].
- [41] Stephen A. Fulling, Kimball A. Milton, Prachi Parashar, August Romeo, K. V. Shajesh, and Jef Wagner. How Does Casimir Energy Fall? *Phys. Rev.*, D76:025004, 2007.
- [42] Kimball A. Milton, Prachi Parashar, K. V. Shajesh, and Jef Wagner. How does Casimir energy fall? II. Gravitational acceleration of quantum vacuum energy. *J. Phys.*, A40:10935–10943, 2007.
- [43] Kimball A. Milton, Stephen A. Fulling, Prachi Parashar, August Romeo, K. V. Shajesh, and Jeffrey A. Wagner. Gravitational and inertial mass of Casimir energy. *J. Phys.*, A41:164052, 2008.
- [44] K. A. Milton, P. Parashar, J. Wagner, K. V. Shajesh, A. Romeo, and S. Fulling. How Does Quantum Vacuum Energy Accelerate? In *Proceedings, 34th International Conference on High Energy Physics (ICHEP 2008)*, 2008.
- [45] Agustn E. Gonzlez. On casimir pressure, the lorentz force and black body radiation. *Physica A: Statistical Mechanics and its Applications*, 131(1):228 – 236, 1985.

Bibliography

- [46] P. W. Milonni, R. J. Cook, and M. E. Goggin. Radiation pressure from the vacuum: Physical interpretation of the casimir force. *Phys. Rev. A*, 38:1621–1623, Aug 1988.
- [47] G Barton. On the fluctuations of the casimir force. *Journal of Physics A: Mathematical and General*, 24(5):991, 1991.
- [48] Qingdi Wang and William G. Unruh. Motion of a mirror under infinitely fluctuating quantum vacuum stress. *Phys. Rev. D*, 89:085009, Apr 2014.
- [49] Qingdi Wang and William G. Unruh. Mirror moving in quantum vacuum of a massive scalar field. *Phys. Rev. D*, 92:063520, Sep 2015.
- [50] Gilad Gour and L. Sriramkumar. Will small particles exhibit Brownian motion in the quantum vacuum? *Found. Phys.*, 29:1917–1949, 1999.
- [51] Marc-Thierry Jaekel and Serge Reynaud. Quantum fluctuations of position of a mirror in vacuum. *J. Phys. I(France)*, 3:1, 1993.
- [52] D. Jaffino Stargen, Dawood A. Kothawala, and L. Sriramkumar. Moving mirrors and the fluctuation-dissipation theorem. 2016.
- [53] Roger Penrose. Gravitational collapse and space-time singularities. *Phys. Rev. Lett.*, 14:57–59, Jan 1965.
- [54] S. W. Hawking. The occurrence of singularities in cosmology. *Proceedings of the Royal Society of London A: Mathematical, Physical and Engineering Sciences*, 294(1439):511–521, 1966.
- [55] S. W. Hawking. The occurrence of singularities in cosmology. ii. *Proceedings of the Royal Society of London A: Mathematical, Physical and Engineering Sciences*, 295(1443):490–493, 1966.
- [56] S. W. Hawking. The occurrence of singularities in cosmology. iii. causality and singularities. *Proceedings of the Royal Society of London A: Mathematical, Physical and Engineering Sciences*, 300(1461):187–201, 1967.
- [57] S. W. Hawking and G. F. R. Ellis. *The Large Scale Structure of Space-Time*. Cambridge Monographs on Mathematical Physics. Cambridge University Press, 2011.
- [58] S. W. Hawking and R. Penrose. The Singularities of gravitational collapse and cosmology. *Proc. Roy. Soc. Lond.*, A314:529–548, 1970.

- [59] A. Einstein and N. Rosen. The particle problem in the general theory of relativity. *Phys. Rev.*, 48:73–77, Jul 1935.
- [60] Abhay Ashtekar. New hamiltonian formulation of general relativity. *Phys. Rev. D*, 36:1587–1602, Sep 1987.
- [61] Ovidiu Cristinel Stoica. *Singular Semi-Riemannian Geometry and Singular General Relativity*. PhD thesis, Bucharest, Polytechnic Inst., 2013.
- [62] O. C. Stoica. On singular semi-riemannian manifolds. *International Journal of Geometric Methods in Modern Physics*, 11(05):1450041, 2014.
- [63] Ovidiu-Cristinel Stoica. Einstein equation at singularities. *Central Eur. J. Phys.*, 12:123–131, 2014.
- [64] Ovidiu-Cristinel Stoica. Beyond the Friedmann-Lemaitre-Robertson-Walker Big Bang singularity. *Commun. Theor. Phys.*, 58:613–616, 2012.
- [65] Ovidiu Cristinel Stoica. The Friedmann-Lemaitre-Robertson-Walker Big Bang Singularities are Well Behaved. *Int. J. Theor. Phys.*, 55(1):71–80, 2016.
- [66] Ovidiu-Cristinel Stoica. Schwarzschild’s Singularity is Semi-Regularizable. *Eur. Phys. J. Plus*, 127:83, 2012.
- [67] Ovidiu Cristinel Stoica. The Geometry of Black Hole singularities. *Adv. High Energy Phys.*, 2014:907518, 2014.
- [68] Ovidiu Cristinel Stoica. The geometry of singularities and the black hole information paradox. In *Proceedings, 7th International Workshop : Spacetime - Matter - Quantum Mechanics. (DICE2014): Castiglione-cello, Tuscany, Italy, September 15-19, 2014*, 2015.
- [69] Ovidiu Cristinel Stoica. Causal Structure and Spacetime Singularities. 2015.
- [70] G.N. Watson. *A Treatise on the Theory of Bessel Functions*. Cambridge University Press, 1995.

Appendix A

Real Massless Scalar Field

In this appendix we give the calculation details about how the quantum vacuum fluctuates all over the spacetime by using the massless scalar field (3.1) as an example.

We first define the covariance of the energy density operator at two spacetime points $x = (t, \mathbf{x})$ and $x' = (t', \mathbf{x}')$

$$\begin{aligned} & \text{Cov}(T_{00}(x), T_{00}(x')) \\ &= \langle \{ (T_{00}(x) - \langle T_{00}(x) \rangle) (T_{00}(x') - \langle T_{00}(x') \rangle) \} \rangle, \end{aligned} \quad (\text{A.1})$$

where the curly bracket $\{ \}$ in (A.1) is the symmetrization operator which is defined as, for any two operators A and B ,

$$\{AB\} = \frac{1}{2}(AB + BA). \quad (\text{A.2})$$

Inserting (3.1) and (3.4) into (A.1) gives the following result

$$\begin{aligned} & \text{Cov}(T_{00}(x), T_{00}(x')) \\ &= \frac{1}{2} \int \frac{d^3k d^3k'}{(2\pi)^6} \frac{(\omega\omega' + \mathbf{k} \cdot \mathbf{k}')^2}{2\omega 2\omega'} \\ & \quad \cdot \cos\left((\omega + \omega')\Delta t - (\mathbf{k} + \mathbf{k}') \cdot \Delta \mathbf{x}\right), \end{aligned} \quad (\text{A.3})$$

where $\Delta t = t - t'$ and $\Delta \mathbf{x} = \mathbf{x} - \mathbf{x}'$ are time and space separation of the two spacetime points x and x' .

If x and x' are timelike separated, we can find a reference frame to set $\Delta \mathbf{x} = |\Delta \mathbf{x}| = 0$. In this case, evaluation of the integral in (A.3) for a high frequency cutoff $|\mathbf{k}| = \Lambda$ gives

$$\begin{aligned} & \text{Cov}(T_{00}(x), T_{00}(x')) \quad (\text{A.4}) \\ &= \frac{1}{24\pi^4 \Delta t^8} \left(\left[-(\Lambda \Delta t)^6 + 21(\Lambda \Delta t)^4 - 72(\Lambda \Delta t)^2 + 36 \right] \cos(2\Lambda \Delta t) \right. \\ & \quad + 6 \left[(\Lambda \Delta t)^5 - 8(\Lambda \Delta t)^3 + 12\Lambda \Delta t \right] \sin(2\Lambda \Delta t) \\ & \quad \left. + 12 \left[(\Lambda \Delta t)^3 - 6\Lambda \Delta t \right] \sin(\Lambda \Delta t) + 36 \left[(\Lambda \Delta t)^2 - 2 \right] \cos(\Lambda \Delta t) + 36 \right). \end{aligned}$$

If x and x' are spacelike separated, we can find a reference frame to set $\Delta t = 0$. In this case, evaluation of the integral in (A.11) for a high frequency cutoff $|\mathbf{k}| = \Lambda$ gives

$$\begin{aligned} & \text{Cov}(T_{00}(x), T_{00}(x')) \\ &= \frac{1}{32\pi^4 \Delta x^8} \left([2(\Lambda \Delta x)^4 - 34(\Lambda \Delta x)^2 + 33] \cos(2\Lambda \Delta x) \right. \\ & \quad - [12(\Lambda \Delta x)^3 - 50\Lambda \Delta x] \sin(2\Lambda \Delta x) \\ & \quad \left. + 16 [(\Lambda \Delta x)^2 - 6] \cos(\Lambda \Delta x) - 64\Lambda \Delta x \sin(\Lambda \Delta x) + 63 \right) \quad (\text{A.5}) \end{aligned}$$

As Δt and Δx goes to 0, both (A.4) and (A.5) reduces to the variance of the energy density,

$$\langle (T_{00} - \langle T_{00} \rangle)^2 \rangle = \frac{2}{3} \left(\frac{\Lambda^4}{16\pi^2} \right)^2 = \frac{2}{3} \langle T_{00} \rangle^2 \quad (\text{A.6})$$

We then investigate the Pearson product-moment correlation coefficient

$$\rho_{x,x'} = \frac{\text{Cov}(T_{00}(x), T_{00}(x'))}{\sigma_x \sigma_{x'}}, \quad (\text{A.7})$$

where

$$\sigma_x = \sqrt{\langle (T_{00}(x) - \langle T_{00}(x) \rangle)^2 \rangle}. \quad (\text{A.8})$$

The correlation coefficient $\rho_{x,x'}$ shows by its magnitude the strength of correlation between two random variables. $\rho_{x,x'}$ is positive if the energy density T_{00} at x and x' are most possibly lying on the same side of the vacuum expectation value $\langle T_{00} \rangle = \Lambda^4/(16\pi^2)$. Thus a positive correlation coefficient $\rho_{x,x'}$ implies the energy density at x and x' tend to be simultaneously greater than, or simultaneously less than the expectation value. Similarly, a negative $\rho_{x,x'}$ implies the energy density tend to lie on opposite sides of the expectation value. We will call the energy density T_{00} at x and x' are positively correlated if $\rho_{x,x'} > 0$ or negatively correlated (anticorrelation) if $\rho_{x,x'} < 0$.

Because of transnational invariance, $\rho_{x,x'}$ is only dependent on the temporal and spatial separation $\Delta t = t - t'$, $\Delta \mathbf{x} = \mathbf{x} - \mathbf{x}'$. For the real massless scalar field (3.1), the behavior of the correlation coefficient $\rho_{x,x'}$ as a function of temporal separation $\Lambda \Delta t$ for the case of $\Delta x = 0$ and as a function of spatial separation $\Lambda \Delta x$ for the case of $\Delta t = 0$ are plotted in FIG. A.1 and A.2 respectively.

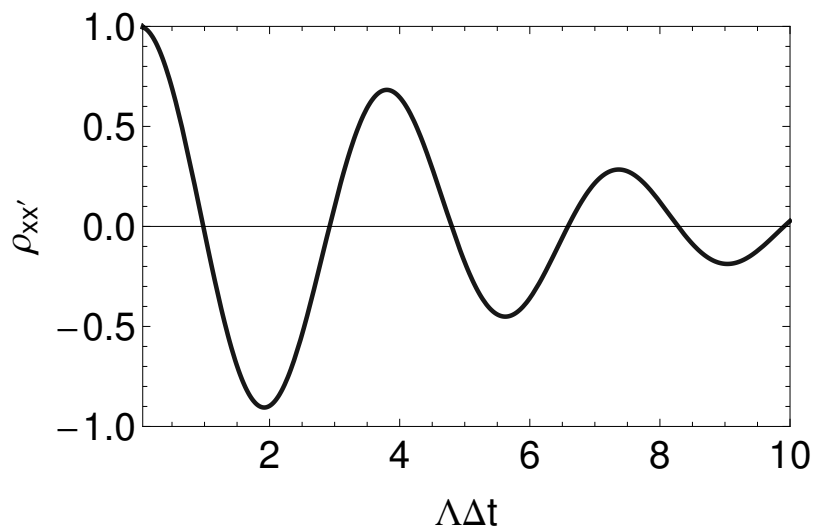


Figure A.1: Plot of correlation coefficient $\rho_{x,x'}$ as a function of time separation $\Lambda\Delta t$ in the case $\Delta x = 0$.

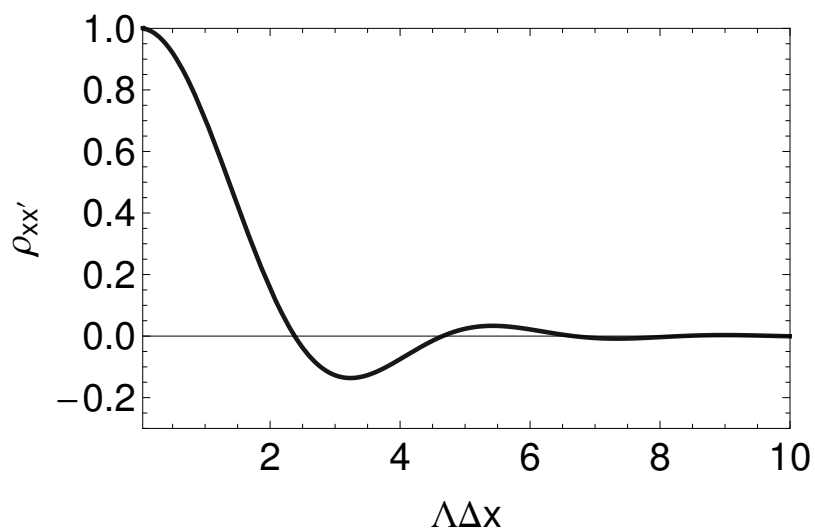


Figure A.2: Plot of correlation coefficient $\rho_{x,x'}$ as a function of spatial separation $\Lambda\Delta x$ in the case $\Delta t = 0$.

In the temporal direction, i.e. the case of $\Delta x = 0$ (Fig. A.1), the correlation coefficient goes quickly from 1 down to around -0.9 in a time scale around $\Delta t = 1.9/\Lambda$ and then goes up to 0.7 in a time scale around $\Delta t = 3.8/\Lambda$ and then goes down and up alternatively from positive values to negative values with decreasing amplitudes. It roughly oscillates as $-\cos(2\Lambda\Delta t)/(\Lambda\Delta t)^2$ with a period π/Λ as Δt is large. Thus at the extremely small time scales $\Delta t \sim 1.9/\Lambda$, ($\Lambda \rightarrow +\infty$), the energy density are strongly anticorrelated. In other words, if at some time the value of the energy density is larger than its expectation value, for example, by an amount of $0.82\langle T_{00}\rangle$, after a short time $\Delta t = 1.9/\Lambda$, its value is most likely to be smaller than the expectation value, for example, by an amount of $0.74\langle T_{00}\rangle$. The difference is $1.56\langle T_{00}\rangle$ only after such a short time.

In the spatial direction, i.e. the case of $\Delta t = 0$ (Fig. A.2), the correlation coefficient goes quickly from 1 down to around -0.14 in a length scale around $\Delta x = 3.24/\Lambda$ and then goes up to 0.03 in a length scale around $\Delta x = 5.4/\Lambda$ and then goes down and up alternatively from positive values to negative values with decreasing amplitudes. Compared to the temporal direction, the decay in the oscillation amplitude of the correlation coefficient is faster in spatial direction. It roughly oscillates as $2\cos(2\Lambda\Delta x)/(\Lambda\Delta x)^4$ with a period π/Λ as Δx is large. These properties show that the strength of the correlation between energy densities at close range in spatial direction is not as strong as in the temporal direction. For larger spatial separations, $\rho_{x,x'}$ approaches zero and the vacuum energy density T_{00} at different x and x' fluctuate independently. These properties result in extreme spatial inhomogeneities of the quantum vacuum which can be characterized by the quantity $\Delta\rho^2$ defined by (3.8) in chapter 3.

The quantity $\Delta\rho^2$ is related to $\rho_{x,x'}$ by

$$\Delta\rho^2 = 1 - \rho_{x,x'}. \quad (\text{A.9})$$

The behavior of $\Delta\rho^2$ has been plotted in FIG. 3.1.

Next we calculate the $\chi(\Delta t)$ defined by (5.3) in section 5.1. Wick expansion of (5.3) gives

$$\chi(\Delta t) = \frac{\langle \dot{\phi}(t_1, \mathbf{x})\dot{\phi}(t_2, \mathbf{x}) \rangle^2 + \langle \dot{\phi}(t_2, \mathbf{x})\dot{\phi}(t_1, \mathbf{x}) \rangle^2}{2\langle \dot{\phi}^2(t, \mathbf{x}) \rangle^2}, \quad (\text{A.10})$$

where the correlation function can be calculated directly by inserting (3.1)

$$\langle \dot{\phi}(t_1, \mathbf{x})\dot{\phi}(t_2, \mathbf{x}) \rangle = \frac{1}{4\pi^2} \int_0^\Lambda k^3 e^{-ik\Delta t} dk. \quad (\text{A.11})$$

Plugging (A.11) into (A.10) gives the following result

$$\begin{aligned}
 \chi(\Delta t) &= \frac{16}{\Lambda^8 \Delta t^8} \left(36 (-2 + \Lambda^2 \Delta t^2) \cos(\Lambda \Delta t) \right. \\
 &+ (36 - 72\Lambda^2 \Delta t^2 + 21\Lambda^4 \Delta t^4 - \Lambda^6 \Delta t^6) \cos(2\Lambda \Delta t) \\
 &+ 6(6 + 2\Lambda \Delta t (-6 + \Lambda^2 \Delta t^2) \sin(\Lambda \Delta t) \\
 &\left. + \Lambda \Delta t (12 - 8\Lambda^2 \Delta t^2 + \Lambda^4 \Delta t^4) \sin(2\Lambda \Delta t) \right). \quad (\text{A.12})
 \end{aligned}$$

The behavior of $\chi(\Delta t)$ has been plotted in FIG. 5.1. It is closely related to the correlation coefficient $\rho_{x,x'}$ as a function of time difference Δt in the case $\Delta x = 0$ (FIG. A.1).

Next we derive the equation (5.29) in section 5.1. First, $\Omega^2(t, \mathbf{0})$ can be expanded as

$$\begin{aligned}
 \Omega^2(t, \mathbf{0}) &= \frac{8\pi G}{3} \int_{\omega, \omega' \leq \Lambda} \frac{d^3 k d^3 k'}{(2\pi)^3} \frac{\sqrt{\omega \omega'}}{2} \quad (\text{A.13}) \\
 &\cdot \left[\left(a_{\mathbf{k}} a_{\mathbf{k}'}^\dagger + a_{\mathbf{k}}^\dagger a_{\mathbf{k}'} \right) \cos(\omega - \omega') t + i \left(-a_{\mathbf{k}} a_{\mathbf{k}'}^\dagger + a_{\mathbf{k}}^\dagger a_{\mathbf{k}'} \right) \sin(\omega - \omega') t \right. \\
 &\left. + \left(-a_{\mathbf{k}} a_{\mathbf{k}'} - a_{\mathbf{k}}^\dagger a_{\mathbf{k}'}^\dagger \right) \cos(\omega + \omega') t + i \left(a_{\mathbf{k}} a_{\mathbf{k}'} - a_{\mathbf{k}}^\dagger a_{\mathbf{k}'}^\dagger \right) \sin(\omega + \omega') t \right].
 \end{aligned}$$

Specially, the vacuum state $|0\rangle$ is an eigenstate of the operator coefficients of the first two terms in the above expression (A.13). If $\mathbf{k} \neq \mathbf{k}'$, the eigenvalues of the operator coefficients of the first two terms are zero. Thus in this case, the first two terms have to both take zero values. If $\mathbf{k} = \mathbf{k}'$, the second term is zero since in this case $\omega = \omega'$ and thus the factor $\sin(\omega - \omega')t = 0$. So only the first term survives and gives the expectation value of $\Omega^2(t, \mathbf{0})$:

$$\Omega_0^2 = \langle \Omega^2 \rangle = \frac{8\pi G}{3} \int_{\omega \leq \Lambda} \frac{d^3 k}{(2\pi)^3} \frac{\omega}{2} = \frac{G\Lambda^4}{6\pi}. \quad (\text{A.14})$$

For the operator coefficients of the last two terms in the expression (A.13), the vacuum state $|0\rangle$ is not an eigenstate. So the last two terms are constantly fluctuating, and the time varying of Ω^2 comes from these two terms.

After some algebraic manipulations, (A.13) can be rewritten as the form of (5.29) for the vacuum state $|0\rangle$, where

$$f(\gamma) d\gamma = \frac{16\pi^2}{\Lambda^4} \int_{\gamma \leq \omega + \omega' \leq \gamma + d\gamma} \frac{d^3 k d^3 k'}{(2\pi)^3} \frac{\sqrt{\omega \omega'}}{2} \left(-a_{\mathbf{k}} a_{\mathbf{k}'} - a_{\mathbf{k}}^\dagger a_{\mathbf{k}'}^\dagger \right), \quad (\text{A.15})$$

$$g(\gamma)d\gamma = \frac{16\pi^2}{\Lambda^4} \int_{\gamma \leq \omega + \omega' \leq \gamma + d\gamma} \frac{d^3k d^3k'}{(2\pi)^3} \frac{\sqrt{\omega\omega'}}{2} i \left(a_{\mathbf{k}} a_{\mathbf{k}'} - a_{\mathbf{k}}^\dagger a_{\mathbf{k}'}^\dagger \right). \quad (\text{A.16})$$

Evaluating the above integrals gives the expectation values

$$\langle f(\gamma)d\gamma \rangle = \langle g(\gamma)d\gamma \rangle = 0, \quad (\text{A.17})$$

and their fluctuations

$$\begin{aligned} & \langle (f(\gamma)d\gamma)^2 \rangle = \langle (g(\gamma)d\gamma)^2 \rangle \quad (\text{A.18}) \\ = & \begin{cases} \frac{4}{35} \left(\frac{\gamma}{\Lambda}\right)^7 \frac{d\gamma}{2\Lambda}, & \text{if } 0 \leq \gamma \leq \Lambda, \\ -\frac{4}{35} \left(40 - 140\frac{\gamma}{\Lambda} + 168\left(\frac{\gamma}{\Lambda}\right)^2 - 70\left(\frac{\gamma}{\Lambda}\right)^3 + \left(\frac{\gamma}{\Lambda}\right)^7\right) \frac{d\gamma}{2\Lambda}, & \text{if } \Lambda \leq \gamma \leq 2\Lambda. \end{cases} \end{aligned}$$

The above expression (A.18) gives the power spectrum density of the varying part of $\Omega^2(t, \mathbf{0})$ (except the constant Ω_0^2 part), which has been plotted in FIG. 5.2.

Appendix B

Wigner-Weyl Description of Quantum Mechanics and Numeric simulations

This chapter explain the principle of the numeric calculations in the main text. Same as the numeric part in the main text, we set $G = 1$ in this chapter. Wigner functions and Weyl transforms of operators offer a formulation of quantum mechanics that is equivalent to the standard approach given by the Schrödinger equation. The Wigner distribution function is a quasi distribution function in the phase space. For a particular quantum wave function $\psi(x)$, its Wigner function is defined as

$$W(x, p) = \int dy e^{-ipy} \psi(x + \frac{y}{2}) \psi^*(x - \frac{y}{2}) \quad (\text{B.1})$$

The Weyl transform of an quantum operator \hat{A} is defined as

$$A(x, p) = \int dy e^{-ipy} \langle x + \frac{y}{2} | \hat{A} | x - \frac{y}{2} \rangle \quad (\text{B.2})$$

Then the expectation value of the operator \hat{A} under the state $\psi(x)$ can be written as

$$\langle \hat{A} \rangle = \int \int dx dp W(x, p) A(x, p) \quad (\text{B.3})$$

These two transformations give the Wigner-Weyl discription for quantum mechanics. The expectation values of physical quantities are obtained by averaging their Weyl transforms over phase space.

For a harmonic oscillator with frequency ω and $m = 1$, the ground state Wigner function is a Gaussian distribution function for both x and p

$$W_0(x, p) = \frac{1}{\pi} e^{-\frac{p^2}{\omega} - x^2 \omega} \quad (\text{B.4})$$

We can easily check that the Weyl transform of an operator $H(\hat{x})$ (or $H(\hat{p})$) is simply replaced the operator \hat{x} by x (or \hat{p} by p). Other than that, another

particular transform we are going to use in this write-up is

$$\hat{x}\hat{p} \rightarrow xp + \frac{i}{2}; \quad \hat{p}\hat{x} \rightarrow xp - \frac{i}{2} \quad (\text{B.5})$$

We can see that the transform of the product does not necessarily equal to the product of transforms. In the following part we are going to get the general expression for the transform of the product.

Before that we notice that Weyl transform can be used to construct the original operator , i.e.

$$\langle x|\hat{A}|y\rangle = \frac{1}{2\pi} \int dp A\left(\frac{x+y}{2}, p\right) e^{ip(x-y)} \quad (\text{B.6})$$

Using this formula we can construct the transform of product of two states:

$$\begin{aligned} & \int dy \langle x + \frac{y}{2} | \hat{A}\hat{B} | x - \frac{y}{2} \rangle e^{-ipy} \\ &= \int dz dy \langle x + \frac{y}{2} | \hat{A} | z \rangle \langle z | \hat{B} | x - \frac{y}{2} \rangle e^{-ipy} \\ &= \frac{1}{4\pi^2} \int dz dy dp_1 dp_2 e^{ip_1(x+\frac{y}{2}-z)} e^{-ip_2(x-\frac{y}{2}-z)} e^{-ipy} \\ & \quad \cdot A\left(\frac{x+y/2+z}{2}, p_1\right) B\left(\frac{x-y/2+z}{2}, p_2\right) \\ &= \frac{1}{4\pi^2} \int dz_1 dz_2 dp_1 dp_2 e^{iz_1(p_2-p)} e^{iz_2(p-p_1)} \\ & \quad \cdot A\left(x + \frac{z_1}{2}, p_1\right) B\left(x + \frac{z_2}{2}, p_2\right) \end{aligned} \quad (\text{B.7})$$

Here we define

$$z_1 = \frac{y}{2} + z - x \quad (\text{B.8})$$

$$z_2 = -\frac{y}{2} + z - x \quad (\text{B.9})$$

We Taylor-expand $A(x + \frac{z_1}{2}, p_1)$ and $B(x + \frac{z_2}{2}, p_2)$ around x and have

$$A\left(x + \frac{z_1}{2}, p_1\right) = \sum_{n=0}^{\infty} \frac{1}{n!} A^{(n)}(x, p_1) \left(\frac{z_1}{2}\right)^n \quad (\text{B.10})$$

$$B\left(x + \frac{z_2}{2}, p_2\right) = \sum_{n=0}^{\infty} \frac{1}{n!} B^{(n)}(x, p_2) \left(\frac{z_2}{2}\right)^n \quad (\text{B.11})$$

and use the facts

$$\frac{1}{2\pi} \int dx x^n e^{ixy} = (-i)^n \delta^{(n)}(y) \quad (\text{B.12})$$

and

$$\int dy \delta^{(n)}(y) f(y) = (-1)^n f^{(n)}(0) \quad (\text{B.13})$$

Therefore, we can write the Weyl transform of operator $\hat{A}\hat{B}$ as

$$\sum_{n,m} \frac{i^n (-i)^m}{2^{n+m} n! m!} A^{(n,m)}(x,p) B^{(m,n)}(x,p) \quad (\text{B.14})$$

The generalized FRW scale factor a satisfies the equation

$$\ddot{a} + \Omega^2(t)a = 0 \quad (\text{B.15})$$

in which

$$\Omega^2(t) = \frac{8\pi}{3} \dot{\phi}^2(t) \quad (\text{B.16})$$

Now we replace all the quantities by operators, assuming that operators still satisfy the previous equation

$$\ddot{\hat{a}} + \hat{\Omega}(t)^2 \hat{a} = 0 \quad (\text{B.17})$$

with

$$\hat{\Omega}^2(t) = \frac{8\pi}{3} \dot{\hat{\phi}}^2(t) \quad (\text{B.18})$$

For a massless real scalar field, we can write it as

$$\hat{\phi} = \int \frac{d^3k}{(2\pi)^{3/2}} (\hat{x}_k \cos(\omega_k t) + \frac{1}{\omega_k} \hat{p}_k \sin(\omega_k t)) \quad (\text{B.19})$$

in which

$$\hat{x}_k = \sqrt{\frac{1}{2\omega_k}} (b_k^\dagger + b_k) \quad (\text{B.20})$$

$$\hat{p}_k = i \sqrt{\frac{\omega_k}{2}} (b_k^\dagger - b_k) \quad (\text{B.21})$$

are the generalized \hat{x} \hat{p} operators for each field modes.

We can write the Weyl transformation of the $\hat{\Omega}(t)$

$$\begin{aligned} \Omega(\{x_k\}, \{p_k\}, t)^2 &= \frac{8\pi}{3} \iint \frac{d^3k d^3k'}{(2\pi)^3} x_k x_{k'} \omega_k \omega_{k'} \sin \omega_k t \sin \omega_{k'} t \\ &+ p_k p_{k'} \cos \omega_k t \cos \omega_{k'} t - 2x_k p_{k'} \omega_k \sin \omega_k t \cos \omega_{k'} t \end{aligned} \quad (\text{B.22})$$

This expression is quadratic in x_k and p_k , so if we apply it to (B.14), only $m + n \leq 2$ terms survive. Assuming $a(\{x_k\}, \{p_k\}, t)$ is the Weyl transform of operator \hat{a} , we have the equation for a as

$$\begin{aligned} \ddot{a} + \Omega^2 a + \frac{i}{2} \sum_k \left(\frac{\partial \Omega^2}{\partial x_k} \frac{\partial a}{\partial p_k} - \frac{\partial \Omega^2}{\partial p_k} \frac{\partial a}{\partial x_k} \right) \\ - \frac{1}{8} \sum_{k,k'} \left(\frac{\partial^2 \Omega^2}{\partial x_k \partial x_{k'}} \frac{\partial^2 a}{\partial p_k \partial p_{k'}} + \frac{\partial^2 \Omega^2}{\partial p_k \partial p_{k'}} \frac{\partial^2 a}{\partial x_k \partial x_{k'}} - 2 \frac{\partial^2 \Omega^2}{\partial x_k \partial p_{k'}} \frac{\partial^2 a}{\partial p_k \partial x_{k'}} \right) = 0 \end{aligned} \quad (\text{B.23})$$

The observed value a is the average over Wigner function $W(\{x_k\}, \{p_k\}, t)$

$$a_o(t) = \int \left(\prod_k dx_k dp_k \right) a(\{x_k\}, \{p_k\}, t) W(\{x_k\}, \{p_k\}, t) \quad (\text{B.24})$$

If the quantum field is in the ground state, then by (B.6)

$$W(\{x_k\}, \{p_k\}, t) = \prod_k \frac{1}{\pi} e^{-\frac{p_k^2}{\omega_k} - x_k^2 \omega_k} \quad (\text{B.25})$$

Local approximation Generally the equation (B.23) depends on not only the value of Ω and a on a particular phase space point (x, p) , but also on the neighboring values (i.e. derivatives). If our solution a is "smooth" enough in the phase space then we can neglect the last two derivative terms in the (B.23). It can be simplified to

$$\ddot{a} + \Omega^2 a = 0. \quad (\text{B.26})$$

Assuming the length of the Universe is L . We can replace the integral by summations. For simplicity, we define

$$\tilde{t} \rightarrow \frac{2\pi t}{L} \quad (\text{B.27})$$

$$\tilde{x}_n \rightarrow \sqrt{2\omega \frac{2\pi n}{L}} x \frac{2\pi n}{L} \quad (\text{B.28})$$

$$\tilde{p}_n \rightarrow \sqrt{\frac{2}{\omega \frac{2\pi n}{L}}} p \frac{2\pi n}{L} \quad (\text{B.29})$$

The equation can be written as

$$\ddot{a} + \frac{2}{3L^2} \Omega(\tilde{t})^2 a = 0 \quad (\text{B.30})$$

with

$$\begin{aligned}
 \Omega(\tilde{t})^2 &= \sum_{\vec{n}, \vec{n}'} \sqrt{nn'} (\tilde{x}_{\vec{n}} \tilde{x}_{\vec{n}'} \sin n\tilde{t} \sin n'\tilde{t} \\
 &\quad + \tilde{p}_{\vec{n}} \tilde{p}_{\vec{n}'} \cos n\tilde{t} \cos n'\tilde{t} \\
 &\quad - \tilde{x}_{\vec{n}} \tilde{p}_{\vec{n}'} \sin n\tilde{t} \cos n'\tilde{t}) \\
 &= \left[\sum_{\vec{n}} \sqrt{n} (\tilde{x}_{\vec{n}} \sin n\tilde{t} - \tilde{p}_{\vec{n}} \cos n\tilde{t}) \right]^2
 \end{aligned} \tag{B.31}$$

Here $\vec{n} = (n_1, n_2, n_3)$, $n_{1,2,3} \in \mathbb{Z}$ and $n = |\vec{n}|$. $\{\tilde{x}_{\vec{n}}\}$ $\{\tilde{p}_{\vec{n}}\}$ are random Gaussian variables with unit standard deviation. We can solve the equation for a randomly generated set of $\{\tilde{x}_{\vec{n}}\}$ and $\{\tilde{p}_{\vec{n}}\}$, and repeat. The result $a_o(t)$ is the average over all solutions as long as our sample size is big enough.

Appendix C

Fourier transforms of the coefficients in (6.42)

In this appendix, we demonstrate the property of the spectrum of the coefficients in (6.42) given by (6.52), (6.54) and (6.56). Observing that the $\cos 2\Theta$, $\sin 2\Theta$ and $\tan \Theta$ in (6.51), (6.53) and (6.55) respectively can all be decomposed as Fourier series sum of the form $e^{i2n\Theta}$, where $n = \pm 1, \pm 2, \dots$, we only need to analyze the spectrum of $e^{i2n\Theta}$.

For simplicity, we only analyze the time component Fourier transform of $e^{i2n\Theta}$. The spatial part has similar property. The phase angle Θ is determined by Ω through (6.9) while Ω is determined by (5.29). The power spectrum of Ω^2 is given by (A.18) (illustrated in FIG. 5.2).

Calculation of the Fourier transform of $e^{i2n\Theta}$ exactly based on (5.29) is complicated. For simplicity, we assume that Ω taking the following simple form which is similar to (5.27)

$$\Omega = \Omega_0(1 + h \cos \gamma t), \quad (\text{C.1})$$

where γ take the peak value of the power spectrum (A.18) which is around $\sim 1.7\Lambda$ (see FIG. 5.2) and $h < 1$ to make sure that $\Omega > 0$.

Then we have

$$\Theta = \Omega_0 t + \frac{h\Omega_0}{\gamma} \sin \gamma t. \quad (\text{C.2})$$

Using the Jacobi-Anger expansion we have

$$e^{i2n\Theta} = \sum_{m=-\infty}^{+\infty} J_m\left(\frac{2nh\Omega_0}{\gamma}\right) e^{i(2n\Omega_0 + m\gamma)t}, \quad (\text{C.3})$$

where J_m is the m th Bessel function of the first kind.

As $|m| \rightarrow \infty$, we have

$$\left|J_m\left(\frac{2nh\Omega_0}{\gamma}\right)\right| \sim \frac{1}{m!} \left(\frac{nh\Omega_0}{\gamma}\right)^{|m|}, \quad (\text{C.4})$$

Appendix C. Fourier transforms of the coefficients in (6.42)

which drops faster than the exponential. Therefore, the Fourier transform of $e^{i2n\Theta}$ is centered around $2n\Omega_0$.

To estimate the magnitude of the Fourier coefficients of $e^{i2n\Theta}$ around zero frequency, we evaluate the Bessel function for

$$m \sim -2n\Omega_0/\gamma \sim \sqrt{G}\Lambda \rightarrow \infty. \quad (\text{C.5})$$

In this case, the zero component Fourier coefficient is asymptotic to (see [70])

$$|J_m(-hm)| \sim \frac{e^{-(\nu - \tanh \nu)|m|}}{\sqrt{2\pi|m|\tanh \nu}} \rightarrow 0, \quad (\text{C.6})$$

since ν is determined by $h = \text{sech } \nu < 1$ that we always have $\nu - \tanh \nu > 0$.

When calculating the Fourier transform of $e^{i2n\Theta}$ exactly based on (5.29), the spectrum becomes continuous instead of discrete. But the distribution of the spectrum should be similar.